THE APPLICATION OF LASER INDUCED BREAKDOWN SPECTROSCOPY SENSOR SYSTEM FOR REAL TIME ORE CLASSIFICATION

by

Rodrigo Fernando Cordova Torres

B.Sc. (Mining Engineering) University of Utah, 2012

A THESIS SUBMITTED IN PARTIAL FULFILLMENT OF

THE REQUIREMENTS FOR THE DEGREE OF

MASTER OF APPLIED SCIENCE

in

THE FACULTY OF GRADUATE AND POSTDOCTORAL STUDIES

(Mining Engineering)

UNIVERSITY OF BRITISH COLUMBIA

(Vancouver)

December 2016

Abstract

Laser Induced Breakdown Spectroscopy (LIBS) is a geoanalytical tool capable of identifying elements, and measuring element concentrations and the composition of rock samples. LIBS is a method based on a laser energy pulse that creates an ablation in the surface of a rock sample and the ionization of photons to produce a breakdown of the sample's elemental composition. The ionization process can be captured to produce a spectrum that contains information about elemental composition. The wavelength is used to identify elements, and its intensity peaks are used to identify the concentrations of the element.

The mining production cycle involves such processes as rock support, drilling, blasting, loading, hauling, dumping, reclamation and ventilation, depending on the mining method. Although pre-sorting, pre-concentration and classification techniques have been applied to aspects of mineral processing after the mining cycle, this research proposes the use of LIBS in the mining cycle, and defines the basic capabilities of a sensor with potential applications in the drilling and loading cycle, particularly with respect to shovels, drills and belt conveyors.

The purpose of LIBS is not to provide an accurate measurement of the target mineral, which in this research is Copper ore, but responses from different elements that can be mineralogically and statistically related to obtain a predicted concentration of the target mineral. In this paper, the methodologies and the foundations of LIBS have been developed as a sensor and proxy to an ore sorting system for the real-time in situ classification of rock material.

The research is based on samples from the Escondida Mine located in the north of Chile. The samples are divided into groups of Oxides and Sulphides. The results reveal the ability to predict Oxides, Sulphides and the discrimination of Oxide and Sulphide ores. The prediction regarding the target ores is obtained by comparing the LIBS data to Certified Analysis with ICP

techniques. The results include models for the prediction of Cu content for Oxides and Sulphide ore types by LIBS analysis, as well as the discrimination of Oxide ores from Sulphide ores using this technology.

Preface

This dissertation is an original intellectual product of the author, Rodrigo Fernando Cordova Torres. The laboratory results reported in Chapter 3:, Chapter 4: and Chapter 5: were obtained at Minesense Ltd. facilities in Vancouver, Canada.

Table of Contents

List of Tables

List of Figures

List of Abbreviations

Acc.	-	Accuracy
Aki	-	Transition probability or Einstein Coefficient
ASS	-	Atomic Absorption Spectroscopy
CCD	-	Charged Coupled Plasma
HFEMS	-	High Frequency Electro Magnetic Spectroscopy
Hz	-	Hertz
ICP	-	Induced Coupled Plasma
ICP-AES	-	Induced Coupled Plasma Atomic Emission Spectroscopy
ICP-MS	-	Induced Coupled Plasma Mass Spectroscopy
ID	-	Identification
l/mm	-	Lines per millimeter
LIBS	-	Laser Induced Breakdown Spectroscopy
mJ	-	Millijoule
MW	-	Mega Watts
NaN	-	Not a number
NIR	-	Near Infra-Red
NIST	-	National Institute of Standards and Technology
nm	-	Nanometer
ppm	-	Parts per million
R	-	Pearson Coefficient
SME	-	Society of Mining, Metallurgy and Exploration
XRF	-	X-ray fluorescence

Acknowledgements

I would like to acknowledge the contributions of Dr. Michael Nelson, my former professor and the director of the Mining Department at the University of Utah, for sharing his previous work with LIBS sensors. I would also like to thank Dr. David Munoz Paniagua, for his academic supervision and support as an expert on Physical Chemistry. I am grateful to Minesense Technologies Ltd. for giving me the opportunity to work on their new potential technology for sorting sensors. I would also like to thank Mitacs for funding in conjunction with Minesense. I offer much gratitude to Dr. Andrew Bamber, and Dr. Bern Klein, my supervisor.

Furthermore, I would like to acknowledge to Matthew Dirks, a current Ph.D. student from the Computer Sciences Department for his support, training and ideas regarding Python Script and computer applications applied to LIBS. Finally, I would like to thank Michael McClintock for his continued support throughout the research process.

Dedication

I would like to dedicate this dissertation to Edgar Cordova and Mariela Torres, my parents and also engineers, because they have inspired me since childhood with a love for science and a passion to provide excellent service.

Also, I would like to share this thought:

> *"Every single organization, society, community in the world is responsible for developing their own technologies to secure their survival, no matter what their conditions or heritage are. Otherwise, they will perish." Rodrigo Fernando Córdova Torres, 2016*

To my beloved country: Peru

Chapter 1: Introduction and Thesis Outline

1.1 Motivation

Laser Induced Breakdown Spectroscopy (LIBS) is an optical spectrochemical method used for the identification of elements. It has a wide variety of applications. LIBS produces a stimulated emission spectroscopy that uses a light beam laser and releases 2 or more photons, resulting in an ionization stage. This spectrochemical method produces a spectrum that is read by a Czerny-Turner monochromator, and is ultimately sent to a photodiode array. This array produces a readable spectrum with data that has been converted into peaks of Intensity (counts-units) on the y-axis and Wavelength (nm-units) on the x-axis.

Minesense Ltd. (the sponsor company for this current research) focuses on the use of sensors for ore sorting. Currently, the main sensor techniques used at Minesense are X-Ray Fluorescence (XRF) and High Frequency Electro Magnetic Spectroscopy (HFEMS). LIBS has been identified as potentially being highly complementary to these modes on account of its use of the direct measurement principle, as well as the superior range of elements that it can detect when compared with, for example, XRF. The ultimate goal of defining LIBS' capabilities is to eventually integrate this technique as a possible sensor for ore sorting at Minesense. In this research, we will review a set of proposed methodologies with the aim of gaining a better understanding of the applications of the LIBS machine in its use as a sensor for sorting ore.

Some of the main challenges currently faced by the mining industry involve creating more effective processes to decrease energy consumption, decrease the costs of extraction, and develop techniques for mining mineral deposits that were not economically feasible in the past due to either their low grade or metallurgical complexity. The majority of the mineral deposits located close to the surface, and with high metal concentrations, have already been mined. As such, mineral

deposits of high complexity have been left underground, waiting for such a time that technology and other developments are advanced enough to allow the deposits to be economically feasible to mine. Ore sorting is a potential solution for the pre-concentration and classification of ores for more cost effective metallurgical extraction.

1.2 Former research work done with LIBS in the mining industry

Several applications of LIBS have been developed for the mining industry such as monitoring grade concentrations, inline volume flow grade analysis of minerals on a belt conveyor, laboratory analysis, and during exploration using fast scanning (SECOPTA). However, no evidence regarding any previous work on LIBS sensors with respect to an ore sorting system in the mining production cycle could be found.

Significant research regarding LIBS applications in mining was conducted by APTI (now British Aerospace) in conjunction with Idaho National Laboratories and the University of Utah (Idaho Nationl Engineering & Environmental Lab, Bechtel BWXT). However, the purpose of work done at APTI was to develop an ore grading device, while the purpose of this research is to develop an automated proxy between the primary target ore and related mineralogy, in order to provide a response for the ore sorting system.

Other academic work has been conducted by the Italian National Research Council (G. S. Senesi) in “Laser-Induced Breakdown Spectroscopy applied to terrestrial and extraterrestrial analogue geomaterials with emphasis to characterize minerals and rocks.” This work provides a chemometric approach to the identification and concentration of elements in rock samples, and discusses the quality and quantity of the data obtained from LIBS in comparison to concentrations determined by chemical analysis.

1.3 Significance of the research

This research provides an initial approach regarding the capabilities of LIBS as a sensor for the sorting of Copper porphyry ores. Ore sorting has been mostly applied to the mineral processing system. This research involves one of the first attempts to include sorting as part of the mining production system. The mining production system is defined in the "SME Mining Engineering Handbook" (Darling) as 10 tasks for surface mining and 8 tasks for underground mining. Primarily, these tasks can be summarized as rock support, drilling, blasting, loading, hauling, dumping, reclamation of the land, and ventilation for underground mining methods. In the mining production cycle, the best location to assess ore quality such that material classified is during drilling and loading. Currently, ore quality is controlled by using reconciliation procedures between the grades of the drill holes and the grade estimated during the exploration cycle. Usually the reconciliation procedure creates a difference between the grades known as discrepancy. This analysis can monitor the expected ore grade, however it does not offer any possibility for control other than through setting the location boundaries of the ore, and estimating its dilution. An ore sorting system could improve grade control by providing an intelligent interface for a shovel operator in the loading cycle to help him/her make decisions regarding the quality of the material in the shovel so that a decision can be made regarding the correct destination for the loaded material.

The sorting would not only provide a reduction in the dilution and pre-concentration of the material, it could potentially be applied to decreasing the cut-off grade of the whole mine operation. This suggests an improvement in flotation capabilities and recovery efficiency during mineral processing.

If sorting systems could improve performance in mine operations, operating cost could be decreased. There is an opportunity to improve performance by increasing control of the grade processed in the concentrator. Also, characterization of ore properties such as Oxide versus Sulphide would allow ore to be diverted to the appropriate process stream (eg heap leach versus flotation).

1.4 Outline

The focus of this dissertation is the presentation of a methodology that could be used to incorporate LIBS as a new sensor for ore sorting systems, and to delineate the capabilities of LIBS in making correlations and yielding results. With respect to the intents of this dissertation, Chapter 2: explains the chemistry basics of LIBS, and highlights the important features of LIBS that need to be considered in order to achieve valid results in characterizing ore materials. Chapter 3: explains the experimental procedures, techniques and algorithms used to process the spectrum and data from LIBS. This chapter further describes some of the mathematical tools used to develop the scripts to acquire data, and also explains some of the challenges posed by laboratory testing, and the ways to address the existing challenges.

Chapter 4: presents a characterization of Oxide porphyry samples using LIBS, and a regression analysis of the results, ultimately providing a potential prediction equation for Cu content. This equation attempts to present a methodology rather than a criterion for sorting ore at the Escondida Mine. Furthermore, the methodology used for regression in Chapter 5:. Chapter 5: presents a characterization of Sulphide porphyry samples using LIBS, as well as regression analysis and prediction equations for Cu content.

Chapter 6: presents a potential methodology for differentiating between Oxide and Sulphide samples for ore sorting systems. Here, the chemistry background needed to understand this distinction is explained. Chapter 7: provides a discussion of the methodology and its potential for improving the results. Finally, Chapter 8: provides a set of conclusions that encompass the outcomes of the LIBS applications found in this research for sorting of Copper porphyry ores.

Chapter 2: Laser Induced Breakdown Spectroscopy Background

2.1 What is LIBS?

LIBS (Laser Induced Breakdown Spectroscopy) is an optical spectrochemical method based on spontaneous emission (DAGDIGIAN) that utilizes an intense laser pulse to determine the elemental composition of a sample. LIBS uses high temperature micro-plasma read by a lens according to a determined time frame. The time frame consists of a 1.5 nanosecond pulse, followed by 10 microseconds of energy dissipation.

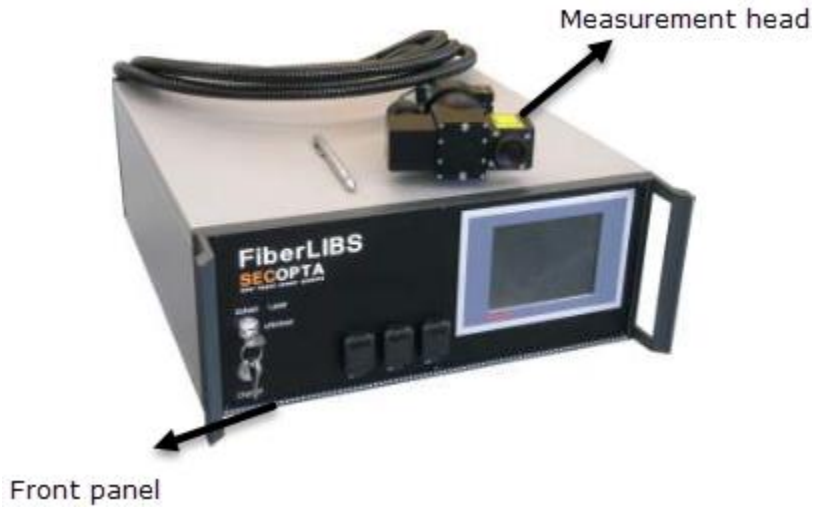

Figure 2-1: LIBS machine used for this experiment: a FiberLIBS model (SECOPTA)

Figure 2-1 shows an image of the LIBS machine that was used for this research project. LIBS emits a laser beam through the measurement head. This laser beam creates a plasmatic formation at the surface of a sample. Once an electrical breakdown is created by the laser in the plasma, LIBS detects the photon movement of the spontaneous emission through a spectrometer and a detector. A detector for LIBS consists of a Charge-Couple Device (CCD) that receives image information from the spectrometer and transforms it into a digital signal. The photon movement

describes the wavelength, which is unique for every ionization stage of an element. This wavelength allows LIBS and the computer to identify the elements in a sample, or elements in specific rock samples in an operation.

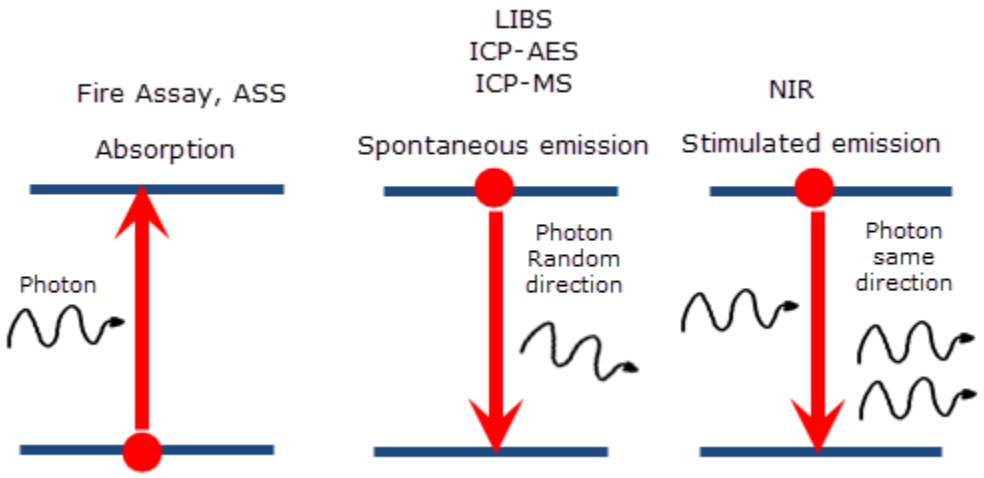

Figure 2-2: Spectrochemical methods for the currently most used sample analysis methods in mining

The current techniques for sample analysis use similar optical spectrochemical methods to those used by LIBS. Figure 2-2 shows the more popular methods for spectrochemical analysis used in mining. This thesis research project bases its calibrations and comparison analysis on Inductively Coupled Plasma – Atomic Emission Spectroscopy (ICP-AES) and Inductively Couple Plasma – Mass Spectroscopy (ICP-MS) Certified Analysis.

The most common type of analysis of Fire Assay beads is either Atomic Absorption Spectroscopy (ASS) or ICP-MS. The method used to determine the Cu content from the samples was by Aqua Regia digestion and ICP-AES.

2.2 Wavelengths

LIBS photon excitation has a random direction that is captured by the lens in the measurement head. LIBS produces a visible spectrum of light that can be seen in ambient conditions. The wavelength is separated by diffraction grating.

The grating is used to diffract the light source generated by the photon excitation that is read by the lens. The grating diffracts the light source into different colours that are calibrated to provide a signal for a determined wavelength. This wavelength bandwidth is processed by a photodiode that calculates the intensity for the different wavelengths.

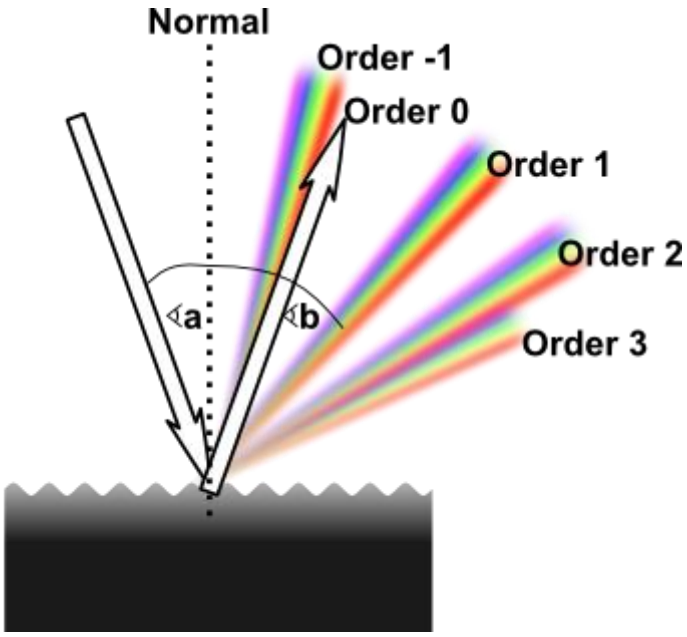

Figure 2-3: Diffraction grating schematic (Fleischer)

LIBS provides factory specifications for wavelengths. The LIBS machine used in this research is a SECOPTA FiberLIBS unit with wavelengths from 2.29*10^-7 to 5*10^-7 m. Different commercial LIBS machines can observe and process wavelengths from approximately 50 nm up to 2000 nm. One characteristic aspect of LIBS wavelengths is that LIBS does not use ionizing radiation as do the XRF and Prompt Gamma methods.

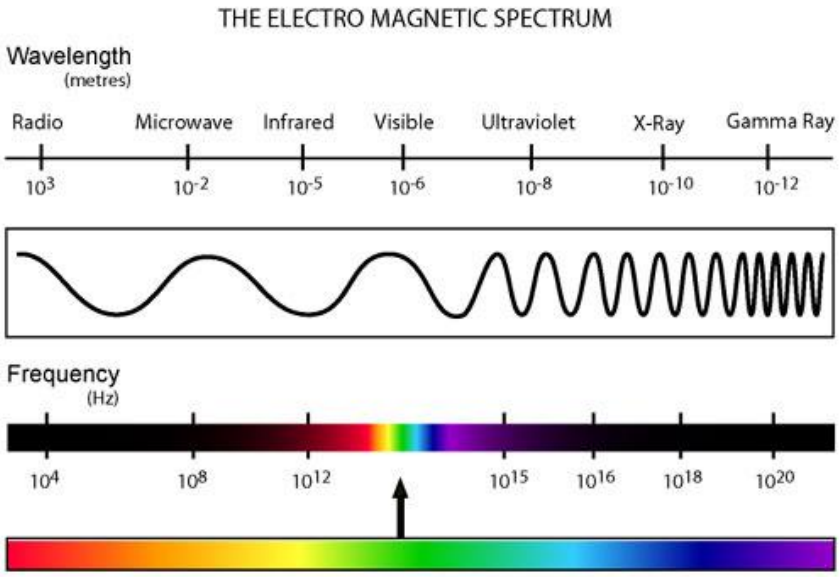

Figure 2-4: Electromagnetic spectrum for light sources (Cyberphysics group)

2.3 Apparatus Fundamentals

Figure 2-5 shows the basic schematic of a LIBS machine. The computer sends a signal to the laser to emit the light beam over the rock sample, resulting in the vaporization of the sample, which is also known as ablation. Once emitted, the optical spectrometer reads the intensity of light as a function of wavelength. A spectrometer consists of a combination of a monochromator and a detector (CCD). There are two types of monochromators: a) Bunsen prism, and b) Czerney-Turner.

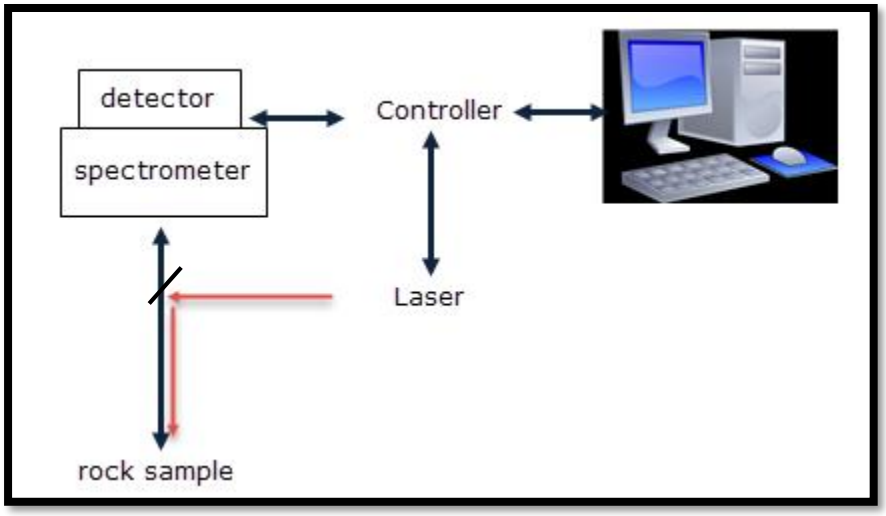

Figure 2-5: Basic schematic of a LIBS machine

LIBS uses the Czerney-Turner monochromator, which is capable of reading wavelengths from 190 to 1000 nm. Optical resolution ranges from a pixel size of 0.05 to 1 nm as part of the spectrometer features. However, the optical resolution, as defined for FiberLIBS, varies from 0.135 nm to 0.15 nm. The FiberLIBS machine used in this research has 2048 pixels with wavelengths from 229.21 to 499.58 nm.

Table 2-1: Specification of FiberLIBS for its spectrometer

Spectrometer	1 or 2 thermal stabilized Czerny-Turner spectrometers
	Wavelength range:190-1000 nm
	Optical Resolution: 0.05 - 1 nm (depending on application)

The monochromator, or spectrometer, acts as a photodiode array that receives the light source diffracted by the grating. The lens works with a slit in the measurement head, allowing the lens to capture only one part of the plasmatic formation that occurs after the ablation of the surface of the rock sample. The laser beam created out of the ablation and radiative flux goes through the slit and reflects on concave mirrors to reflect over the grating, and then once again

over another concave mirror. This effect allows the light beam to be diffracted, as shown in Figure 2-6.

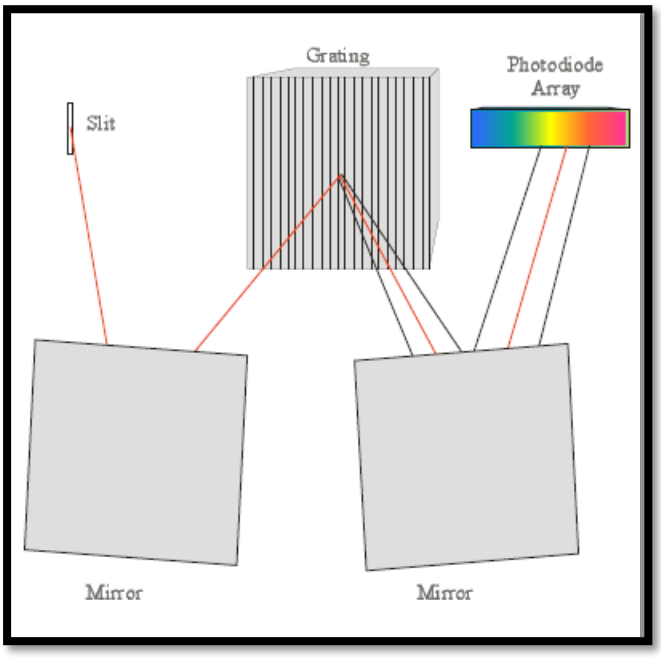

Figure 2-6: Schematic of LIBS spectrometer (Rehse)

2.4 Importance of the Diffraction Grating

2.4.1 Young's Double Slit example

In order to explain the importance of the grating in the LIBS apparatus, it is necessary to define how the spectrum is generated. A simple way to explain the functionality of LIBS from a physics perspective is through an understanding of Young's Double Slit experiment. Young's Double Slit experiment can be performed with a laser pen and 3 pencil leads. Three leads are held parallel so that two slits are created on either side of the center lead. The laser pen has to light through 2 slits created by the 3 pencil leads that are held parallel to each other, and reflected on a wall. The diffraction of the laser pen will result in the laser beam multiplying the reflected light on the wall with a high intensity in the center, and a lower intensity as it gets farther from the center.

The same principle is at play with the LIBS machine. The effect of the grating is similar to that which occurs in Young's Double Slit experiment. As seen in Figure 2-7, the light sources pass through two slits. The interaction of the waves creates both constructive and destructive harmonics. The central $\Delta x = 0$ has a complete constructive harmonic and defines the higher intensity peak in the spectrum. The location of this point can be found by following the center of the two waves exactly in the middle of the 2 wavelets. When $\Delta x = 0.5\lambda$, the superposition of the waves is destructive. The next harmonic $\Delta x = \lambda$ already has the destructive effect and the intensity is lower than $\Delta x = 0$. After the third harmonic, the signal to noise ratio is too high and is no longer considered efficient. This spectrum is the main indicator of efficiency in the Czerney-Turner monochromator. The spectroscope spectrum reflects the intensity of light that is read by the detector as intensity, and the intensity is calibrated in order to calculate the concentration of the photon excited by the light source.

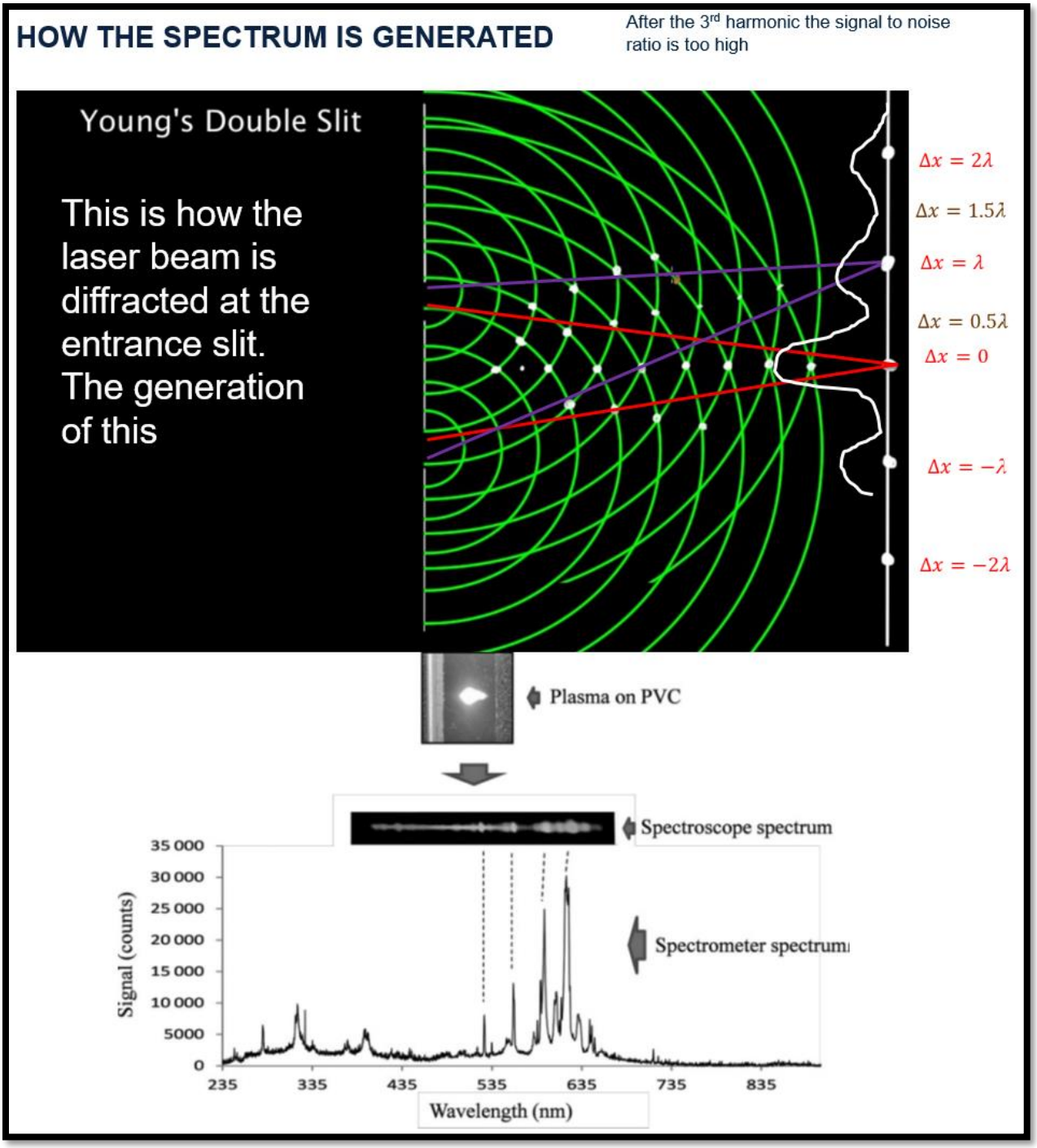

Figure 2-7: How the spectrum is generated in LIBS (Cremers and Radziemski)

2.4.2 Diffraction grating calculation

Even though the design of the LIBS machine is not part of the ore sorting analysis, it is important to have a full understanding of the internal specifications of the LIBS machine. This is important in order to hold control over the quality of the responses and the concentrations measured as outputs of the spectrum. The equation for the incident angle of the light beam over the grating is shown in Figure 2-8. The incident light is reflected over the grating with "d" as the spacing between slits, "α" as the incident light beam and "β" as the diffracted light beam.

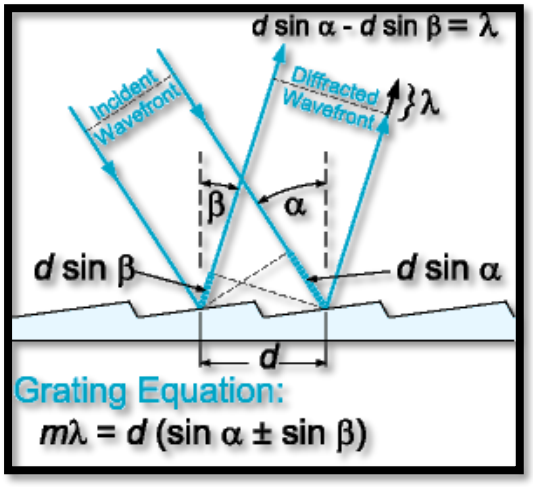

Figure 2-8: Incident light beam over a grating (Ryer)

Table 2-2: Specifications for average spectrometers used in the construction of LIBS sensors

Spectrometer	
Type	Czerny-Turner
Bandwidth	190 to 800 nm
Grating	2400 l/mm & 600 l/mm
Resolution	2 angstroms
Coverage	65 nm

"m" in Figure 2-8 or "n" in the equation below is the harmonic. For this example, the calculation uses data from the TRACER™ 2100 Laser Element Analyzer, a grating slit of 2000 lines per millimeter (l/mm), an incident angle of 48 degrees and a diffracted (or refractive "r") angle of 20 degrees.

$$n\lambda = d[sen(i) + sen(r)]$$

$$d = \frac{1mm}{2000l/mm} * 10^6 \frac{nm}{mm} = 500 \frac{nm}{l}$$

$$\lambda = \frac{500}{n = 1} nm(sen(48) + sen(20) = 548.58nm$$

"d" is transformed to nm/l units and λ is calculated for the first harmonic. Table 2-3 shows the calculation for the harmonic with varying refracted angles.

Table 2-3: Harmonic calculation for the grating

	n		
r	**1**	**2**	**3**
20	542.58	271.29	180.86
10	458.40	229.20	152.80
0	371.57	185.79	123.86
-10	284.75	142.37	94.92
-20	200.56	100.28	66.85

Table 2-3 shows that for a given wavelength of 500 nm of the laser beam and a spacing of 2000 l/nm, the harmonics has an effective bandwidth from 180 to 540 nm. Also, the table suggests that readings in the range of 180 to 270 nm will be less responsive or noisy in terms of the spectrum

because these wavelengths belong to the second or third harmonic. As explained through Young's Double Slit experiment, these harmonics are less intense and slightly noisier. It is not recommended to work with harmonic values greater than 3 because the spectrum becomes too noisy to give a good reading.

2.5 LIBS machine specifications

The LIBS machine used for this research work is the FiberLIBS from Secopta. The basic specifications for its laser are provided in Table 2-4. LIBS machines have ranges from 1 mJ to 10 mJ of pulse energy. This machine has a frequency of 100 Hz as a pulse rate, meaning that it is capable of taking 100 readings in 1 second.

Table 2-4: Laser specification for FiberLIBS

Laser	
Wavelength	1064nm
Pulse energy	3 mJ
Peak power	2 MW
Max pulse rate	100 pulse per second
Pulse width	1.5 ns

Table 2-5: Spectrometer specification for FiberLIBS

Spectrometer	
Type	Czerny-Turner
Bandwidth	229 to 500 nm
Grating	1200 l/mm
Resolution FWHM	0.18-0.22
Entry slit	10 um

The spectrometer for FiberLIBS has a10 micron entry slit and a bandwidth of 229.21 to 499.58 nm. The resolution of a peak varies from 0.135 nm to 0.15 nm, which is described by the Resolution Full Width at Half Maximum (FWHM). This term shows the half power point resolution for the peak.

2.6 White colouring problem

LIBS has difficulty reading white surfaces since white surfaces are more likely to reflect the laser beam rather than absorb the light energy and as a result a good spectrum is not generated by the LIBS machine. If the laser is reflected and not absorbed, then the plasma formation and ablation will not produce enough breakdown of the photon to reproduce the desired spectrum in order to identify elements and measure concentrations. The reason for the reflectance of the laser beam or any other light source is that molecules and atoms of white surfaces do not absorb any of the visible colours of light, while other colours do absorb the light.

Current industrial laser cutters use intense power to cut steel accurately. It is a common practice with this technology to paint the surface black prior to the cutting procedure as the black surface improves the effectiveness of the laser. At the very least, the surface must have a dark colouration in order to allow the molecules and atoms on the surface to absorb the energy so that the material could be cut successfully.

The Kirchhoff rules of spectroscopy indicate that a good reflective material is a poor absorber, while a good absorber is a good re-emitter. This means that if LIBS reads a material that reflects the light spectrum, then the amount of energy absorbed will be low. If not enough energy is captured by the surface of a rock material, then LIBS won’t be able to create the plasma formation and subsequently, readings will be noisy and of poor spectrum quality.

Chapter 3: Experimental Approach

A key goal of this research project is to develop a sensor that is capable of collecting data from elements that are not traceable with XRF and HFEMS. The objectives of this program are to develop and demonstrate the effectiveness of the LIBS system in characterizing Copper porphyry ore, to test and analyze the repeatability of the bench scale LIBS system, and to demonstrate the efficiency of the LIBS system for Copper ore. In particular, there was a desire to explore the applications of LIBS in discriminating Oxides vs. Sulphides, where XRF has been shown to be ineffective.

Although current XRF sensors at Minesense Ltd. (the sponsor company for this research) are similar to the LIBS sensor, the physical-chemical analysis conducted by both systems is significantly different. In XRF sensors, the X-ray process involves the electromagnetic radiation of a short wave produced by the deceleration of electrons (Skoog y Leary). In contrast, LIBS involves plasma formation as a result of an intense laser pulse of a high-temperature followed by the process of optical spectroscopy. LIBS is considered by many material manufacturers as the new option for sensing alloy properties that XRF is not capable of accomplishing. This relegates the XRF to the position of a proven technology that nevertheless is limited in certain areas. However, no real research has been conducted regarding the use of LIBS responses in correlations for ore sorting sensors.

One of the improvements with respect to material recognition in which LIBS is superior to XRF is the lack of radiation passing over the work area. Current technology has improved significantly, and has evolved to the point where portable LIBS systems have been developed for use as hand tools. For this reason, the topic of radiation is an important one to consider.

This chapter highlights the details of the experiment that was performed for this research, as well as the challenges involved in developing a LIBS sensor for sorting ore.

3.1 Experimental design

The experiment was divided in 2 parts:

1. Project initiation: LIBS identification and calibration
2. LIBS correlation

3.1.1 Project Initiation: LIBS Identification and Calibration

The rock samples for this research were taken from ore deposits from the Escondida Mine, in Chile. Escondida is a Copper mine in the Atacama Desert.

Figure 3-1: Escondida Mine samples. Left: sample #26 Oxide sample, Right: sample #12 Sulphide sample

This research used forty-one samples from the Oxide ores, 38 samples from the Sulphide ores, and 1 chipped sample of the Sulphide ore was not ultimately used in this research.

One of the characteristics of LIBS is that it does not require any sample preparation. This research therefore took an “as-is” approach regarding the rock samples that were taken from the mine site and as such, they were not washed, polished, or cut.

The samples were weighed, and then scanned by the LIBS machine. The samples were read with the LIBS on 4 faces of the rock, and 10 readings were taken per face. In the initial phases of experimentation and trial, readings were taken randomly, usually at the default value of 100 readings per shot. One of the most time-consuming tasks during this stage was to solve the white colouring problem with respect to the Sulphide rock samples.

Upon the completion of this stage, the experiment was focused on the identification and characterization of the rock samples. To identify the rocks, it was important to have a valid reference regarding the wavelength and spectroscopy observed in the LIBS spectrums. In order to understand the behaviour of the LIBS system, it was necessary to shoot over the known surfaces, such as the pure Copper or steel layers, in order to start developing an understanding regarding how the literature and online references matched the reality of the LIBS spectrum.

Finally, the construction of a Python Script was initiated in order to transform the spectrum information into a readable format. The development of the initial script was attempted in MATLAB, but as a result of the amount of information processed, and the continuous data coming from LIBS, it was decided to migrate the data and algorithms to Python. Several techniques from the computer sciences, data analysis, and liner programming were applied into this construction in conjunction with the basics of physical chemistry.

3.2 Geology and Geochemistry of Escondida Mine Rocks for Correlation

Escondida Mine is a Copper porphyry deposit that is located in the north of Chile, and is one of the largest mining operations in the world. It belongs to a big supergene Copper deposit morpho-techtonic with the intervention of shallow gravel-filled basins.

The mineralogy groups are as follows:

1. Hypogene Sulphides
2. Supergene sulfides
3. Copper Oxides

In order to decide which Mineralogy group should be accepted into the equation, Table 3-1 was developed to provide detailed information about each mineral, or type of rock expected from every geological region (Ruben Padilla Garza). This table consolidates information from a variety of reference sources, but has a strong focus on "Geology of the Escondida Porphyry Copper Deposit, Antofagasta Region, Chile" (Ruben Padilla Garza). Mineralogical references are very important at this stage in order to create associations between the elements and minerals. Although no direct mineral association can be made here because LIBS is not able to identify minerals directly, we can create associations between the elements and the ion responses.

Table 3-1: Summary of Mineralogy of Escondida Mine by Mineralogical Groups and Elements

Mineralogical group	Mineral/Rock	Elements								
Advanced Argillic Alteration	Pyrite	Fe	S							
	Bornite	Cu	Fe	S						
	Chalcopyrite	Cu	Fe	S						
	Sulfides	S								
	Covellite	Cu	S							
	Enargite	Cu	As	S						
	Chalcocite	Cu	S							

Mineralogical Group	Mineral/Rock	Elements								
	Galena	Pb	S							
	Sphalerite	Zn	Fe	S						
	Alunite	K	Al	S	O	H				
Quartz-Sericite	Quartz	Si	O							
	Sericite	Na	Al	Si	O	H				
	Chalcopyrite	Cu	Fe	S						
	Pyrite	Fe	S							
	Molybdenite	Mo	S							
Sericite-Chlorite	Chalcopyrite	Cu	Fe	S						
	Pyrite	Fe	S							
	Molybdenite	Mo	S							
Biotitic	Biotite	K	Mg	Fe	Al	Si	O	H	F	
	Chlorite	Mg	Fe	Ni	Mn	Al	Si	O	H	Cl
Potassic Alteration k-feldspar	Biotite	K	Mg	Fe	Al	Si	O	H	F	
	Anhydrite	Ca	S	O						
	Chalcopyrite	Cu	Fe	S						
	Bornite	Cu	Fe	S						
	Orthoclase	K	Al	Si	O					
Potassic Alteration Biotitic	Biotite	K	Mg	Fe	Al	Si	O	H	F	
	Magnetite	Fe	O							
	Bornite	Cu	Fe	S						
	Chalcopyrite	Cu	Fe	S						
Propylitic Alteration	Calcite	Ca	C	O						
	Chalcopyrite	Cu	Fe	S						
	Grossular	Ca	Al	Si	O					
	Chlorite	Mg	Fe	Ni	Mn	Al	Si	O	H	Cl
	Epidote	Ca	Al	Fe	Si	O	H			
Sulfide enrichment blanket	Chalcocite	Cu	S							
	Andesite	Si	O							
	Atacamite	Cu	Cl	O	H					
The best Copper grades of the supergene zone	Covellite	Cu	S							
	Digenite	Cu	S							
	Idaite	Cu	Fe	S						
	Pyrite	Fe	S							
Leached capping zone	Limonite	Fe	O	H						
	Hematite	Fe	O							
	Covellite	Cu	S							
Copper Oxides	Brochantite	Cu	H	S	O					
	Antlerite	Cu	S	O	H					

Elements
Al
As
C
Ca
Cl
Cu
F
Fe
H
K
Mg
Mn
Mo
Na
Ni
O
Pb
S
Si
Zn

Mineralogical Group	Mineral/Rock	Elements								
	Atacamite	Cu	Cl	O	H					
	Chrysocolla	Cu	Al	Si	H	O				
	Tenorite	Cu	O							
	Chlorite	Mg	Fe	Ni	Mn	Al	Si	O	H	Cl
	Sericite	Na	Al	Si	O	H				
	Andesite	Si	O							

3.3 LIBS correlation

To use LIBS as a measuring device, the quality of the response relies on the limits of detection, the concentration calibration that is based on the analysis of pure samples (Cremers and Radziemski). At its core, this research investigates another method through which to develop correlations with respect to the LIBS spectrum. This in turn makes a difference with respect to other LIBS research projects. It was not the intention of this project, however, to develop LIBS' capabilities in accurately calculating the grade of a rock because this is not the purpose of an ore sorting sensor.

The technical capabilities of LIBS can be seen with respect to LIBS' ability to function as an ore sorting sensor. It is necessary to define which elements can be identified, and compare these to a certified analysis. The technical capabilities represent the basic resources through which to build correlations from the responses to the target element, Cu content, for this project.

From this perspective, this section of the research was focused on:

1. Completing the identification of wavelengths for the elements.
2. Comparing the readings of the elements obtained from LIBS with the readings of the elements obtained from the Certified ICP analysis.
3. Developing a logical thought process regarding to how the spectrums can be processed with the tools and resources available.

4. Application of several types of regression analysis in a trial and error scheme to develop correlations.
5. Validation of the data.

3.4 Main problems expected when using LIBS as an ore sorter

While attempting to record LIBS spectra, two measurement challenges were encountered. Firstly, it was difficult to obtain good quality spectrum from white surfaces and secondly how to assess LIBS for sorting applications as compared to sample analysis.

3.4.1 White colouring problem solution approach

Initially, LIBS was expected to be able to read any surface or rock sample. As explained in section 2.6, the white colour on a surface stops the absorption of the energy of a laser beam because white colours reflect the light. After the initiation of the project, several samples were used in experimentation, including white rocks that belonged to the categories of Escondida Sulphides and “mixto” ore (Spanish word for “mixed” that refers to the geological interaction zone between Oxide and Sulphide ores). The initial reading process using LIBS was to place the measurement head in a static position at the indicated distance provided by the manufacturer. The white samples could not be read for several weeks. The problem was solved by taking the measurement head and moving it along the surface. It was an unexpected solution that may be related to the Interaction of Light with Matter Theory and the low absorption capabilities of white minerals, as explained in section 2.6.

3.4.2 Spectrum analysis

One of the key problems to solve involved how to train LIBS as an ore sorting sensor rather than a laboratory measurement device. In contrast to in the laboratory, in mining, bulk material handling systems using either in a shovel or a belt conveyor will not allow the operation to stop in order to read one rock several times at the exact same spot. As such, it was necessary to develop a reliable method that was capable of reading data instantly, and that did not involve repetitive readings. Even though a moving rock can be hit twice, or even several times, it is very unlikely that it will be hit in the exact same point in subsequent hits.

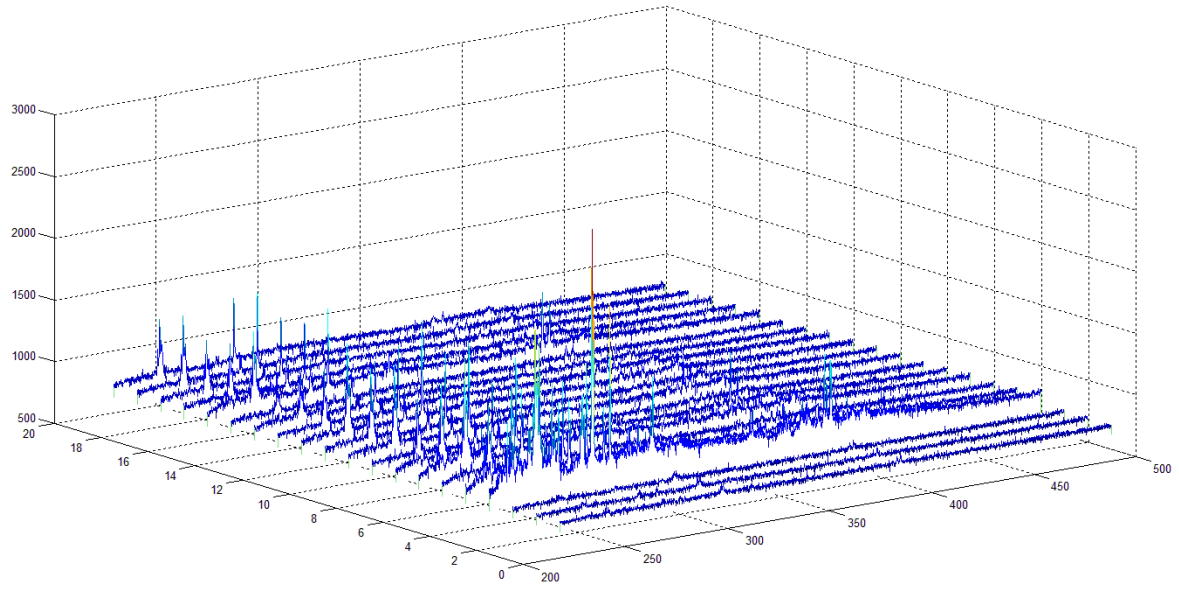

Figure 3-2: Twenty readings of Silica/Oxide sample spectrum from Escondida mine

Figure 3-2 provides evidence that the spectrum can vary due to impurities or to the white colouration effect. The first three peaks differ from the fourth peak; and after the fifth reading, the spectrum develops stability. The peak in red is likely to be a bad reading, and LIBS has the option to average all peaks to avoid this variation in the spectrum. However, a LIBS sensor for ore sorting

cannot focus on the same point over several milliseconds which is required to average several peaks.

For this reason, it was necessary to build an algorithm or computer script to reveal which peaks should, and should not, be used. The development of this script was based on statistics and basic methods in Artificial Intelligence. This script evolved according to the needs of the project's changing parameters, as will be explained later.

3.5 Sulphide samples difficult to read with LIBS

The Sulphide samples were difficult to be read with the LIBS sensor because of the white colouration of the rocks. As shown in Figure 3-3 and Figure 3-4, several attempts were made to obtain responses from the LIBS machine. The rocks were placed both horizontally and vertically, measuring the respective mirror's effective focal lengths, as described in the machine's manual.

Figure 3-3: LIBS reading Sulphide samples from the top

Figure 3-4: LIBS reading Sulphide samples from the side

Figures 3-3 and 3-4 shows the laser beam shooting the rock samples at different positions. The structure that holds the laser measurement head kept the laser beam perpendicular with respect to the rock surface. Even though several angles were attempted, problems came up while taking the readings. Figure 3-5 illustrates the LIBS computer screen as data is being collected while LIBS is working. “Mat.” stands for the type of material, and consists of input information that is not relevant for our correlation. “Sampl.” is the sample number for the current set of readings, e.g. 4 samples were taken with 10 readings per sample. For the last example, the number of readings requested by the LIBS operator is reflected in “spectra.” “Now” indicates the current number of readings obtained until that moment. Finally, “del” shows the number of samples deleted because they did not fit the LIBS machine default threshold. As seen, there are 7896 samples deleted, and only 1 that was accepted. When the machine ran for several minutes, if the number of readings requested were not obtained, it automatically stopped the reading.

Figure 3-5: LIBS computer screen for Sulphide samples

Figure 3-6: LIBS computer screen for Sulphide sample #14

This difficulty in reading the samples will prove to be a serious problem if the LIBS sensor reaches the stage of proof of concept. As such, it is likely that some of the data for the Sulphide samples is not as reliable as it is for the Oxide samples, which do not show the white colouring. Good data is obtained, but over longer periods of times, and this data does not depend on the length of exposure of the laser to the rock surface, as with the XRF sensors. Rather, obtaining reliable data depends on how much power the laser beam emits while not being interrupted by the light reflection. Figure 3-6 indicates that although good spectrums are being obtained, it takes relatively long to acquire the data. As seen within Table 3-6, 10 readings were obtained after deleting 50283. If the sensor has a frequency of 100 Hz, then the 10 readings took 60 seconds instead of 0.1 seconds.

3.6 Identification of Wavelength List

The wavelength list identifies the characteristic wavelength of a particular ion of an element from the periodic table. In order to create this wavelength list, certain parameters, which will be discussed later, were taken into account. Figure 3-7 shows the spectrum of a pure Copper layer sample. The peaks can be recognized by matching the wavelength from the x-axis with the ID wavelength proposed in Table 3-5. This ID wavelength acts as a primary key for the identification of elements in the Python Script that is described in section 3.7, and attached in Appendix C .

To build a table for the identification of wavelengths, data was acquired from the National Institute of Standards and Technology (NIST) database (Laboratory). The selection regarding the ID wavelength is based on the likelihood and certainty of finding the ionization stage in that

particular wavelength. For this reason, the main parameter for quantifying this likelihood is the Aki, which is the transition probability, also known as the Einstein Coefficient.

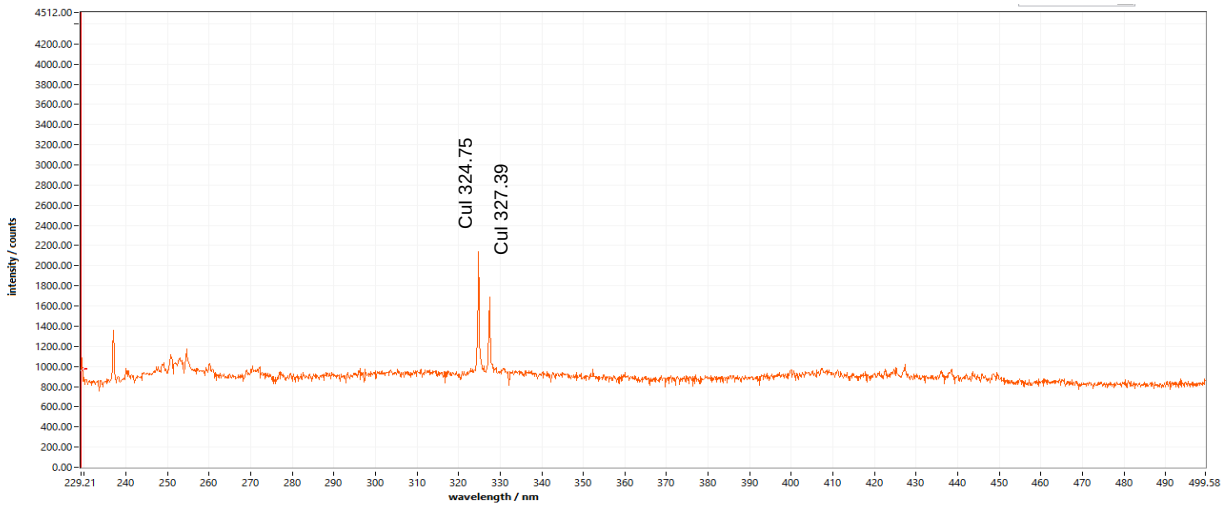

Figure 3-7: Spectrum of pure Copper layer sample showing the characteristic peaks at 324.75 and 327.39 for Cu I

Furthermore, Aki is the emission transition probability of the ion stage excited to move to another ionization stage, and which has been excited by the LIBS laser. Another element related to the likelihood of this transition is the Absorption Oscillator Strength (f_{ik}), also known as the f-value. However, the Aki is directly proportional to the f-value, and because of this, it is redundant to analyze the f-value as well.

It was very important to have certainty with respect to the readings. The best indicator is the Accuracy (Acc.). Accuracy can be understood as a rating for the likelihood that a transition of the ionization stage takes place. David A. Cremers defines it as*: "how close a measurement result is to the "true" value of the property measured"* (Cremers and Radziemski). The likelihood is measured in the NIST database following the pattern shown in Table 3-2. Relevant information was retrieved from the NIST website (National Institute of Standards and Technology NIST).

Table 3-2: Accuracy for transition strength

AAA	≤	0.30%
AA	≤	1%
A+	≤	2%
A	≤	3%
B+	≤	7%
B	≤	10%
C+	≤	18%
C	≤	25%
D+	≤	40%
D	≤	50%
E	>	50%.

Table 3-3 shows a proposed set of values for each accuracy rating in order to quantify the accuracies, and include them with the Relative Intensity. The weighting factors were created for this project as a tool through which to provide significance to the values with higher Acc. ratings. The logic used was to provide a maximum of 400 for an Acc. of 400. Subsequently, decrease 50 units to the next lower levels of Acc. The sequence was intended to end at D+ where the accuracy is not significant for the selection of wavelengths.

Table 3-3: Weighting factors

AAA	400
AA	350
A+	300
A	250
B+	200
B	150
C+	100
C	50
D+	1
D	1
E	1
	1

This pattern was created in order to quantify the Acc. rating into numbers, and to highlight the elements that are likely to be seen in the spectrum. The relative Intensity number (14000) in Table 3-4 has been multiplied by the Acc. values from Table 3-3 (150). This value is shown in the column titled "Weighted Relative Intensity in Table 3-4. The final Weighted Relative Intensity is 2100000 is used to sort the higher values for Weighted Relative Intensity, and depends on likelihood and the intensity. The final proposed pattern for the ID wavelength is presented in Table 3-5 below.

Table 3-4: Example of the database and the classifications of the ratings

Ion	Observed Wavelength Air (nm)	Ritz Wavelength Air (nm)	Acc.	Rel. Int. number	Weighted Rel. Intensity
Ca III	289.9785	289.9785	B	14000	2100000
Ca III	337.2671	337.2679	B	10000	1500000
Ca III	292.4326	292.4331	B	7000	1050000

Table 3-5 was included in the Ritz Wavelength. The main difference between the observed wavelength and the Ritz wavelength is that the Ritz is a calculated wavelength, while the Observed Wavelength refers to the results of experiments. Most of the Observed Wavelengths have been tracked and repeatedly found from different experiments. NIST provides detailed information about the wavelengths. A Python Script was developed for the purposes of this research. Observed wavelength is being used here unless only a Ritz Wavelength is available. Although it is suggested to use the Observed Wavelength, the Ritz wavelength provides critical information in Chapter 6: with respect to the discrimination of Oxides and Sulphides. For this reason, it is important to include this value as part of the input for the Python Script.

Table 3-5: ID Wavelength proposed for the LIBS machine used in this research

Ion	Observed Wavelength Air (nm)	Ritz Wavelength Air	Acc.	Rel. Int. number	Aki
Ag II	232.02	232.02	B	730000	2.9E+08
Ag II	241.32	241.32	B+	470000	2.1E+08
Al II	281.62	281.62	A	4000	3.6E+08
As I	234.98			350	3.1E+08
Au I	267.60	267.59		3400	1.6E+08
Au I	242.80	242.79		2600	2E+08
Ba I	350.11	350.11	B	860	3.5E+07
Ba II	455.40	455.40	B	9300	1.1E+08
Be II	272.89	272.89	AA	310	3.2E+07
Be II	482.82	482.81	A	710	7870000
Be III	448.73	448.70	AAA	100	2.1E+08
Bi I	289.80	289.79		4000	1.5E+08
Bi I	306.77	306.77		9000	1.7E+08
Br I	447.77			20000	1300000
C I	247.86	247.86	C+	800	2.8E+07
C II	283.67	283.67	B+	1000	3.3E+07
C III	229.69	229.69	A+	800	1.4E+08
Ca I	422.67	422.67	B+	50	2.2E+08
Ca II	317.93	317.93	C	180	3.6E+08
Ca III	289.98	289.98	B	14000	2.5E+08
Cd II	274.85			1000	2.8E+08
Cl II	479.46	479.46	C	99000	1E+08
Cl II	481.01	481.01	C	29000	9.9E+07
Co I	347.40	347.40	B	8000	5.6E+07
Co II	258.03	258.03	B+	210000	2.1E+08
Co II	237.86	237.86	B+	140000	1.9E+08
Cr I	427.48	427.48	B	2500	3.1E+07
Cr I	425.44	425.43	B	2480	3.2E+07
Cu I	324.75	324.75	AA	10000	1.4E+08
Cu I	327.40	327.40	AA	10000	1.4E+08
Cu II	271.35			700	6.8E+07
F II	350.56	350.56	C	220	2.9E+08
Fe I	374.95	374.95	A	1150000	7.6E+07
Fe II	234.35	234.35	A+	1000000	1.7E+08
Fe II	238.20	238.20	B+	1800000	3.1E+08
Ga I	294.36	294.36			1.3E+08
Ge I	265.12	265.12			2E+08
Hf I	368.22	368.22		2200	2.6E+07
Hg II	284.77	284.77		3500000	3E+08
In II	294.10	294.10	B	9600	3.4E+08
Ir I	269.42	269.42		3000	4.8E+07
Mg I	285.21	285.21	A	50	4.9E+08
Mg II	279.55	279.55	A+	13	4.8E+08
Mg III	239.51	239.52	A	20	1.7E+08
Mn I	279.83	279.83	C	5100	3.6E+08

Ion	Observed Wavelength Air (nm)	Ritz Wavelength Air (nm)	Acc.	Rel. Int. number	Aki
Mn II	261.02	261.02	C	10000	3E+08
Mo VI	329.33	329.33		30000	7.2E+08
Mo VI	338.70	338.70		50000	4.5E+08
N II	399.50	399.50	A	1000	1.2E+08
N IV	347.87	347.87	B	570	1.1E+08
Na II	298.42	298.42	B	1300	1.7E+07
Na II	307.83	307.83	A	550	1.2E+08
Ni I	349.30	349.30	C+	5500	9.8E+07
Ni I	341.48	341.48	C	8200	5.5E+07
O V	278.10	278.10	B	1000	1.4E+08
O III	245.50	245.50	B	200	3.4E+08
O III	393.48	393.48	C+		9.93E+07
P IV	334.77	334.77	C+	650	2.1E+08
P I	253.56	253.56	C	950	9.5E+07
Pb I	283.31	283.31		35000	5.8E+07
Pb I	280.20	280.19		25000	1.6E+08
Pd I	340.46	340.46		24000	1.3E+08
Rh I	369.24	369.24		9400	9.1E+07
Ru I	372.80	372.80		11000	8.2E+07
S VI	420.08	420.08	AA	50	4.8E+07
S VI	419.89	419.89	AA	120	2.9E+08
Sb I	231.15	231.15		2500	1.7E+08
Sc III	273.40	273.40	D	230	3.3E+08
Sc III	269.91	269.91	C	350	3.4E+08
Si I	288.16	288.16	B	1000	2.2E+08
Si II	413.09	413.09	B	500	1.7E+08
Sn II	328.31	328.31	B+	15000	1.7E+08
Sn II	335.20	335.20	B+	13000	1.8E+08
Ta I	362.66			980	7100000
Te I	238.58	238.58		1200000	8.1E+07
Ti I	399.86	399.86	A	10000	4.8E+07
Ti II	376.13	376.13	A	11900	1.2E+08
Ti III	251.61	251.60	D	25	3.4E+08
Tl I	276.79	276.79		4400	1.3E+08
Tl I	351.92	351.92		20000	1.2E+08
V I	411.18	411.18	B	8900	1E+08
V II	292.40	292.40	B	2400	1.7E+08
W I	400.88	400.87	B	1000	1.6E+07
W II	248.92	248.92	B	422	7E+07
Y I	410.24			1800	1.3E+08
Y II	371.03			13000	1.5E+08
Zn I	334.50			800	1.7E+08
Zn II	491.16			800	1.6E+08
Zr III	266.43	266.43		5000000	3.2E+08
Zr III	262.06	262.06		10000000	3.9E+08

3.7 The Python Script

The Python Script is attached in Appendix C . This script uses the ID Wavelength file and the spectrum data from LIBS as input. An extraction of this file is shown in Table 3-6. This table contains the wavelength from 229.21 to 499.58 nm in the columns, and shows each rock sample (Su1), the shot number (S1) and the reading number (1,2,3,…) in the rows.

The script starts with asking the sample wanted to be plotted, and the user has the option to select the spectrum to plot. The Python Script attempts to solve the problem of reading data that is not averaged because within the mining cycle, it is impossible to take several readings in 1 spot.

Table 3-6: Extraction of the spectrum data from LIBS

wavelength	Su1,S1,0	Su1,S1,1	Su1,S1,2	Su1,S1,3	Su1,S1,4	Su1,S1,5	Su1,S1,6	Su1,S1,7	Su1,S1,8
229.21	856	809	699	700	703	901	820	735	828
229.36	907	869	730	717	685	1011	854	766	909
229.5	856	815	705	694	721	943	826	763	844
229.65	756	733	691	723	690	795	745	694	738
229.79	806	749	685	699	731	810	743	725	775
229.94	786	770	737	692	701	822	770	729	766
230.08	759	722	677	674	668	745	719	701	730
230.22	784	785	708	723	704	797	767	721	762
230.37	776	778	685	725	725	795	748	741	763
230.51	763	756	710	711	699	745	751	720	765
230.66	753	751	682	704	712	759	733	714	739
230.8	689	737	710	669	692	732	735	688	723
230.95	766	734	712	675	682	756	731	678	739
231.09	750	747	710	736	724	753	732	690	695
231.24	759	742	713	703	707	726	741	714	732
231.38	736	745	705	698	720	713	700	713	725
231.53	744	726	725	704	698	762	723	724	727
231.67	703	753	696	697	715	744	731	715	729

Due to the heterogeneity of the geology and the constant movement of a belt conveyor or mining shovel, it was necessary to gather LIBS data that had previously been validated. In contrast to laboratory test work, samples in a production line cannot be taken apart for analysis because of the mining production cycle and the efficiency expected with respect to mining machinery. As

such, it was necessary to build data filters to simulate that which could be read in several readings in one static test, in only one reading, and in constant movement.

There are 3 filters proposed for validating the data without the need to average several readings over a static sample:

1. Minimum peak of 10 counts
2. Local maximum using the second derivate kernel smoother density at 1.0
3. A low pass filter analyzing the noise frequency using the Fast Fourier Transform (FFT)

3.8 Technical potential

Table 3-7 provides a summary of the 43 elements obtained from the responses of LIBS over the porphyry Copper samples from Escondida Mine. Table 3-7 has been constructed based on data that was collected, and is attached in Appendix A and Appendix F . This table indicates which elements LIBS has been able to detect based on wavelength identification. In contrast, Table 3-8 shows only the 26 elements that have been identified through LIBS and the ICP Certified Analysis for both Oxide and Sulphide samples of Escondida Mine.

Table 3-7: Technical potential summary

Ag	Cd	Hg	Ni	Sn	Zr
Al	Cl	In	O	Ta	Co
Au	Cr	Ir	P	Ti	Sc
Ba	Cu	Mg	Pb	Tl	
Be	F	Mn	Pd	V	
Bi	Fe	Mo	S	W	
C	Ga	N	Sb	Y	
Ca	Hf	Na	Si	Zn	

Table 3-8: Technical potential summary skewed by Certified ICP Analysis

Ag	Ca	Mg	Sb	Co

Al	Cd	Mn	Si	Sc
Au	Cr	Mo	Sn	
Ba	Cu	Na	Ti	
Be	Fe	Ni	Zn	
Bi	Hg	Pb	Zr	

3.9 The Pearson Correlation

The Pearson Correlation is a ratio or percentage of the dependence between 2 variables. This value is calculated by dividing the covariance by the partial standard deviations.

$$r = \frac{\sigma_{sy}}{S_x S_y}$$

Equation 1 Pearson Correlation Coefficient

This coefficient is used to measure the dependence of the Certified ICP Results and the LIBS responses.

3.10 Confidence level over technical potential

The identification of elements through LIBS is based on the likelihood of the occurrence of the transition of ionization stage. Wavelengths with possible false identification are summarized in this section. The main reason for this problem is the lack of an Identification of Wavelength set provided by the manufacturer of FiberLIBS, for that reason the wavelengths are vulnerable to error. Even when identified precisely, wavelengths can have error with respect to overlap (Cremers and Radziemski). As such, the best approach to verifying the wavelengths is through comparing them with the results of the Certified ICP analysis of the Oxide and Sulphide samples.

Table 3-9: Confidence levels for technical potential to detect elements

	ICP data			
	unit	Min	Max	Confidence
Ag II@232.02	ppm	<2	<2	Good
Ag II@241.32	ppm	<2	<2	Good
Al II@281.62	%	0.41	1.94	Good
Au I@242.8				Unknown
Ba II@455.4	ppm	<5	64	Good
Be II@272.89	ppm	<0.5	<0.5	Poor
Be III@448.73	ppm	<0.5	<0.5	Poor
Bi I@306.77	ppm	<5	<5	Poor
C I@247.86				Unknown
C III@229.69				Unknown
Ca I@422.67	%	<0.01	0.13	Good
Ca II@317.93	%	<0.01	0.13	Poor
Cd II@274.85	ppm	<11	<11	Poor
Cl II@481.01				Unknown
Co I@347.4	ppm	<1	47	Good
Cr I@427.48	ppm	<1	3	Poor
Cu I@324.75	ppm	393	25700	Very Good
Cu I@327.4	ppm	393	25700	Very Good
Cu II@271.35	ppm	393	25700	Poor
F II@350.56				Unknown
Fe I@374.95	%	0.07	8.31	Very Good
Fe II@234.35	%	0.07	8.31	Very Good
Fe II@238.2	%	0.07	8.31	Very Good
Ga I@294.36				Unknown
Hf I@368.22				Unknown
Hg II@284.77	ppm	<1	1	Poor
In II@294.1				Unknown
Ir I@269.42				Unknown
Mg I@285.21	%	0.01	0.51	Very Good
Mg II@279.55	%	0.01	0.51	Good
Mg III@239.51	%	0.01	0.51	Good
Mn I@279.83	ppm	6	296	Poor
Mn II@261.02	ppm	6	296	Poor
Mo VI@329.33	ppm	7	1830	Poor
Mo VI@338.7	ppm	7	1830	Poor

	ICP data			
	unit	Min	Max	Confidence
N IV@347.87				Unknown
N II@399.5				Unknown
Na II@298.42	%	0.03	0.11	Very Good
Na II@307.83	%	0.03	0.11	Good
Ni I@341.48	ppm	<1	10	Good
Ni I@349.3	ppm	<1	10	Poor
O III@393.48				Unknown
O V@278.1				Unknown
P I@253.56	%	<0.01	0.05	Good
P IV@334.77	%	<0.01	0.05	Good
Pb I@280.2	ppm	<2	154	Very Good
Pb I@283.31	ppm	<2	154	Good
Pd I@340.46				Unknown
S VI@419.89	%	0.08	4.48	Poor
S VI@420.08	%	0.08	4.48	Poor
Sb I@231.15	ppm	<5	<5	Poor
Sc III@269.91	ppm	<0.5	1.1	Good
Si I@288.16*	%	45.9	70	Very Good
Si II@413.09	%	45.9	70	Poor
Sn II@335.2	ppm	<10	<10	Poor
Ta I@362.66				Unknown
Ti I@399.86	%	<0.01	0.07	Good
Ti II@376.13	%	<0.01	0.07	Good
Ti III@251.61	%	<0.01	0.07	Good
Tl I@276.79				Unknown
Tl I@351.92				Unknown
V I@411.18	ppm	3	38	Poor
V II@292.4	ppm	3	38	Poor
W I@400.88	ppm	<10	<10	Good
W II@248.92	ppm	<10	<10	Good
Y II@371.03	ppm	<0.5	4.3	Unknown
Zn I@334.5	ppm	<1	207	Good
Zn II@491.16	ppm	<1	207	Good
Zr III@262.06	ppm	<0.5	1.5	Good
Zr III@266.43	ppm	<0.5	1.5	Very Good

* Si calculated based on SiO concentrations

Table 3-9 provides a summary of the confidence levels for the technical potential of the whole sample in providing a source of information with respect to choosing the ions for prediction equations. The confidence levels are classified as follows:

- Very good: Wavelengths with obvious correlation to those identified in the ICP
- Good: Wavelengths with some correlation to those identified in the ICP

- Poor: Wavelengths that are present in the LIBS responses, but no real correlation can be identified
- Unknown: Wavelengths seen in LIBS spectrum but not in the ICP

The values in this table define the limits for the identification of elements, and classify the elements as either belonging to the area of chemical analysis or to that of mining technology, the latter of which is the focus of this thesis.

Based on the approach that was used for this study, elements corresponding to wavelengths that have very low concentrations, as indicated by ICP, are likely to be falsely identified and therefore the wavelengths are likely represent a different element. However, the regression analysis indicated that the magnitude of the peak at this wavelength is significant, and therefore the unknown elements associated with the wavelength are considered significant.

For the purpose of this thesis and for ease of presentation, for the elements identified by the approaches used in this chapter, the element label is used to represent the wavelength.

Chapter 4: Analysis of Oxide Rock Samples with Laser Induced Breakdown Spectroscopy

The purpose of this research is to generate a response for a sensor using correlations between LIBS responses and Certified ICP assays, and not to measure the actual grades. One significant obstacle in developing a response from LIBS involves being able to generate repeatability with respect to the sensor. This is because the spot area that LIBS targets on the rock surface is 1 mm, which represents a statistically small sample size for classifying a much larger particle and rock sample. Rock samples of this research were in the size range of 3 to 5 cm. Following an idealization of a perfect spherical rock sample, the typical rock used had a surface area of 11,309 mm^2. This signifies that there is a chance of 0.008% (1 mm^2/ 11,309 mm^2) that LIBS is able to hit the same point on a rock sample.

Previous research has demonstrated that LIBS capabilities are superior in terms of accuracy to those of other techniques such as ICP-AES, therefore, as a system, LIBS is favoured (G. S. Senesi). LIBS has shown a higher degree of accuracy in a variety of studies, and has reached accuracies from 1.82% to 6.25% based on ICP-AES Certified Analysis as compared with prepared and homogenized rock samples from Phosphate mines (INEEL). One of the significant problems encountered however, is the small amount of area covered by the laser beam that takes the reading. The analysis of the samples starts with the compilation of the data taken from all of the samples and put into one data file. The LIBS data was processed through the use of a Python Script, as explained in Chapter 3:. Output data is shown in Appendix A .

A spectrum from the Oxide samples is shown in Figure 4-1. The spectrum was processed with the Python script proposed in Appendix C . The blue line belongs to the spectrum representing a

potential peak in the area highlighted in grey. Some notable readings can be seen close to wavelengths 324 and 327 in the x-axis, leading to a correspondence of both wavelengths to Copper. Furthermore, another characteristic feature includes the 3 peaks from 394 to 396, which this thesis proposes as a ratio for Oxides versus Sulphides.

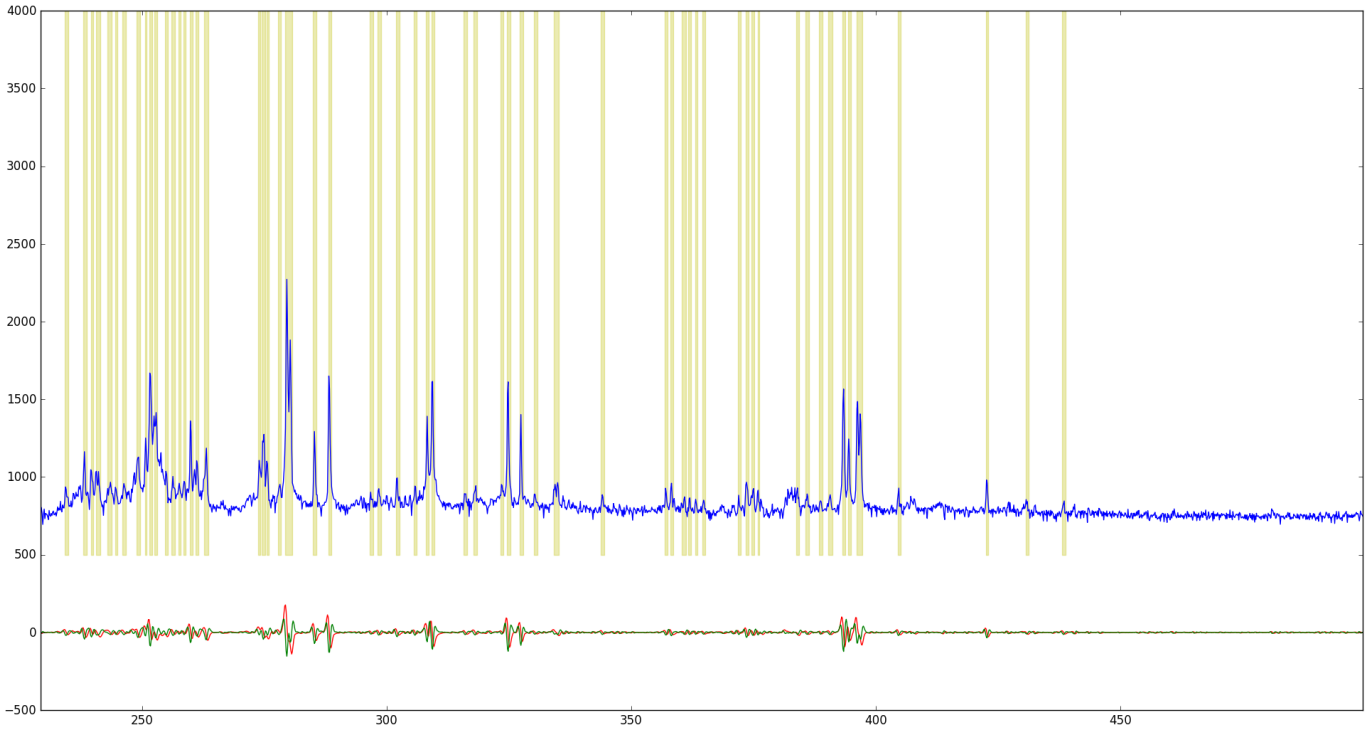

Figure 4-1: Characteristic Oxide sample spectrum processed with the Python script

The data shown in Table 4-1 includes the rock sample name, followed by the face-sample that it was taken from (S1 to S4), and then the reading taken (0 to 9). In order to obtain a significant measurement, 4 faces of the rock were sampled, with 10 readings for each sample, yielding a total of 40 readings per rock. In total there were 21,458 elements identified (including repetitions in the same rock) along with all of the readings.

"Peak Wavelength" refers to the wavelength read in the sample that might differ from the theoretical wavelength shown in the column "Observed Wavelength Air." The difference between these columns occurs because LIBS needs a calibration of the wavelengths along its photodiode array.

Table 4-1: Output of Python Scripts for the Oxide samples from Escondida Mine (Wavelength are in nm).

	Sample Rock	Peak Wavelength	Element	Intensity	Acc.	Observed Wavelength Air
0	15B1,S1,0	350.55	F II	1119	C	350.563
1	15B1,S1,0	294.46	Ga I	957		294.3636
2	15B1,S1,0	279.56	Mg II	1332	A+	279.5528
…	…					…
21455	21B1,S4,9	288.15	Si I	1612	B	288.1579
21456	21B1,S4,9	251.54	Ti III	1588	D	251.6053
21457	21B1,S4,9	276.73	Tl I	955		276.787
21458	21B1,S4,9	266.53	Zr III	887		266.4286

"Element" shows the ionization state of the element. "Intensity" measures the relative concentration of the element, and has arbitrary units since different LIBS machines will have different Intensity scales. This intensity varies from experiment to experiment depending on the configuration and features of the LIBS machine in use. In the same way, the NIST database (Laboratory) provides a Relative Intensity that consists of a ratio of the Intensity to its real concentration, which is used to represent the strengths of the lines in the spectrum. This might vary depending on the machines used. "Acc" (Accuracy), as described in Table 3-2, is a rating for the likelihood that a transition of the ionization stage occurs. This rating represents a direct "quality" factor of confidence for the data read.

4.1 Data integration and analysis

Once the data has been processed through the Python script, the data is grouped by element and ionization stage. This table groups data according to ion and element, as shown in Appendix A . The units of the table are considered to be “counts” or “arbitrary units.”

Each of the blank values in Appendix A represent readings that cannot be detected using the filters in the Python script. One of the main challenges of grouping elements is determining the uncertainty of the ID wavelength chosen for the Python script.

4.2 Regression Analysis for the Oxide Rocks

Once the samples had been reviewed with respect to any possibility for error, the data was taken into a regression analysis. A Stepwise regression was used to develop this correlation. The main purpose of this research was to elicit a response from the sensor to provide an indicator of the presence of ore, Sulfide or Oxide. It is possible to elicit such a response by conducting a multilinear regression analysis that will predict the target element, in this case Copper.

4.3 Correlation of LIBS Cu Oxides response to ICP analysis

This section presents an analysis of the direct correlation between the LIBS responses with respect to Copper versus those of the ICP Copper assays. The direct response of Copper has been obtained through the LIBS response. The Copper wavelengths analyzed correspond to Cu I at 324.75 and Cu I at 327.39. The wavelengths provide readings only in the areas covered by the LIBS laser beam, and it is for this reason that the LIBS response might not represent an accurate measurement of the Copper. However, as shown below, useful results have been obtained.

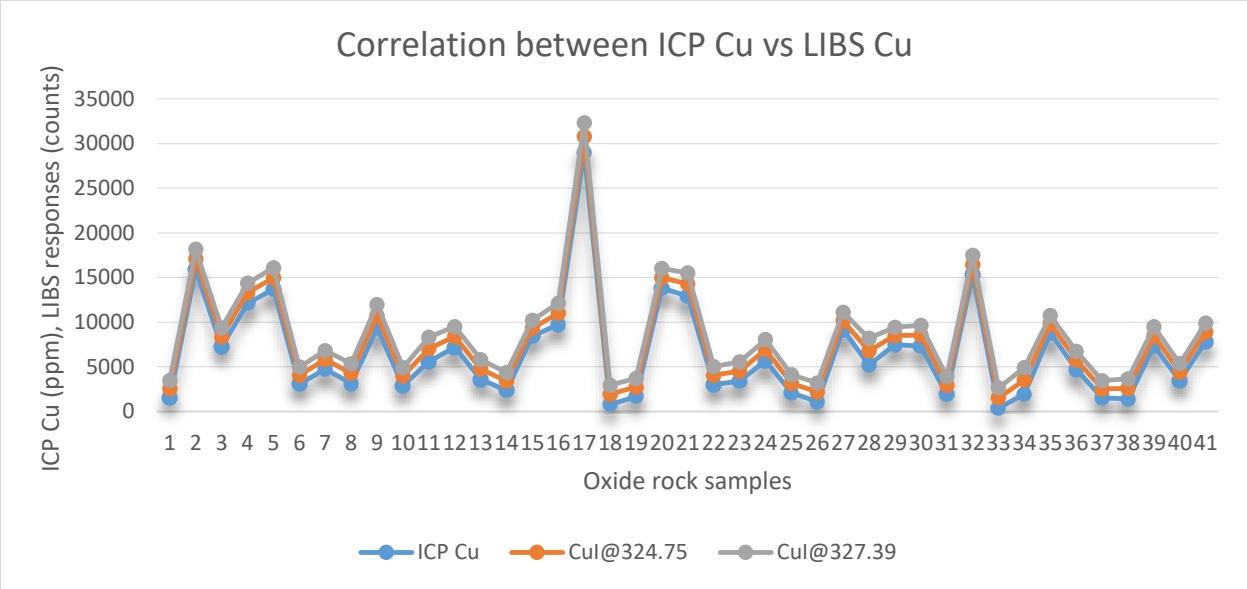

Figure 4-2: LIBS responses for Copper at wavelengths 324.75 and 327.39 vs ICP Cu (ppm)

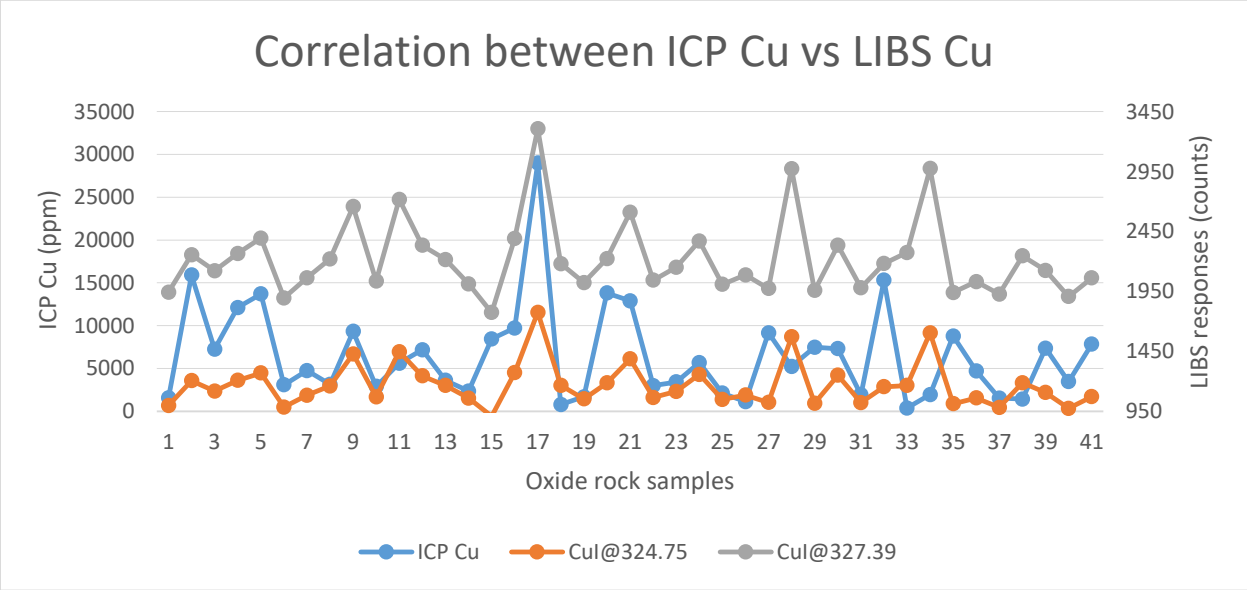

Figure 4-3: LIBS responses for Copper at wavelengths 324.75 and 327.39 vs ICP Cu (ppm) with secondary axis

The intention behind showing two charts with the same information is to provide a perspective regarding the relationship of the correlation between the LIBS response and the ICP assays for Copper. Figure 4-2 provides the correlation using the same primary axis, and Figure 4-3

shows the correlation with different axes. The correlation shown in Figure 4-4 is a normalization (from 0 to 1) of the two variables, and the Pearson Correlation Coefficient is 0.48.

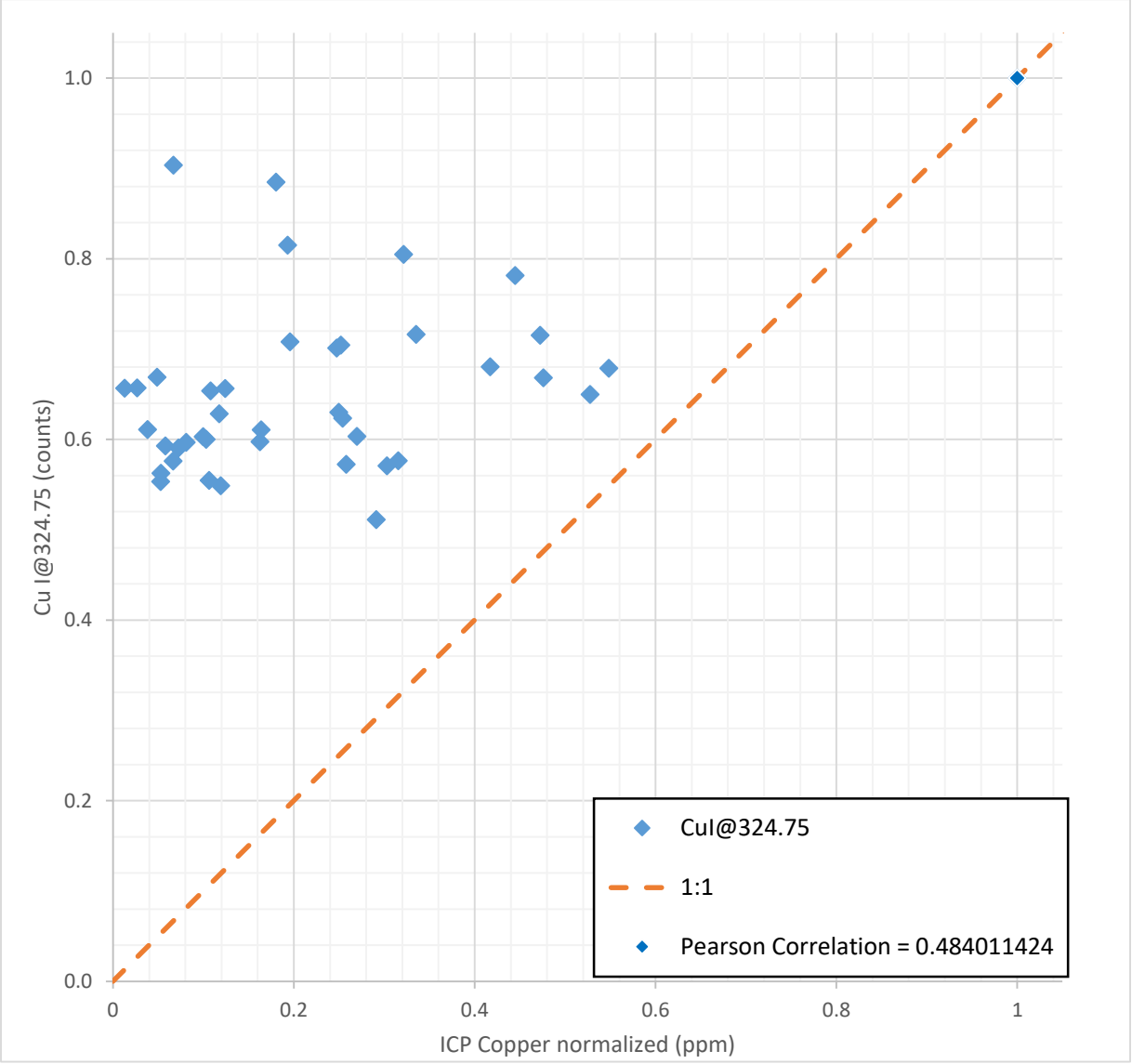

Figure 4-4: Correlation of Cu I at 324.75 nm

The reason that these variables have been normalized is because they do not have a common unit, as it is ppm for ICP Cu, and counts for LIBS Cu. The optimum number would be 1 on this regression, however obtaining a value of 0.48 means that the value is significant for the whole correlation developed in later sections of this chapter.

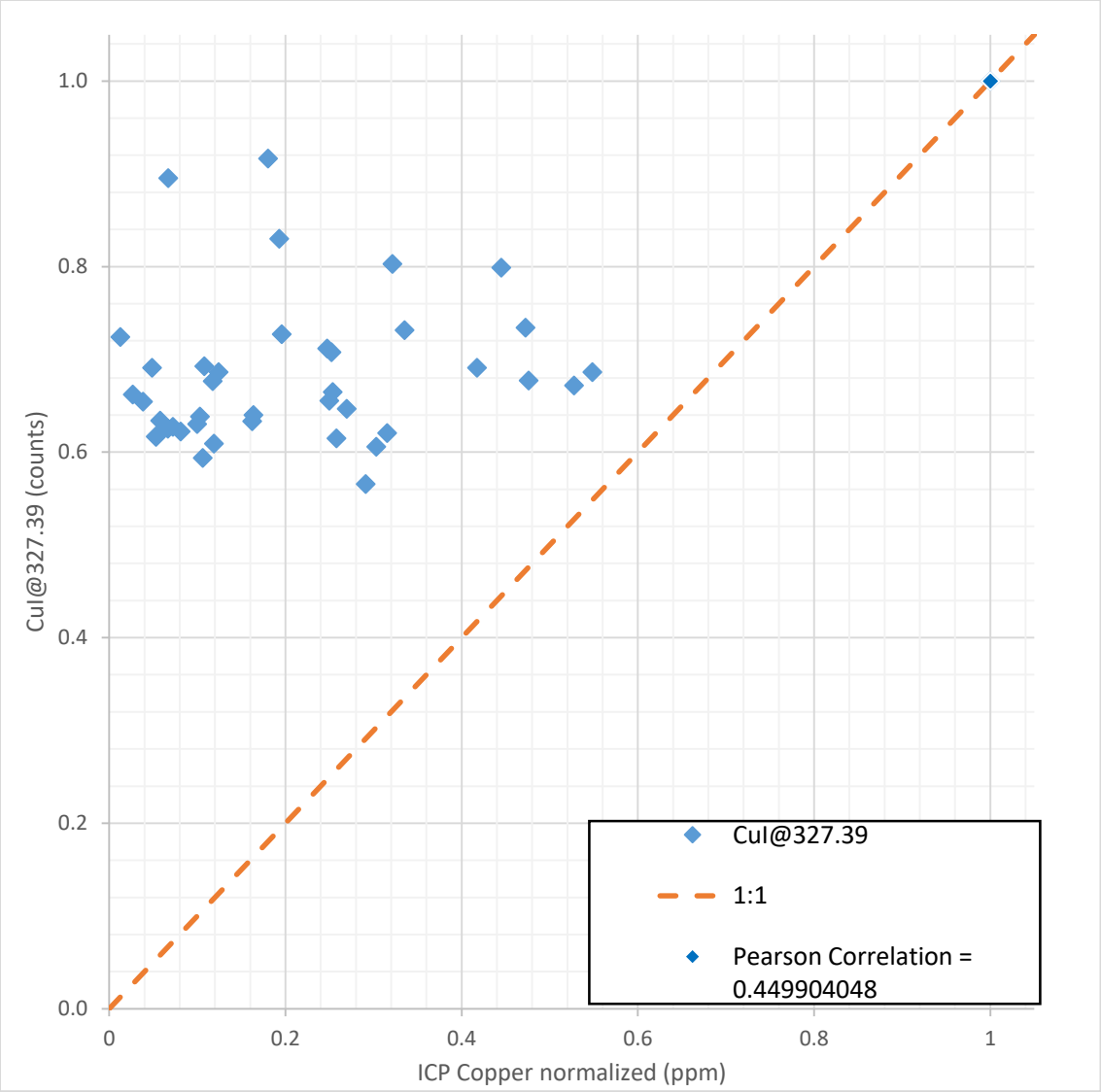

Figure 4-5: Correlation of Cu I at 327.39

In the same way, Figure 4-5 shows the correlation between the ion Cu I at 327.39 nm. The Pearson Correlation Coefficient is 0.45, and the interaction between these two variables is more clear in Figure 4-3. However, a coefficient in the range of 0.5 +-0.1 suggests a moderate uphill relationship. Direct LIBS correlations is recommended depending on the geology type. For example, coal seams that have low heterogeneity and can produce a good response using this direct correlation. Copper

ore deposits do not match these characteristics, and as such, LIBS responses will not follow properly with this type of correlation.

4.4 Element regression analysis for Oxide samples

The data, as shown in Appendix A , is a compendium of the large database of responses from LIBS readings over Oxide rocks. Appendix B shows the results of the Certified ICP results. The responses were taken into MATLAB to process the Stepwise Fit regression analysis. The input data is 0 and the second input to fit all of these elements is Cu concentration (ppm) from Appendix B .

As shown in Table 4-2, the results of this analysis provide a coefficient for the ion, a standard deviation and a p-value. The regression selection is based on the p-value, which represents the null-hypothesis where the coefficient is equal to zero.

It is important to mention that the software (MATLAB) does not accept empty data into the matrices to create this correlation. This is a source of non-measurable error because empty cells are being filled with zeros “0” in order to calculate the correlation prediction. There is no solution to this problem because the LIBS responses and the predictions may be contaminated as a result of garbage data even when the LIBS responses are compared with the ICP assays because ICP provides a geochemical analysis for the entire sample rather than a surface reading, as does LIBS. Although not directly the subject of this research, it is therefore recommended to develop a mathematical algorithm that does not fill empty spaces with zeros in the matrices when calculating the predictions using Stepwise regression.

Table 4-2: Results of regression analysis over LIBS responses

Element	Coefficient	Std. Error	p value
Ag II@232.02	3.665	2.203	0.105
Ag II@241.32	1.402	1.157	0.234
Al II@281.62	-1.719	1.039	0.107
Ba II@455.4	0.369	2.018	0.855
Be II@272.89	0.165	1.002	0.86
Be III@448.73	0	22.10	1
Bi I@306.77	-1.96	1.007	0.060
Ca I@422.67	-1.12	12.78	0.9302
Ca II@317.93	-0.7	1.059	0.465
Cd II@274.85	-2.38	2.635	0.371
Cl II@481.01	0.365	2.149	0.8661
Co I@347.4	-2.776	4.350	0.527
Cr I@427.48	4.0494	2.058	0.057
Cu I@324.75	50.50	18.02	0.0083
Cu I@327.4	-56.6	24.00	0.024
Cu II@271.35	-1.3188	0.95	0.174
F II@350.56	-1.261	1.413	0.378
Fe I@374.95	-1.013	1.493	0.502
Fe II@234.35	1.0135	2.75	0.714
Fe II@238.2	-3.157	3.531	0.3776
Ga I@294.36	-0.02	1.597	0.9851
Hf I@368.22	-2.6298	3.501	0.4579
In II@294.1	-0.822	1.369	0.552
Ir I@269.42	-1.38	1.1206	0.225
Mg I@285.21	-4.744	12.72	0.711
Mg II@279.55	-0.615	3.604	0.8654
Mg III@239.51	-4.3487	4.3426	0.323
Mn I@279.83	7.7559	1.713	7.01E-05
Mn II@261.02	-1.55	6.0825	0.799
N II@399.5	-0.5061	2.4213	0.835
N IV@347.87	-1.0638	1.615	0.514
Na II@298.42	0.5653	3.01	0.852
Na II@307.83	-2.2515	0.700	0.0028
Ni I@349.3	-0.162	1.3748	0.906
O III@393.48	9.80552	15.88	0.541
O V@278.1	1.52244	0.899	0.100
P I@253.56	0.3609	1.098	0.744
P IV@334.77	-0.7648	0.77	0.332
Pb I@280.2	-1.156	0.98	0.248
Pb I@283.31	0.67120	1.443	0.645
S VI@419.89	-0.612	1.407	0.66
S VI@420.08	-0.28	1.2408	0.821
Sc III@269.91	5.417	3.580	0.13
Si I@288.16	-26.35	5.374	2.29E-05
Si II@413.09	-0.042	1.241	0.9730
Sn II@335.2	4.7879	2.123	0.0305
Ta I@362.66	-0.63	3.34	0.849
Ti I@399.86	0.44	1.37	0.745
Ti II@376.13	0.453	1.66	0.787
Ti III@251.61	-15.76	12.8	0.229
Tl I@276.79	0.32	1.76	0.855
Tl I@351.92	1.07	1.899	0.575
V II@292.4	0.1568	1.285	0.903

Element	Coefficient	Std. Error	p value
W I@400.88	5.140	3.397	0.139
W II@248.92	-0.29	1.117	0.795
Y II@371.03	0.824	1.183	0.490
Zn I@334.5	1.712	1.266	0.185
Zn II@491.16	5.479	3.622	0.139
Zr III@266.43	0.124	1.233	0.920

The p-value represents how extreme the measure is with respect to its model. The p-value for this statistical analysis provides the significance of the term inside the regression analysis. For practical purposes, only p-values below 0.05 will be considered for the regression. In Table 4-2, p-values with values below 0.05 have been highlighted in red. A summary of the results, including the intercept for the equation, is shown in Table 4-3 below.

Table 4-3: Selected elements for regression analysis

Element	Coefficient	Std. Error	p value	Occurrence	Occurrence%
Cu I@324.75	50.505	18.021	8.31E-03	1461	90%
Cu I@327.39	-56.664	24.009	2.41E-02	1334	82%
Mn I@279.82	7.756	1.714	7.01E-05	1	0%
Na II@307.83	-2.252	0.701	2.88E-03	82	5%
Si I@288.15	-26.351	5.375	2.29E-05	1247	77%
Sn II@335.19	4.788	2.123	3.07E-02	4	0%
Intercept	42,336				

$$Predicted\ Cu(ppm)$$
$$= 42{,}336 + [50.50 * Cu\ I@324.75] - [56.66 * Cu\ I@327.39]$$
$$+ [7.75 * Mn\ I@279.82] - [2.25 * Na\ II@307.83] - [26.35 * Si\ I@288.15]$$
$$+ [4.78 * Sn\ II@335.19]$$

This formula was used to plot the y-axis for Figure 4-6. For the purposes of this chart, the size ratio was adjusted to 1:1 to provide a realistic graphical plot of the predictive model.

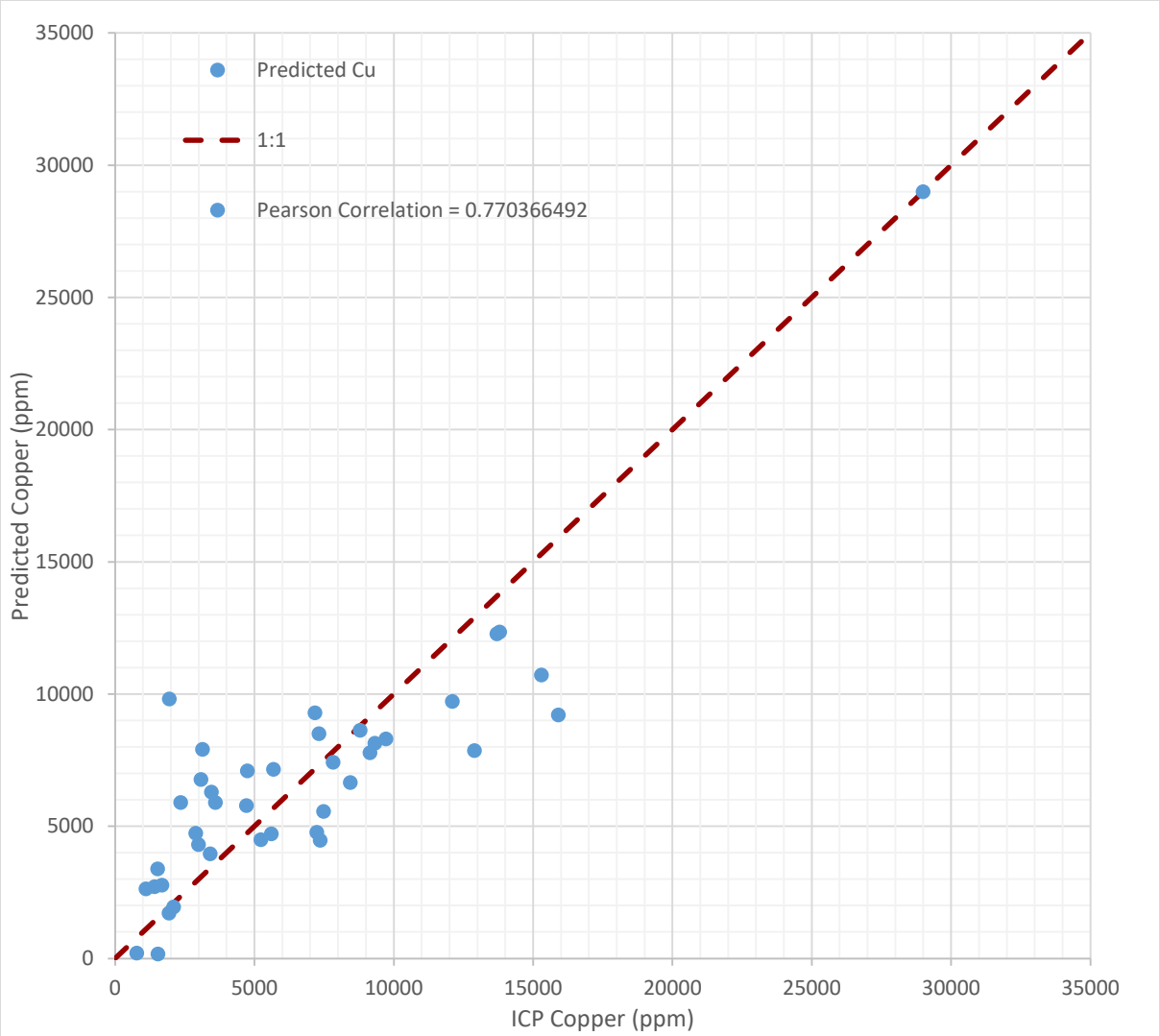

Figure 4-6: Predicted Copper vs Certified ICP Copper (ppm)

The Pearson Correlation provides an idea of how disperse the 2 models are. It also resembles a moment of inertia, and can be considered to be a precision. In this case, the correlation does not appear to be a reliable model for sorting. Although there is no standard with respect to dispersion for sorting sensors, some logic standards can be used as a pattern. The average cut-off grade for an open pit mine operation ranges between 0.27% to 0.5% Cu, or 2700 to 5000 ppm. Ideally, the results would fall along the 1:1 line, however this is not the case. The prediction tells

us that 23% (1-0.7703) will be off the predicted value. This means that if we work with a cut-off of 0.27% Cu, we might attain readings of 0.2% Cu or vice versa, which could result in wrong sensor responses and indeed, loose ore.

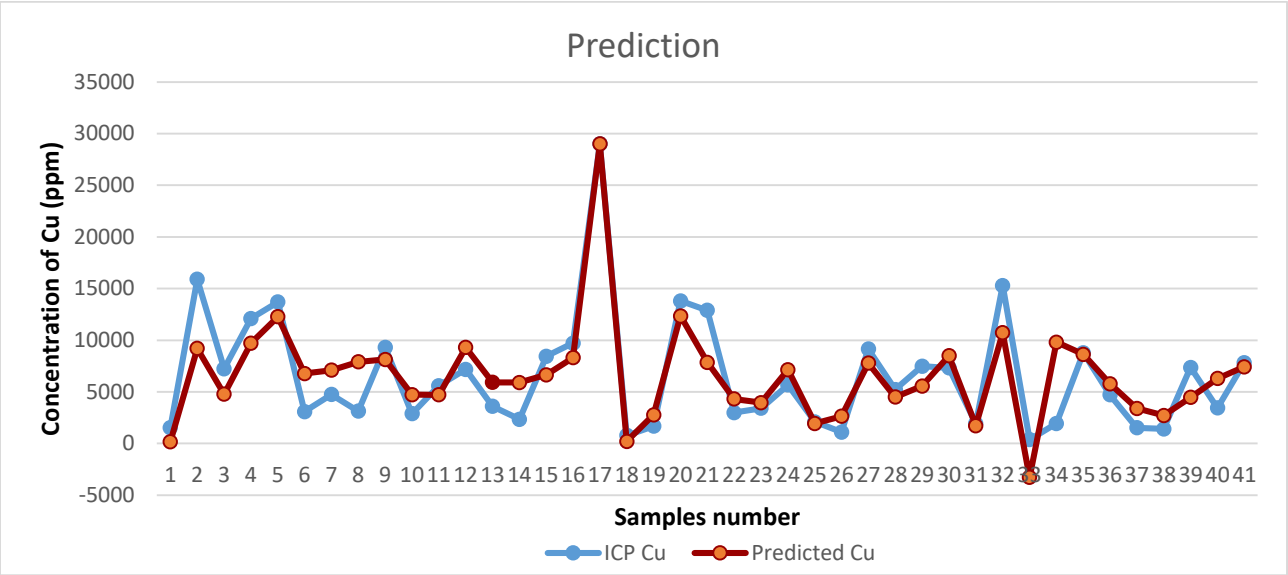

Figure 4-7: ICP Cu vs Predicted Cu trending line along the 41 rock samples

Figure 4-7 shows the predicted Copper levels versus those of the certified analysis for the sample. This figure provides an idea of the accuracy of the sensor prediction through a basic multivariable regression analysis. The accuracy for this response has been calculated as the average of the individual accuracies, giving a final value of 77%. The individual accuracies have been calculated as:

$$Accuracy = \frac{abs(ICP\ Cu - Predicted\ Cu)}{ICP\ Cu}$$

Equation 2 Accuracy calculation for the correlation

Table 4-4: ICP Cu vs Predicted Cu values in ppm

Accuracy	ICP Cu	Predicted Cu
89%	1540	172
42%	15900	9207
34%	7240	4772

Accuracy	ICP Cu	Predicted Cu
20%	12100	9721
10%	13700	12271
120%	3080	6770
49%	4750	7099
153%	3130	7905
13%	9320	8139
64%	2890	4735
16%	5600	4710
30%	7170	9291
64%	3600	5903
151%	2350	5901
21%	8440	6653
15%	9720	8303
73%	774	209
65%	1680	2773
11%	13800	12350
39%	12900	7865
44%	2990	4307
16%	3410	3956
26%	5680	7147
7%	2100	1947
138%	1110	2637
15%	9150	7779
14%	5230	4494
26%	7480	5562
16%	7310	8498
11%	1930	1718
30%	15300	10725
986%	370	-3280
406%	1940	9809
2%	8790	8626
23%	4710	5784
122%	1530	3390
92%	1410	2713
39%	7360	4470
83%	3450	6298
5%	7820	7425
79%		

The accuracy of the response is 79%. In previous chapters it was explained that, as a result of the time frame and LIBS capabilities with respect to number of readings, accuracy is not as important as precision. Accuracy can be estimated and improved upon by taking more than one reading per sample once the sensor is working in a sorting system. However, 79% means that only 21% of the readings are aimed at the target. This might be critical, even if a high level of precision is expected.

In contrast, precision can be achieved if we understand the statistical behavior of the sample.

Table 4-5: Histogram data of the 41 Oxide samples

Bin	*Frequency*	*Cumulative %*
-3	0	0.00%
-2	1	2.50%
-1	4	12.50%
0	13	45.00%
1	17	87.50%
2	4	97.50%
3	1	100.00%
More	0	100.00%

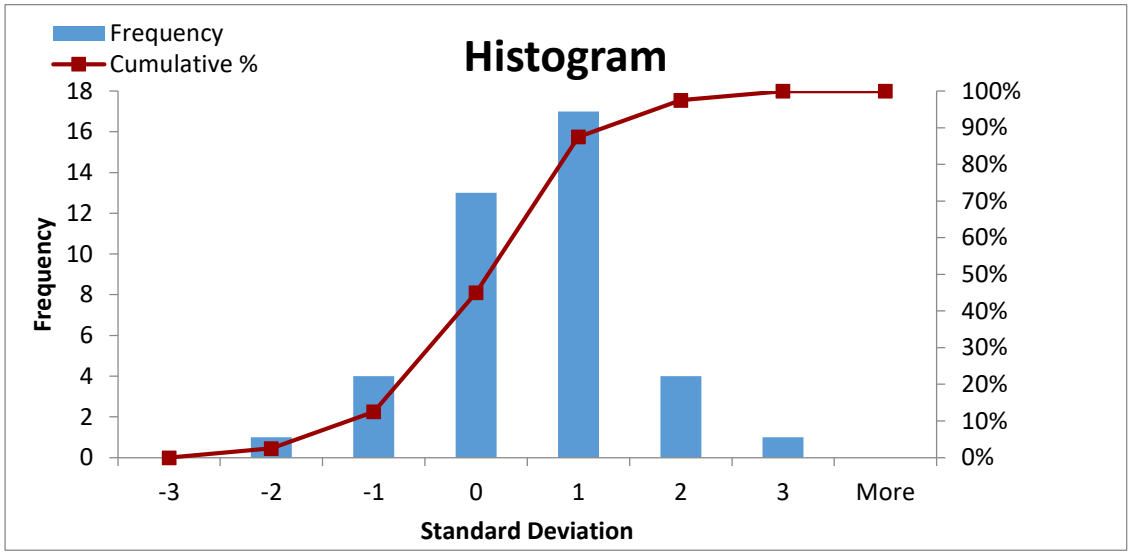

Figure 4-8: Histogram of the 41 Oxide samples

Figure 4-8 and Table 4-5, shows the historic data of the regression analysis. This chart is a Pareto chart that has been calculated with the 3 standard deviations obtained from the correlation of ICP Cu and Predicted Cu. The histogram plays a significant role with respect to the correlation because we are taking responses from cut-off grades. The histogram suggests that the bias tends to the positive side (mean is greater than the predicted value) and is less likely to trend to the negative side (mean is lesser than the predicted value). This suggests that if there is a cut-off grade

of 0.3% Cu, then 25% will be below the cut-off, and the other 75% will be around or greater than the target. In contrast, in Figure 4-9 the trend indicates that from 0 to 3% Cu, the prediction turns to be negative.

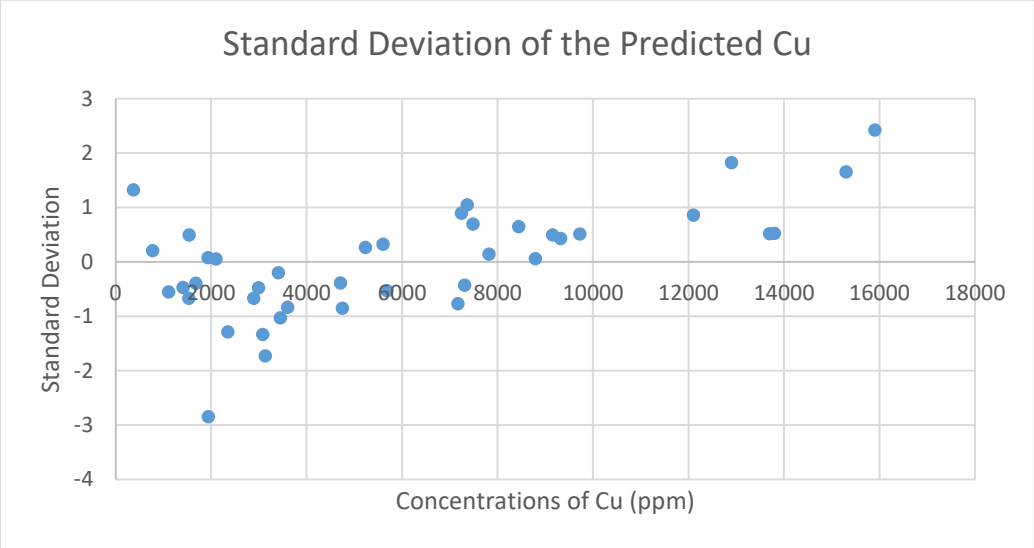

Figure 4-9: Standard Deviation dispersion of the predicted Copper

4.5 Interaction effect analysis using multilinear regression analysis for Oxide samples

The analysis of the interaction effects begins with the development of another Python Script to multiply each element response by another element response. The input of this script is shown in the table in Appendix A . In the script there are 59 elements, giving an output of 3481 interaction effects of elements, including repetitions such as "Ag II@232.02*Ag II@232.02". The problem described in section 4.4 in terms of zeros in the matrices calculations is increased here. Every single space has been calculated as the multiplication of 2 responses, and if one or two of the responses are empty (or zero for the calculation), then the result will also be empty, or zero.

Table 4-6: Truth Table using AND logic

AND		
A	B	AB
0	0	0
0	1	0
1	0	0
1	1	1

To gain an understanding of how this will effect the results of the calculations, Table 4-6 shows the results of a Truth Table with the operator AND. In this case, A represents one ion and B another ion in the multiplication script. A zero represents an empty space, and 1 represents a numeric response different than an empty space. As such, it is indicated that only 25% of the possibilities will provide a numeric response for the 3481 binomial elements. This increases the potential for error, and it is recommended that this situation be investigated in more detail.

The multiplication provides responses that are in the numerical range of squared power because they have been multiplied. Evidence of this is shown in the extract of the output of the script in Table 4-7. This chart simply provides a random extraction from the whole table. This portion of the table, however, has been shown on purpose to provide at least some visible data because most of the tables have no interaction effect responses.

The interaction effects are developed with the purpose of creating links between the target ore (Copper) and the host minerals. The mineralogy of the bearing minerals of the target ore provides a good trace for the presence of the target element. However, this approach is appropriate for ores such as gold, in that direct gold readings are unlikely through LIBS or any other sensor, due to particle size. Massive ore bodies such as Copper porphyries do not allow for the creation of strong links to a specific mineralization because of the natural and complex geological formation of the ore body. Because of this, the current research focuses on the statistical analysis of the interaction of the elements and not on the mineral-bearing association of host minerals, also

referred to as ore genesis. For example, host minerals of gold provide a strong response to the presence of gold because the fine, or very fine grain size of gold might not be read by a sensor. As such, the gold associated to Tellurides, Sulphides, Arsenopyrites or Carbonaceous materials, and can be difficult to read as gold. However, the association to gold would be easier if the predictive equation searches for Arsenic, Antimony or Tellurium, depending on the local ore genesis. This would provide a good tool for searching over high grade veins where gold is occluded into the mentioned host minerals. However, if the ore body is a massive disseminated porphyry, then the interaction effect might limit the statistical capacity of predicting the element concentration by not accepting some of the elements. Indeed, the best approach to the interaction effect is to provide some logical acceptance or rejection of the variables under the geological perspective based on their mineralogical associations. Copper porphyry deposit genesis typically belongs to a hydrothermal magmatic fluid for which a better approach might be geo-spatial characterization via geostatistical analysis rather than heterogeneity and host mineralization.

Table 4-7: Extract of binomial multiplication of the ion responses from LIBS

Rock	Mg I@285.21*Be III@448.73	Mg I@285.21*Bi I@306.77	Mg I@285.21*Ca I@422.67	Mg I@285.21*Ca II@317.93	Mg I@285.21*Cd II@274.85	Mg I@285.21*Cl II@481.01	Mg I@285.21*Co I@347.4
1			1052956		1173146.9		
2			1012570		1194120.2		
3			1045180	1062383.85	1129281.0		
4			1045832		1197269.8		
5			1051358	996808.1515	1037441.6	823450.2	
6			978493		1067929.7		
7			1045516		1052351.5		
8		1361130.225	1034371		1455831.0		
9			1111389	1161952.0	1315768.1	957001.3	
10		1260264.6	1045583		1420121.4		
11			1117576	1508004.4	1268463.3		
12		1269411.11	1014349	1078216.8	2131788.4		
13			1040576		1190350.9		
14			949752		1134324.3		
15			867266		979689.1		
16			1026289		1089395.4	936682	
17	973928.7		959216	1093710.791	1170050.6		
18		1095843.214	1070755	1127179.8	1792358.7		

Rock	Mg I@285.21*Be III@448.73	Mg I@285.21*Bi I@306.77	Mg I@285.21*Ca I@422.67	Mg I@285.21*Ca II@317.93	Mg I@285.21*Cd II@274.85	Mg I@285.21*Cl II@481.01	Mg I@285.21*Co I@347.4
19		1099832.767	1033135	1112472.288	1362796.2		
20		1034505	1047562	1082070.9	1076614.5		
21			971638	956096.7	1191059.4	895723.2	
22		1444833.113	1032193		1732889.3		
23		1254677.907	1002130		1184938.5		
24		1131976.625	1054606	1237411.5	1486248.5		1032334.8
25			1014031	1057703.4	1150800.1		
26		1242154.05	1048500	1004045.2	1410501.7		
27			1084227	1168885.1	1198292.6		
28			1028212	1084348.35	1398646.7		
29			1058327		1140914.1		
30			1021557	1130917.282	1368772.1		
31			990900		1287859.9		
32			991509		1266436.2		
33			1044814		1116409.9		
34			1040522	1008561.8	1128178.6	981586.075	
35			1102378	1144697.88	1389501.3		
36			1003450	1050617	1112683.3		
37			1007754	1009750.3	1239945.7		
38		1396766.7	1085700	1093554	1904927.6		
39			997601		1494442.3		
40			1087467	1109302.074	1031189.2		
41			1088747		1314198.8	1003087.05	

This numerical range will disable the sensitivity of the ion responses from LIBS because the numbers are higher in quantity than are the raw LIBS responses. As such, values in Table 4-7 were re-calculated as the square root for all of the values. As in Table 4-7, this part is shown on purpose for the reason of providing some visible data.

Table 4-8: Extract of the square root of the binomial multiplication of the ion responses

Rock	Zr III@266.43*Ag II@232.02	Zr III@266.43*Ag II@241.32	Zr III@266.43*Al II@281.62	Zr III@266.43*Ba II@455.4	Zr III@266.43*Be II@272.89	Zr III@266.43*Be III@448.73
1	0	0	900	0	912	0
2	0	0	0	0	926	0
3	0	0	0	0	0	0
4	0	0	0	0	0	0
5	0	0	946	0	0	0
6	0	0	0	0	0	0
7	0	0	0	0	0	0
8	0	0	1153	0	1263	0
9	0	1060	1025	0	1321	0
10	0	0	0	0	1015	0
11	0	0	996	916	1207	0

Rock	Zr III@266.43*Ag II@232.02	Zr III@266.43*Ag II@241.32	Zr III@266.43*Al II@281.62	Zr III@266.43*Ba II@455.4	Zr III@266.43*Be II@272.89	Zr III@266.43*Be III@448.73
12	0	1021	0	0	1244	0
13	0	0	0	994	1084	0
14	0	0	0	0	0	0
15	0	0	0	0	0	0
16	0	0	0	0	0	0
17	0	0	0	914	1059	929
18	0	0	966	0	1033	0
19	0	0	0	0	1046	0
20	0	0	920	0	957	0
21	0	0	0	856	924	0
22	0	0	1069	0	1245	0
23	0	1062	1081	0	1314	0
24	0	0	989	0	1089	0
25	0	0	0	0	951	0
26	0	0	0	0	1153	0
27	0	0	0	0	0	0
28	0	0	0	939	1100	0
29	0	0	0	0	0	0
30	0	0	0	842	940	0
31	0	0	0	0	1045	0
32	1084	1242	0	0	0	0
33	0	1084	1068	1079	1240	0
34	0	0	884	844	0	0
35	0	0	0	0	1028	0
36	0	0	0	0	0	0
37	0	0	0	0	1072	0
38	0	0	0	0	1161	0
39	0	0	0	0	978	0
40	0	0	0	0	0	0
41	0	0	0	0	1179	0

An extraction of the 3481 square rooted binomials is shown in Table 4-8. This numerical range is similar to that of the LIBS responses. The empty spaces were filled with zeros to make the computing of the responses possible. Table 4-8 will not be included into this thesis due to its size, but can be easily replicated through the use of the Python Script included in Appendix D .

4.6 First procedure run analysis for the regression for Oxide samples

The first run for the regression uses data from Table 4-8. The entire table was processed with the MATLAB Stepwise fit function, providing statistical results for the 3481 binomials. The

results indicate that 3443 values, or 98.9 % of all of the binomials provided a NaN result for the p-value. MATLAB (MathWorks) describes NaN returns as "Not-a-Number" values that result from operations with undefined numerical results. For all of these NaN results for p-value, the calculated coefficient was zero. Table 4-9 shows the calculated values of p-values and coefficients in MATLAB for the first run in the algorithm. It is expected that the calculated p-value of zero "0" is due to the large amount of variables processed by the software. The values were calculated for Copper in ppm from the ICP Certified Results (ICP certified assay results for the 41 Oxide Escondida samples), a target dependent variable. The maximum allowed p-value was set at 0.05.

Table 4-9: Results of the first run using Stepwise Fit regression in MATLAB for Copper

Binomials	p-value	Coefficient
Al II@281.62*Ba II@455.4	0	4.7660
Ba II@455.4*Ca II@317.93	0	-0.7830
Ba II@455.4*Fe I@374.95	0	-3.7101
Be II@272.89*Ca I@422.67	0	-13.306
Be II@272.89*Cu I@324.75	0	163.232
Be II@272.89*Cu I@327.4	0	-132.49
Be II@272.89*Na II@298.42	0	-19.509
Be II@272.89*Ti I@399.86	0	-13.512
Be III@448.73*Cr I@427.48	0	6.0267
Ca I@422.67*Mg III@239.51	0	7.2111
Ca II@317.93*Al II@281.62	0	0.2186
Ca II@317.93*Cl II@481.01	0	-2.3148
Ca II@317.93*Cr I@427.48	0	-4.6994
Cd II@274.85*Mn II@261.02	0	-0.0390
Cd II@274.85*Ti II@376.13	0	0.0333
Cl II@481.01*Ir I@269.42	0	1.0694
Cr I@427.48*P I@253.56	0	-0.078
F II@350.56*Si II@413.09	0	0.5143
Fe I@374.95*Fe I@374.95	0	-2.0133
Fe II@234.35*P I@253.56	0	-13.075
Ga I@294.36*Ni I@349.3	0	1.7984
Ga I@294.36*Pb I@280.2	0	0.0006
In II@294.1*W II@248.92	0	0.4223
In II@294.1*Y II@371.03	0	0.0001
Mg III@239.51*Si I@288.16	0	-31.205
N II@399.5*P I@253.56	0	-2.7507
O III@393.48*P I@253.56	0	15.6554
O III@393.48*P IV@334.77	0	-0.206
P I@253.56*F II@350.56	0	-6.006
P I@253.56*Zr III@266.43	0	0.0197

Binomials	p-value	Coefficient
P IV@334.77*Sn II@335.2	0	-0.6383
P IV@334.77*Ti II@376.13	0	-1.0461
Pb I@280.2*Tl I@276.79	0	0.7423
Pb I@280.2*Tl I@351.92	0	0.8022
S VI@419.89*V II@292.4	0	0.2601
Ti I@399.86*V II@292.4	0	-0.6404
Ti I@399.86*Zr III@266.43	0	9.3700
Ti II@376.13*Tl I@276.79	0	2.1956

Table 4-9 represents a preselection of the set of variables from Table 4-8. All of these interaction effects have a higher statistical interdependence with respect to the target value, and were selected based on t-statistics assumptions in order to build an equation with respect to which variables provide a better fit to the target dependent variable (Cu ppm).

4.7 Second procedure run analysis for the regression

Once the first set of variables was selected, the set of responses for each of these binomials was re-entered into MATLAB in order to process the data. The same process employed in the first run was used for this stage, but the dataset consisted of the binomials selected in Table 4-10.

Table 4-10: Second run using Stepwise Fit regression in MATLAB

Binomials	p-value	Coefficient
Be II@272.89*Ti I@399.86	1.26E-16	-13.512
Ti I@399.86*Zr III@266.43	2.00E-16	9.370
Be II@272.89*Cu I@324.75	9.34E-16	163.23
P I@253.56*F II@350.56	1.50E-15	-6.006
Al II@281.62*Ba II@455.4	8.78E-15	4.765
Be II@272.89*Cu I@327.4	1.41E-14	-132.5
Mg III@239.51*Si I@288.16	1.43E-14	-31.21
Ca II@317.93*Cr I@427.48	5.45E-14	-4.699
Ca II@317.93*Cl II@481.01	5.92E-14	-2.314
Ba II@455.4*Fe I@374.95	1.15E-13	-3.709
O III@393.48*P I@253.56	1.21E-13	15.65
N II@399.5*P I@253.56	2.27E-13	-2.750
Fe I@374.95*Fe I@374.95	2.71E-13	-2.014
Ti II@376.13*Tl I@276.79	2.88E-13	2.196
Be II@272.89*Na II@298.42	2.99E-13	-19.50
Fe II@234.35*P I@253.56	4.06E-13	-13.07
Be III@448.73*Cr I@427.48	4.79E-13	6.026
Pb I@280.2*Tl I@276.79	1.02E-12	0.742

Binomials	p-value	Coefficient
Ga I@294.36*Ni I@349.3	3.64E-12	1.798
Ba II@455.4*Ca II@317.93	6.56E-12	-0.783
Ca I@422.67*Mg III@239.51	9.90E-12	7.202
F II@350.56*Si II@413.09	1.66E-11	0.515
Be II@272.89*Ca I@422.67	1.87E-11	-13.30
Pb I@280.2*Tl I@351.92	2.19E-11	0.801
Ti I@399.86*V II@292.4	3.28E-11	-0.640
Cl II@481.01*Ir I@269.42	5.62E-11	1.0676
P IV@334.77*Ti II@376.13	8.94E-11	-1.046
Ca II@317.93*Al II@281.62	4.36E-10	0.2193
P IV@334.77*Sn II@335.2	6.11E-10	-0.638
S VI@419.89*V II@292.4	1.99E-09	0.260
In II@294.1*W II@248.92	2.57E-09	0.42
O III@393.48*P IV@334.77	4.64E-08	-0.205
Cr I@427.48*P I@253.56	1.08E-06	-0.076
Cd II@274.85*Ti II@376.13	5.44E-06	0.03
P I@253.56*Zr III@266.43	7.25E-05	0.018
Cd II@274.85*Mn II@261.02	0.0044785	-0.032
Ga I@294.36*Pb I@280.2	0.2195562	0.0003
In II@294.1*Y II@371.03	0.5953761	-0.0003

The calculations depend on the number of statistical variables because they are matrix multipliers, and as such, p-values might change for different runs. Values highlighted in red do not fit the minimum standard of 0.05 for p-value, and will be removed from the set of variables. The above table is sorted from smallest to largest p-value.

4.8 Proposed Method A

The variables with the smaller p-values were taken from the set of values in Table 4-10 to continue with the algorithm. The reason for choosing this set of values is that a reasonable equation for predicting Copper values cannot hold "too many variables," meaning that there should be no more than 10 or 12 variables in the equation. Smaller p-values show a higher interdependence between the dependent and interdependent variables, which is the key target in the sorting algorithm.

For this method, we used the first 20 interaction effects shown in Table 4-10. These effects have the smallest p-values in the correlation matrix, and are added to the 6 elements from Table

4-3. The reason that it is necessary to add elements to this binomial set is because the geological variable interaction corresponds directly to some presence of the elements. In this case, our target is Copper, and Copper alone must be added. Silicon, Magnesium and Sodium are found in abundance on the earth's crust (Yaroshevsky), and they show a statistical correlation with the target variable (ICP Copper assays).

The final input for the computation of the correlation will include 26 variables, as shown in Table 4-11. This table indicates the p-values and the coefficients for each variable computed. Unexpectedly, the p-value for elements such as Cu, I, or Na II are high, and do not fit with the standards suggested for inclusion into a prediction equation.

Table 4-11: Results for correlation for Oxide rocks

Variables	p-value	Coefficient
Be II@272.89*Ti I@399.86	1.95E-12	-11.883
Ti I@399.86*Zr III@266.43	9.52E-11	8.623
Be II@272.89*Cu I@324.75	7.36E-10	142.45
P I@253.56*F II@350.56	2.98E-09	-4.478
Al II@281.62*Ba II@455.4	4.72E-04	2.99
Be II@272.89*Cu I@327.4	1.03E-06	-119.8
Mg III@239.51*Si I@288.16	6.70E-09	-25.62
Ca II@317.93*Cr I@427.48	0.0786	-1.492
Ca II@317.93*Cl II@481.01	0.056	-1.253
Ba II@455.4*Fe I@374.95	0.006	-2.585
O III@393.48*P I@253.56	4.63E-07	3.07
N II@399.5*P I@253.56	0.0012	-2.943
Fe I@374.95*Fe I@374.95	0.012	-1.805
Ti II@376.13*Tl I@276.79	0.0064	1.446
Be II@272.89*Na II@298.42	0.00019	-24.93
Fe II@234.35*P I@253.56	0.825	-0.678
Be III@448.73*Cr I@427.48	1	0
Pb I@280.2*Tl I@276.79	0.027	0.919
Ga I@294.36*Ni I@349.3	0.188	0.68
Ba II@455.4*Ca II@317.93	0.011	-2.6411
Cu I@324.75	0.601	-1.188
Cu I@327.4	0.560	-1.669

Variables	p-value	Coefficient
Mn I@279.83	9.39E-06	3.2323
Na II@307.83	0.354	0.291
Si I@288.16	0.755	-0.999
Sn II@335.2	0.275	0.839

Appendix A shows the responses for Mn I at 279.83 nm. For this particular ion, only one response was found. While the stepwise regression suggests that the Mn term is significant, it does not provide a significant amount of information and was therefore eliminated from the model.

By comparing Table 4-11 and Table 3-1, some of the interaction effects proposed for building the predicted Copper formula can be confirmed. Magnesium and Silicon are likely to be found together, and to create a numerical correlation to Copper because the Biotitic and Quartz-Sericite mineral groups contain these two elements. The elements shown in the mineralogical group are not necessarily good predictors for copper. The 1st and 2nd Interaction Effect indicators show the confidence level of the identification of each. These indicators are based on Table 3-9.

Table 4-12: Final prediction equation for Predicted Copper

1st I. E.	2nd I. E.	Variables	Coefficient	p-value
Poor	Good	Be II@272.89*Ti I@399.86	-11.78	1.33E-08
Good	Very Good	Ti I@399.86*Zr III@266.43	8.71	1.14E-07
Poor	Very Good	Be II@272.89*Cu I@324.75	157.8	1.63E-08
Good	Unknown	P I@253.56*F II@350.56	-3.16	0.00041
Poor	Very Good	Be II@272.89*Cu I@327.4	-160.5	3.16E-08
Good	Very Good	Mg III@239.51*Si I@288.16	-30.32	1.11E-07
Unknown	Good	O III@393.48*P I@253.56	1.968	0.01079
Poor		Mn I@279.83	4.11	0.0002

Intercept: 37480.607

The values were computed with Stepwise Fit in MATLAB, the variables in this table are used to build the predictive equation for copper. This final equation with its intercept, is used to plot Figure 4-10. This chart shows a very good correlation of 0.9614 that has the highest Pearson

Coefficient found for the Oxide samples. However, this method is inconsistent, and needs to be subject to revision.

$Predicted\ Cu(ppm) = 37480.6 - 11.78 * \text{Be II@272.89} * \text{Ti I@399.86} + 8.71 * \text{Ti I@399.86} * \text{Zr III@266.43} + 157.87 * \text{Be II@272.89} * \text{Cu I@324.75} - 3.16 * \text{P I@253.56*F II@350.56-160.59*} \text{Be II@272.89*Cu I@327.4-30.32*} \text{Mg III@239.51*Si I@288.16+1.96*} \text{O III@393.48*P I@253.56+4.11*} \text{Mn I@279.83}$

Equation 3 Predicted Copper for Oxide samples - Method A

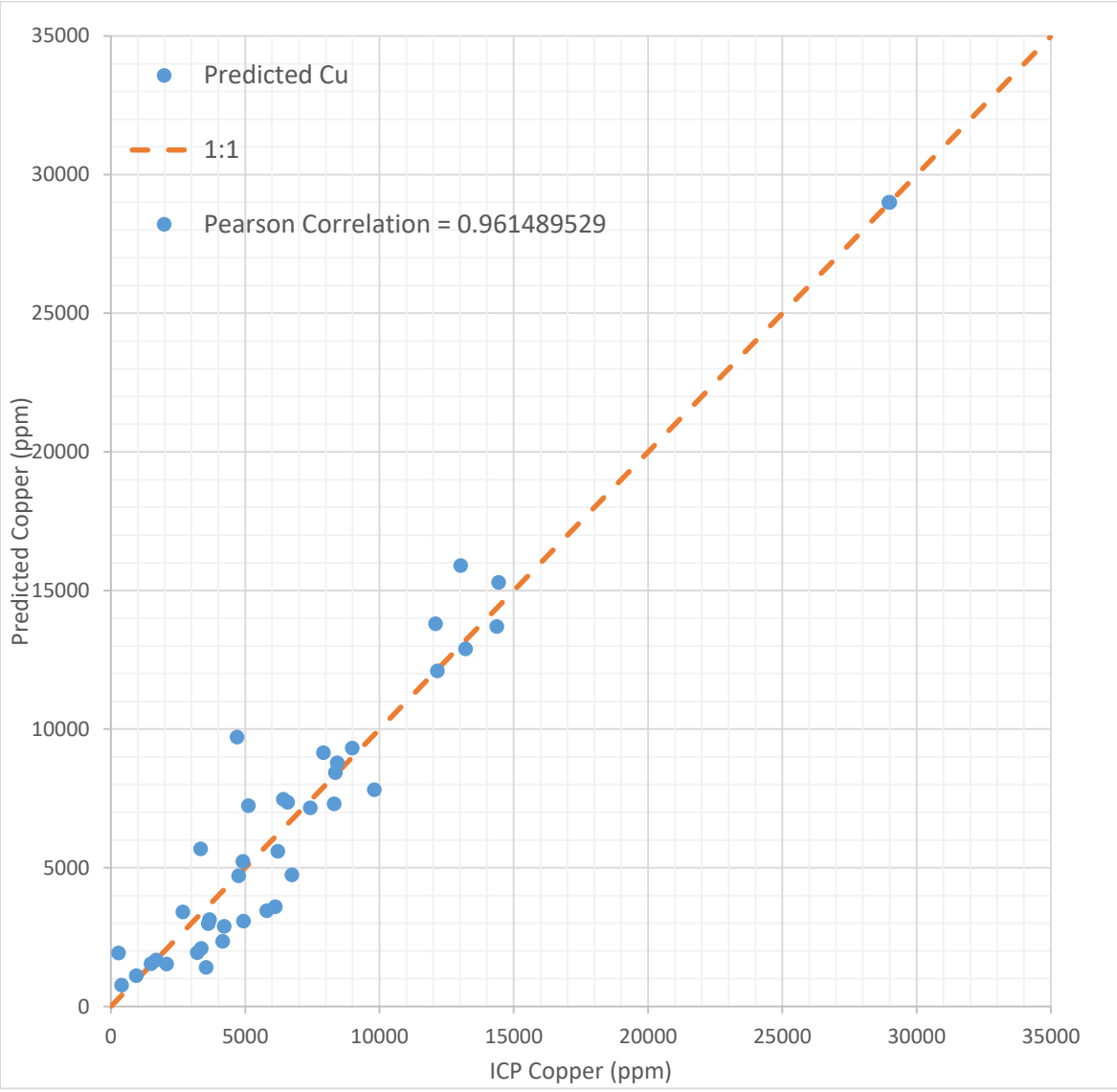

Figure 4-10: Correlation equation for LIBS Copper responses

The negative coefficient indicates that there is an inverse correlation between the Copper grade and the response parameter or element. For example, the high concentration of an element associated with a gangue mineral would imply a low concentration of Copper.

A common mistake that is made while developing regression analysis is to follow the patterns that had been developed during former projects. In this case, LIBS has a different set of values. This set of values varies with regard of the amount of information present, such as for example, Mn I at 279.83 nm.

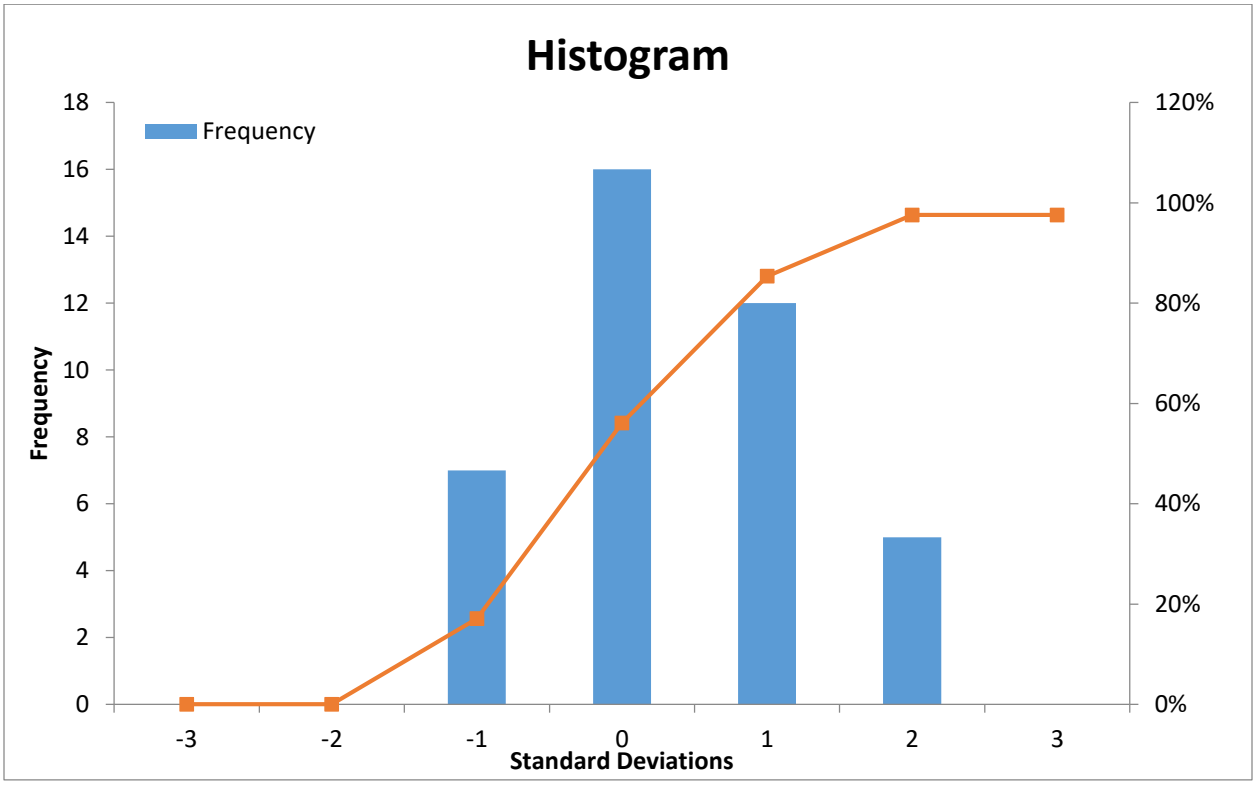

Figure 4-11: Histogram for the correlation equation for LIBS Copper responses

The LIBS responses fit very well, and this histogram shows how the trend does not reach the limits of the third standard deviation which demonstrate an excellent fit to the prediction. Some of the data barely reaches the 1st or 2nd standard deviation for the whole set.

As mentioned, this information is quite good, and fits very well with respect to the intended target. However, this method is not reliable because it does not consider the number of responses available from the interaction effects. It is necessary to see how many responses can be counted in order to fill this regression.

Also, the number of responses available are not explicitly shown in Appendix A because this is a pivot table that provides a lump sum of the total responses from LIBS. The real responses are shown in Table 4-1. The data fits very well in this prediction, but will not function well in the real world once the sensors are built-in to the belt conveyors, or the buckets of shovels or front end loaders.

4.9 Proposed Method B

This method is similar in procedure to Method A but includes the amount of responses obtained from LIBS in its analysis. Appendix E indicates the amount of LIBS responses attained for each of the 41 samples from Escondida Mine. It is important to know the number of responses in order to determine the mathematical error. Calculating mathematical error does not need to be considered because it will be assessed as part of the proof of concept but it is expected to be taken into account once the algorithm is applied to a sensor system either on a belt conveyor or a mining shovel, for ore sorting. The mathematical error refers to the availability of responses for the terms in the Predicted Formula. Some variables, such as Pb I@280.2 or Tl I@276.79 included in Table 4-11, have a positive statistical correlation with the target variable and are mathematically viable. However, once inserted into a correlation equation, they will not work as expected because there are not enough responses to feed the model in a sorter device.

As a result of the mathematical error, LIBS will loose its potential to produce the elements used for the interaction effects. If one of the elements needed for one interaction effect variable is not easily read in the first readings, then the predictive equation will be incomplete and the prediction inaccurate. The reading will not necessarily be taken several times on the same rock, and the likelihood of getting a response from a binomial with two ions will be low, and as such, will result in a high level of inaccuracy and low level of precision. A clear presentation of this problem will be done later in this chapter.

It is important to mention that a low amount of data for an independent variable provides higher correlation because there is less squared error to be taken into account. These variables can be computed successfully, but will not provide optimal results.

4.9.1 Quantification of the number of responses

In order to quantify which independent variables should be chosen to create a prediction, one proposed method is to weigh the p-values times the occurrences of the response along the whole data set.

Table 4-13 shows an extraction of the way in which these readings have been quantified. It is true that the average value for each ion can be processed to calculate the binomial value for the predictive equation. However, there is no guarantee that each single rock will be shot with LIBS enough times to elicit a valid response. A valid response is understood as a reading using LIBS capable to generate values for all of the elements in the predictive equation, particularly elements in the interaction effects. In order to fix this potential hazard, it is necessary to obtain an individual analysis for each LIBS reading. Table 4-13 below indicates the rock number and its

respective readings. As mentioned previously, every rock sample was shot 40 times, obtaining 4 samples (S1 to S4) of 10 readings per sample.

Table 4-13: Extraction of the quantification process for the binomials

Rock	Reading	Be II 272.89	Ti I 399.86	5
1				
	S1,2	1		
	S1,9		1	
	S4,3		1	
	S4,4		1	
	S4,5		1	
	S4,6		1	
	S4,7		1	
	S4,8		1	
	S4,9		1	
2				
	S1,6		1	
	S3,2		1	
	S4,7	1		
	S4,8	1	1	1
3				
	S1,2		1	
	S1,8		1	
	S3,8		1	
4				
	S1,0		1	
5				
	S2,2		1	
6				
	S2,3		1	
	S2,5		1	
	S3,9		1	
7				
	S3,3		1	
	S4,8		1	
8				
	S1,2	1		
	S1,3	1		
	S1,4	1	1	1
	S1,5	1	1	1
	S1,7	1		
	S1,8	1		
	S1,9	1		
	S2,3		1	
9				
	S2,9	1	1	1
	S4,0	1	1	1

Rock	Reading	Be II 272.89	Cu I 327.4	125	
1					
	S1,0		1		
	S1,1		1		
	S1,2	1	1		1
	S1,3		1		
	S1,6		1		
	S1,8		1		
	S1,9		1		
	S2,0		1		
	S2,1		1		
	S2,2		1		
	S2,3		1		
	S2,4		1		
	S2,5		1		
	S2,6		1		
	S2,7		1		
	S2,8		1		
	S2,9		1		
	S3,0		1		
	S3,1		1		
	S3,2		1		
	S3,3		1		
	S3,4		1		
	S4,1		1		
	S4,2		1		
	S4,3		1		
	S4,4		1		
2					
	S1,0		1		
	S1,3		1		
	S1,4		1		
	S1,5		1		
	S1,6		1		
	S1,7		1		
	S1,8		1		
	S1,9		1		
	S2,0		1		
	S2,1		1		
	S2,2		1		
	S2,3		1		
	S2,4		1		
	S2,5		1		

An individual analysis of these readings provides a clear breakdown of what we can get from LIBS as a sorting sensor. The "1" in the third column means that there exists a reading for the ion Be II@272.89, and the same for Ti I@399.86. The next column can show either a "1" meaning a valid reading for each of the two components of the interaction effect; or "-", meaning no valid interaction. For example, no valid value can be obtained for the interaction from rock 1. For rock 2 only one valid interaction value can be obtained. The lump sum of all possible valid binomial values is 5 for Be II@272.89*Ti I@399.86. For the next interaction effect, Be II@272.89*Cu I@327.4, a valid lump sum of 125 binomial values is obtained. In this way, the values were obtained for each pre-selected binomial. Table 4-14 provides a summary of the number of responses of LIBS for each ion, and for each of the 41 samples. The maximum possible value of number of responses is 40 readings x 41 numbers of readings/samples, resulting in 1640.

Table 4-14: Summary of number of responses for the 41 Oxide samples

Maximum	264
Maximum possible	1640
Number of samples	40
Number of readings/sample	41

1640 is the maximum number of responses that could be obtained for any binomial or ion variable in this project for the 41 Oxide samples. Table 4-15 shows the 20 binomials that were pre-selected from Table 4-10 with higher p-values. It is curious to note that the computation of this set of interaction effects included Fe I@374.95*Fe I@374.95, but Fe I@374.95 alone was not included when computing the ions in Table 4-2, obtaining a p-value of 0.71 (the maximum ideal p-value allowed is 0.05).

The maximum number of responses that could be obtained from this pre-selection is 266. The number of occurrences per maximum number of occurrences from Table 4-15 is 32/264=12%, and for the number of occurrences per maximum possible occurrences, it is 32/1640=1.95%.

Table 4-15: Number of occurrences for the binomials analyzed

Binomials	Number of occurrences	N occurrences / Max N occurrences	N occurrences / Max possible
Be II@272.89*Ti I@399.86	32	12%	1.95%
Ti I@399.86*Zr III@266.43	46	17%	2.80%
Be II@272.89*Cu I@324.75	126	47%	7.68%
P I@253.56*F II@350.56	4	2%	0.24%
Al II@281.62*Ba II@455.4	0	0%	0.00%
Be II@272.89*Cu I@327.4	120	45%	7.32%
Mg III@239.51*Si I@288.16	158	59%	9.63%
Ca II@317.93*Cr I@427.48	0	0%	0.00%
Ca II@317.93*Cl II@481.01	0	0%	0.00%
Ba II@455.4*Fe I@374.95	1	0%	0.06%
O III@393.48*P I@253.56	35	13%	2.13%
N II@399.5*P I@253.56	0	0%	0.00%
Fe I@374.95*Fe I@374.95	266	100%	16.22%
Ti II@376.13*Tl I@276.79	26	10%	1.59%
Be II@272.89*Na II@298.42	127	48%	7.74%
Fe II@234.35*P I@253.56	32	12%	1.95%
Be III@448.73*Cr I@427.48	1	0%	0.06%
Pb I@280.2*Tl I@276.79	91	34%	5.55%
Ga I@294.36*Ni I@349.3	16	6%	0.98%
Ba II@455.4*Ca II@317.93	1	0%	0.06%

This method provides a mathematical quantification to allow a greater significance for the binomials that are more likely to be seen. Table 4-16 shows the full pre-selection of ions and binomials, and it is already sorted by p-value/occurrence. For each of these independent variables, their respective coefficient, p-value, occurrence ratio and p-value per occurrence are shown.

Table 4-16: Weighting of the binomials

Binomials & Elements	Coefficient	p-value	Occurrence %	p-value / Occurrence
Be II@272.89*Ti I@399.86	-11.883	1.95E-12	1.95%	9.98918E-11
Ti I@399.86*Zr III@266.43	8.6230	9.52E-11	2.80%	3.39557E-09
Be II@272.89*Cu I@324.75	142.45	7.36E-10	7.68%	9.5787E-09
Mg III@239.51*Si I@288.16	-25.625	6.70E-09	9.63%	6.95332E-08
P I@253.56*F II@350.56	-4.478	2.98E-09	0.24%	1.22368E-06

Binomials & Elements	Coefficient	p-value	Occurrence %	p-value / Occurrence
Be II@272.89*Cu I@327.4	-119.80	1.03E-06	7.32%	1.41409E-05
O III@393.48*P I@253.56	3.0743	4.63E-07	2.13%	2.17127E-05
Be II@272.89*Na II@298.42	-24.9375	0.00019267	7.74%	0.00248
Mn I@279.83	3.2323	9.39E-06	0.06%	0.0154
Fe I@374.95*Fe I@374.95	-1.805	0.012	16.22%	0.0754
Ti II@376.13*Tl I@276.79	1.4465	0.0064	1.59%	0.4084
Pb I@280.2*Tl I@276.79	0.91964	0.0279	5.55%	0.5040
Cu I@324.75	-1.1882	0.6015	91.46%	0.6577
Cu I@327.4	-1.6698	0.5600	83.66%	0.6695
Si I@288.16	-0.999	0.7555	78.60%	0.9613
Na II@307.83	0.2915	0.3545	6.46%	5.485
Ba II@455.4*Fe I@374.95	-2.585	0.0060	0.06%	9.851
Ba II@455.4*Ca II@317.93	-2.641	0.0115	0.06%	19.006
Ga I@294.36*Ni I@349.3	0.6803	0.188	0.98%	19.353
Fe II@234.35*P I@253.56	-0.6785	0.8258	1.95%	42.32427175
Sn II@335.2	0.8393	0.2757	0.24%	113.04
Be III@448.73*Cr I@427.48	0	1	0.06%	1640
Al II@281.62*Ba II@455.4	2.990	0.0004	0.00%	No occurrence
Ca II@317.93*Cr I@427.48	-1.492	0.0786	0.00%	No occurrence
Ca II@317.93*Cl II@481.01	-1.253	0.056	0.00%	No occurrence
N II@399.5*P I@253.56	-2.9436	0.0012	0.00%	No occurrence

The idea behind this statistical sort is to select the interaction effects or ions with the smaller p-values and the higher occurrences. The values with smaller p-value/occurrence ratios are located at the top of the table, while those with higher ratios are at the bottom.

$$\frac{p-value\ \downarrow}{Occurrence\ \%\ \uparrow}$$

Some of these variables have no occurrence. However, while being computed, these values could have been selected for correlation. This provides clear evidence of the error and the importance of analyzing the variables independently.

4.9.2 Final correlation for the Oxide samples

The final selection of the variables consists of the top 8 binomials listed in Table 4-16. Furthermore, the two Copper ions available from LIBS responses were also added because they have a high occurrence, and provide a direct response for the predicted copper. Silicon was also

included as part of the variables because it has a high occurrence, and it is geologically related to Copper. The 1st Interaction Effect (I.E.) and 2nd Interaction Effect provide a reference for the confidence of the value with regard to the identification of the elements.

Table 4-17: Final correlation for Copper Oxides

1st I. E.	2nd I. E.	Elements/Binomials		Coefficient	p-value
Poor	Good	Be II@272.89*Ti I@399.86		-11.867	2.63E-07
Good	Very Good	Ti I@399.86*Zr III@266.43		8.243	5.49E-06
Poor	Very Good	Be II@272.89*Cu I@324.75		158.5	1.10E-06
Good	Very Good	Mg III@239.51*Si I@288.16		-36.10	1.74E-08
Good	Unknown	P I@253.56*F II@350.56		-3.835	0.0002
Poor	Very Good	Be II@272.89*Cu I@327.4		-160.4	2.06E-06
Unknown	Good	O III@393.48*P I@253.56		2.317	0.009
Poor	Very Good	Be II@272.89*Na II@298.42		-10.13	0.343
Very Good	Very Good	Cu I@324.75		-1.43	0.946
Very Good	Very Good	Cu I@327.4		6.111	0.041
Very Good	Very Good	Si I@288.16		5.678	0.2876
		Intercept	37480.6		

The final proposed predictive equation for Oxide Copper given the 41 samples is:

$$Predicted\ Cu(ppm) = 37480.6 - 11.86 * Be\ II@272.89 * Ti\ I@399.86 + 8.24 * Ti\ I@399.86 * Zr\ III@266.43 + 158.59 * Be\ II@272.89 * Cu\ I@324.75 - 36.10 * \text{Mg III@239.51*Si I@288.16-3.83* P I@253.56*F II@350.56 - 160.45*Be II@272.89*Cu I@327.4} + 2.31\ \text{O III@393.48*P I@253.56-10.13* Be II@272.89*Na II@298.42-1.43* Cu I@324.75} + 6.11\ \text{Cu I@327.4} + 5.67\ \text{* Si I@288.16}$$

Equation 4 - Predicted Copper for Oxide Samples Method B

The prediction has a Pearson Correlation Coefficient of 0.949. Although it shows a slightly lower value than the coefficient in the last regression of 0.961, this value is more reliable. The standard deviation is 1779. The histogram below provides evidence that the Predicted Cu values tend to be lower values than the real values (assumed as the ICP Copper). Figure 4-14 shows a map of standard deviations for the 41 samples. The critical numbers for correlation prediction land on values near to those for the cut-off of the mine. 0 to 5000 ppm (0 to 0.5%) is a typical range for cut-off grades. Further research is suggested in order to group grade ranges for different mines so that error could be better controlled at grades close to the cut-off ranges.

It is notable that there is a negative correlation between the Copper concentration, as indicated by the coefficient for the wavelength 324.75. As shown in Table 4-4 there is a positive correlation between Copper grade and the magnitude of the Copper peak from LIBS at this wavelength. Therefore, the negative correlation is an artifact of the regression analysis that uses more than 1 wavelength to represent Copper.

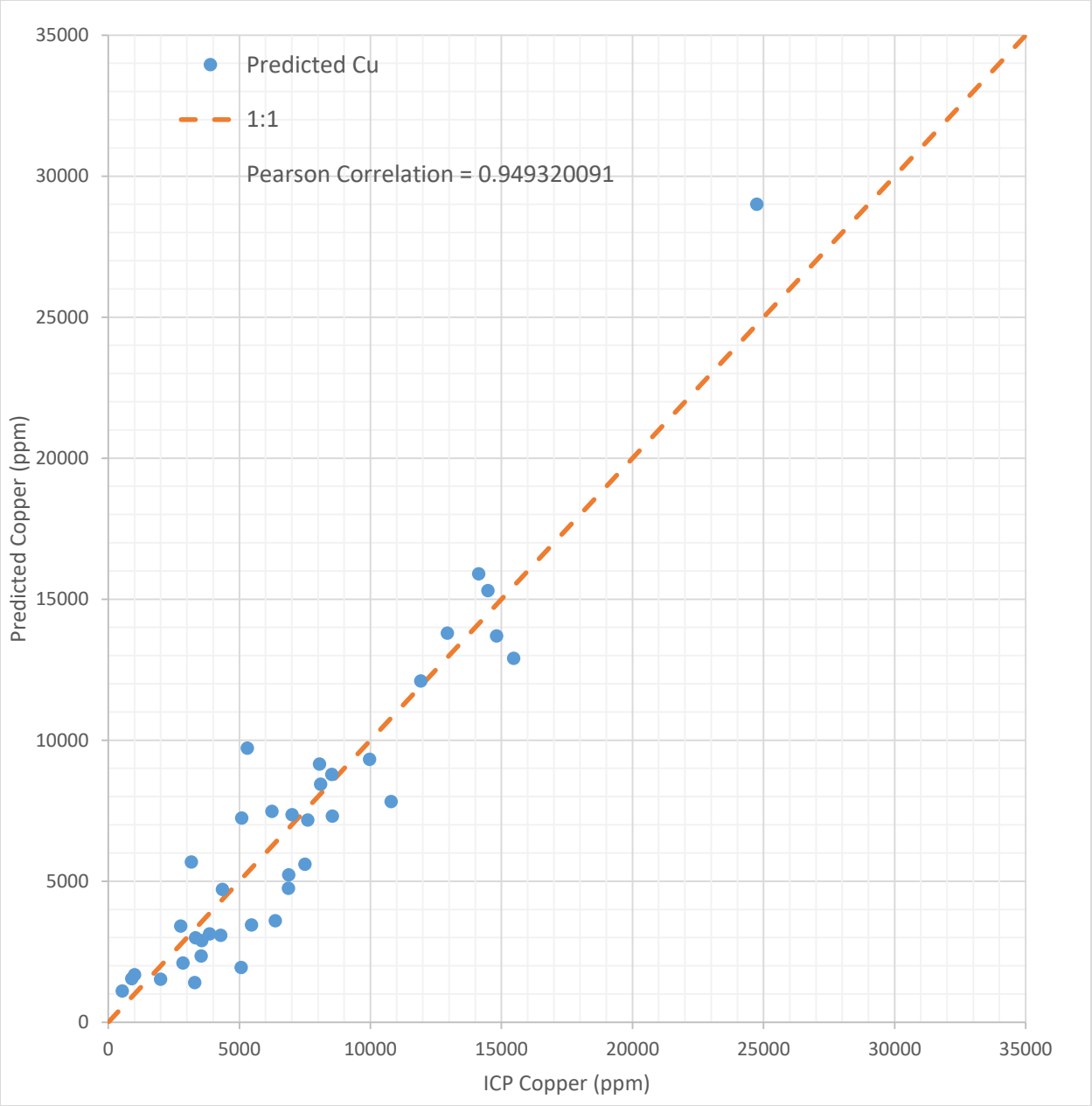

Figure 4-12: Final correlation for Copper Oxides

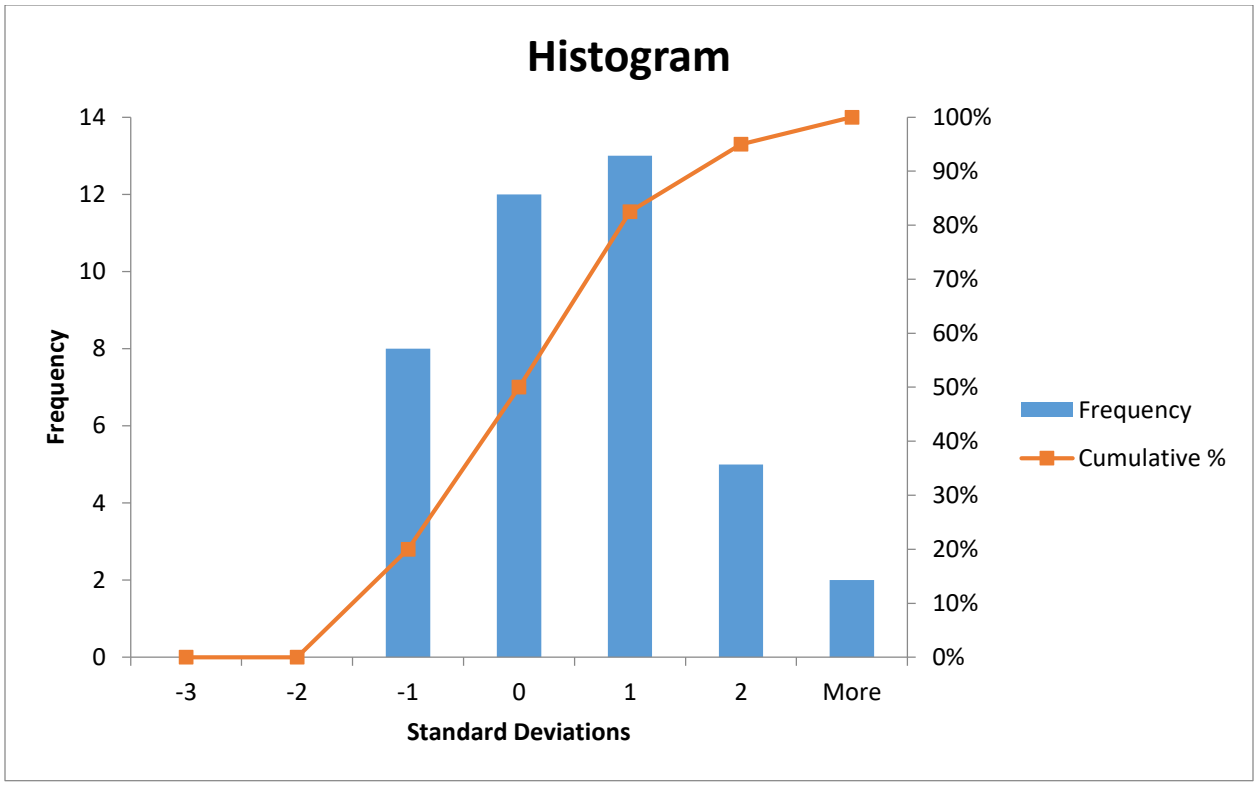

Figure 4-13: Histogram for the final correlation of Oxide samples

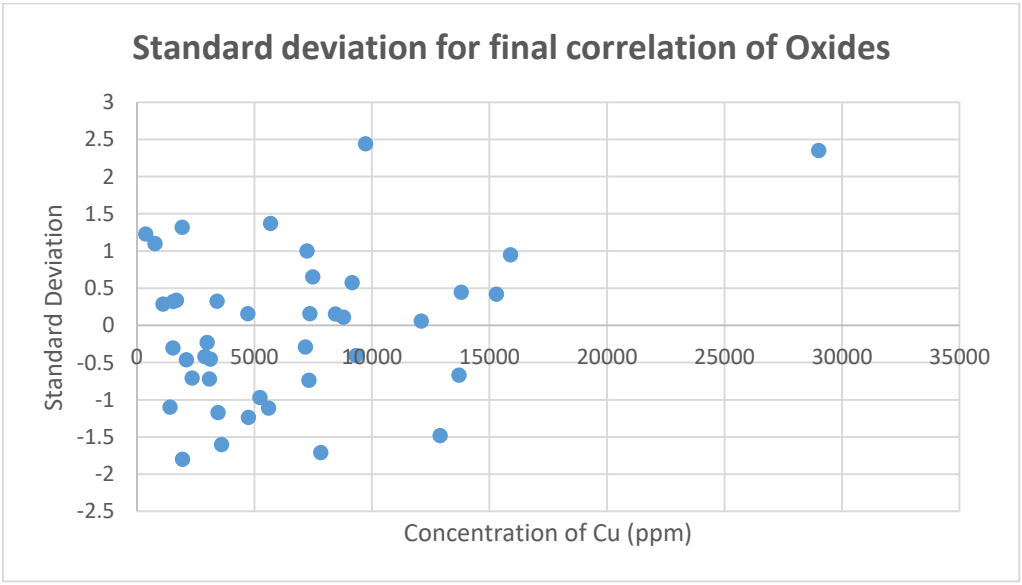

Figure 4-14: Standard deviation for the final correlation of Oxide samples

Chapter 5: Analysis of Sulphides with Laser Induced Breakdown Spectroscopy

LIBS responses were obtained by shooting 38 Sulphide samples from Escondida Mine. Each sample was shot on 4 faces, had 10 readings per face, with a total of 40 readings per sample. The methodology for the analysis of the Sulphide samples is similar to the methodology used for the Oxide samples. Thirty-eight Sulfuro (Sulphide) samples were analyzed with LIBS, and the responses are attached in Appendix F . The ICP Sulfuro results shown in Appendix H include Sulfuro-3, which is not included in the LIBS responses. Sulfuro-3 is a dust-type material that is difficult, if not impossible, to read it using LIBS. Because of this, it was not included in this analysis.

An extraction of the output of the Python Script for the Sulphide sample analysis is shown in Table 5-1, and the compiled output is attached in Appendix F . Table 5-1 includes the rock sample, as well as each ion identified in the reading of that rock.

Table 5-1: Extraction of the output of the Python Script for the Sulphide samples

	Sample Rock	Peak Wavelength	Element	Intensity	Acc.	Observed Wavelength Air
0	Su1,S1,0	274.89	Cd II	1211		274.854
1	Su1,S1,0	324.82	Cu I	2530	AA	324.754
2	Su1,S1,0	327.43	Cu I	2145	AA	327.3957
3	Su1,S1,0	374.88	Fe I	1002	A	374.9485
4	Su1,S1,0	234.42	Fe II	897	A+	234.3495
5	Su1,S1,0	238.17	Fe II	1100	B+	238.2037
6	Su1,S1,0	285.2	Mg I	860	A	285.2127
7	Su1,S1,0	279.56	Mg II	942	A+	279.5528
8	Su1,S1,0	239.61	Mg III	1012	A	239.5149
9	Su1,S1,0	298.37	Na II	927	B	298.4186
10	Su1,S1,0	419.97	S VI	841	AA	420.083
11	Su1,S1,0	419.97	S VI	841	AA	419.89
12	Su1,S1,0	288.15	Si I	1220	B	288.1579

5.1 Correlation of LIBS Cu Sulphide response to ICP analysis

The initial LIBS correlations for the Sulphide samples using only the LIBS responses for Copper ions are shown in Figure 5-1. In comparison to the values shown in Figure 4-4 and Figure 4-5, these samples reveal a very low correlation coefficient of 0.077 for Cu I at 327.4, and -0.06 for Cu I at 324.75. The correlation coefficient is based on the standard deviations. The same value for the correlation coefficient was obtained using the raw data from LIBS, or through normalizing the data. The normalization of the data was initially done by taking the maximum peak of a spectrum and then setting that value as 1. The noise was calculated in a similar manner as it had been for Table J-4, with the noise value set at 0. However, the correlation coefficient is the same. It is important to note that the Sulphide samples have a white colouration, which makes it more difficult to read using LIBS, and increases the noise in the spectrum.

In order to improve this correlation coefficient, it is suggested to determine the Lower Limit of Detection and the range for the LIBS machine. The Lower Limit of Detection can be calculated by reading pure metal samples with known concentration to develop a calibration curve for each ion. Such a calibration renders LIBS a powerful device for measuring concentration. However, this research does not aim to develop the measuring capabilities of LIBS, but rather its intention is to develop LIBS' correlation capabilities in a geological environment.

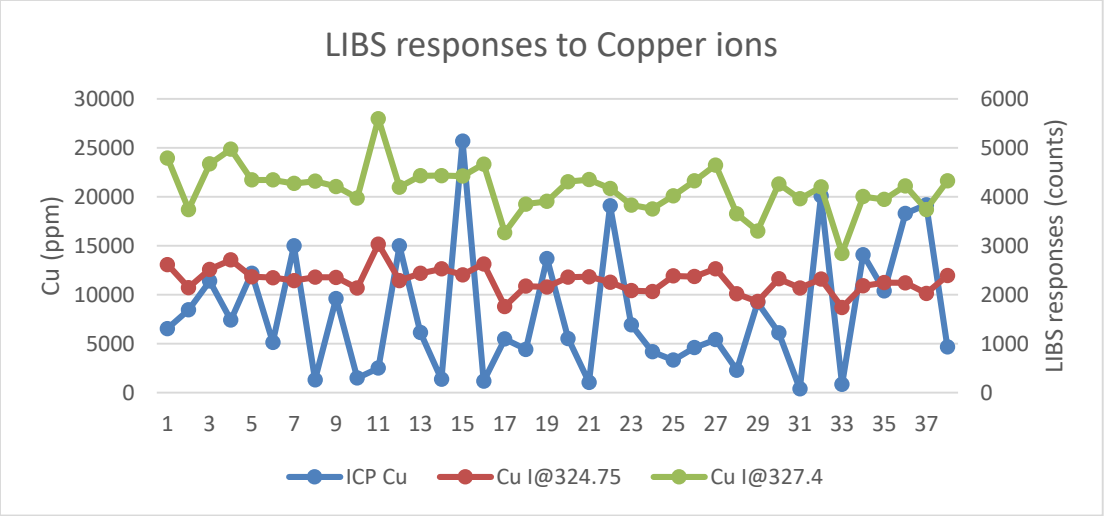

Figure 5-1: LIBS responses for Copper ions for Sulphide samples

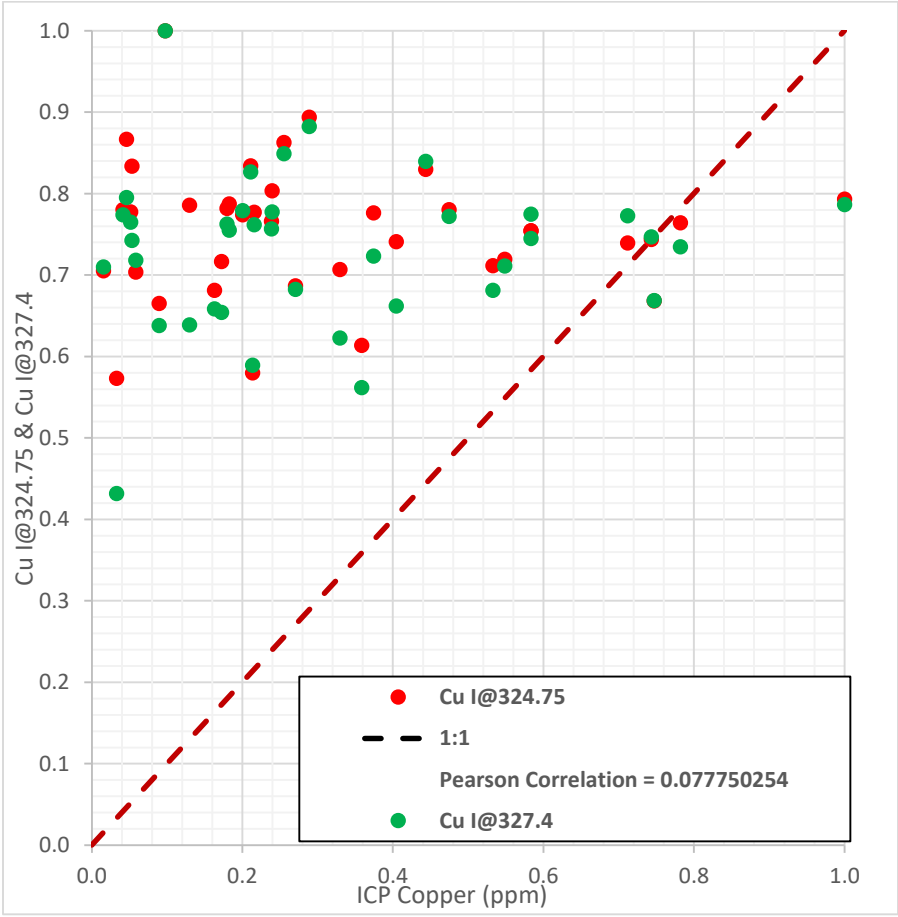

Figure 5-2: Basic correlation between ICP Cu vs LIBS Copper ions responses

5.2 Element correlation for LIBS responses for Sulphide samples

The ion responses in Appendix F were used to build a basic correlation based on "t-statistics" and p-values. The first interpretation of this correlation suggests a new unexpected component with respect to the list of ions for Sulphides - the presence of the Carbon element. The presence of C III at 229.69 was not expected to be present, and the ICP results in Appendix H do not report the presence of Carbon. In addition, there are no readings of C III at 229 in the Oxide LIBS responses, making the presence of the element even more suspicious. However, even small responses in LIBS could be accepted as good responses because of the particle size of the elements. ICP is bulk testing while LIBS is a superficial test. Appendix G shows the number of responses for the C III ion, and as expected, the responses are small in number in comparison to other ions in the same table.

A geological interpretation of this unexpected scenario may be that Sulphide oxidation takes place during the natural weathering process, thus generating acid that will dissolve carbonates. As such, Carbon responses are not present in the Oxide samples.

The predicted Copper correlation was conducted in MATLAB once the responses were processed in the Python Script. The results for the basic correlation are shown in Figure 5-2. They have a Pearson Correlation Coefficient of 0.824, which is high in comparison to the 0.77 coefficient for the Oxide samples that were seen in Figure 4-6.

Table 5-2: Predicted Copper correlation using ions for Sulphide samples

Elements	Coefficient	Std. Error	p-value	Occurrence	Occurrence%
C III@229.69	-6.036	2.0991	0.0075	29	2%
Ag II@241.32	6.1057	2.0347	0.0055	79	6%
Al II@281.62	-6.317	1.6232	0.0005	57	4%
Ba II@455.4	-6.816	2.0373	0.0023	31	2%
Ga I@294.36	-6.959	2.2109	0.0038	144	11%
Mg III@239.51	-4.554	1.2981	0.0015	421	32%
Ta I@362.66	-7.451	2.8549	0.0142	4	0%
Zr III@262.06	-3.819	1.6705	0.0297	37	3%
Intercept	23165				

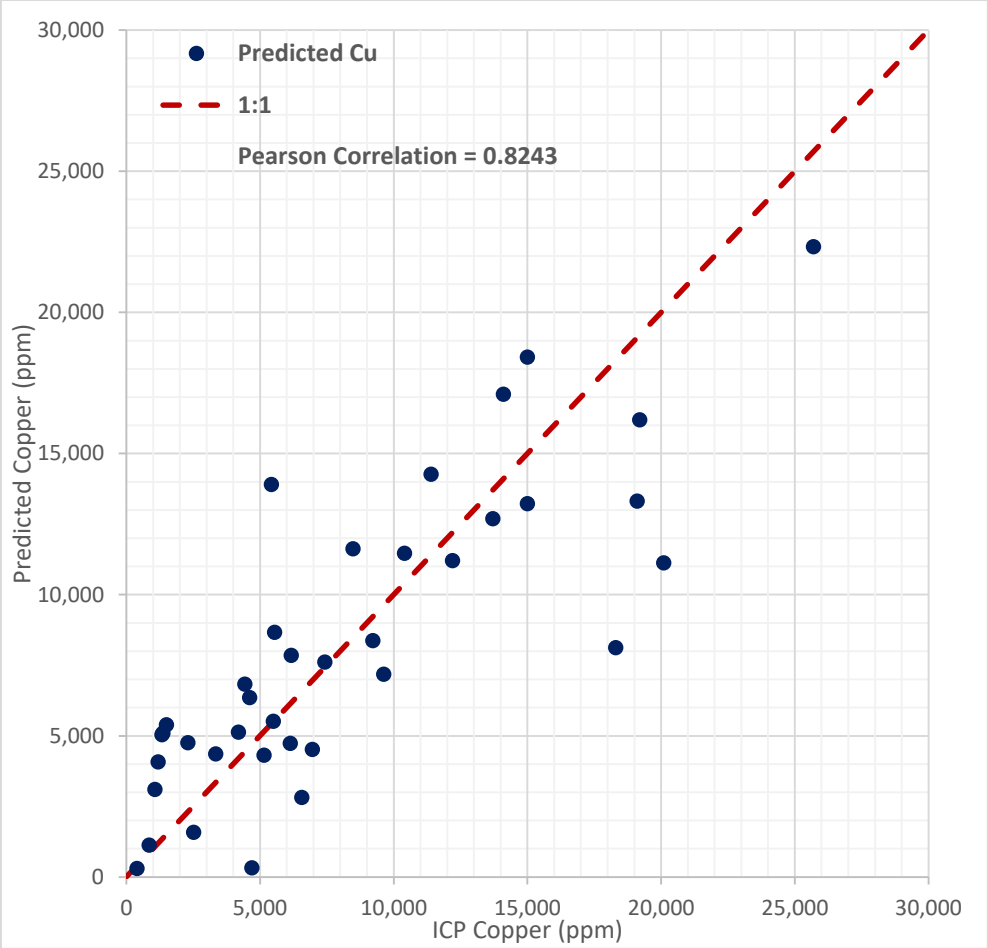

Figure 5-3: Predicted Copper correlation using ions for Sulphide samples

One issue not discussed in the chapter regarding the Oxide sample analysis was the relationship to the low p-value, which is the key element for the selection of the independent variables. A suspiciously high correlation coefficient was found in Table 5-2. There exists a relationship between the p-value, standard error, and the number of responses obtained from LIBS. As in Table 4-3, Table 5-2 shows that the p-value is significantly small (good for correlation) when occurrence is low. Occurrence calculation involves the sum of responses for each ion, and the percentage is based on the maximum number of responses for all of the ions. The discrepancy

between the two tables mentioned provides evidence to affirm that there is a relationship between the low number of responses and a possible low p-value.

Sections 4.8 and 4.9 explain in detail the reasons that a low occurrence of responses in a laboratory research project should be avoided.

5.3 Interaction effect analysis using multilinear regression analysis for Sulphide samples

Binomial regression analysis is performed to find possible interaction effect variables that can generate a good response for the LIBS sensor correlation. Much like the methodology described for the Oxide samples, the Sulphide samples were processed using the Python Script that can be found attached in Appendix C . The 65 samples from Appendix F were processed, obtaining 4225 binomials. These binomials will generate numbers in different magnitudes than found in the ion responses. To solve this issue, the square root was applied to all the binomials obtained from the Python Script. Once the sheets were ready to be processed, the data was analysed with MATLAB in order to find potential interaction effect responses to meet the requirements for mathematical correlation.

The mathematical correlation defines the p-value at 0.05 as a standard, which means that 1 in 20 samples will exceed the 2 standard deviations. The Stepwise procedure will remove elements from the list that do not meet this criterion.

The LIBS responses were processed using the Python Script that is attached in Appendix D . This multiplication was processed in MATLAB using the Stepwise Fit procedure. The correlation was not successful with respect to the small number of significant interaction effects and the geological interpretation of those effects. Table 5-3 shows the binomial correlation if a p-value of 0.05 is imposed.

Table 5-3: Binomial correlation for Sulphide samples with maximum 0.05 p-value

Binomial	Coefficient	p-value	Std. Error
Al II@281.62*Cd II@274.85	-5.48	4.11E-04	1.394
Ba II@455.4*Ca II@317.93	-14.52	7.49E-04	3.908
C III@229.69*Ga I@294.36	-9.61	9.86E-06	1.844
Cu I@324.75*Cu I@324.75	-8.16	1.38E-02	3.139
Intercept	33084.15		

In comparison to the Oxide samples that used a p-value of 0.05, using 0.05 for the Sulphide rocks does not provide a good output to use for correlation. Only 4 binomials passed the p-value requirement, and one of them is Cu I@324.75*Cu I@324.75, which has a bigger p-value when analyzed through the element analysis described in section 5.2.

This regression analysis was not successful because of the small number of significant variables. Therefore, other types of linear correlation were attempted. One of the functions tested was Stepwiselm in MATLAB, which performs a linear regression analysis using forward and backward elimination for arriving at the final model, and provides a decision based on the Akaike Information Criterion (AIC). The AIC value for this correlation is 747.93. A lower number for the AIC represents a better correlation. The AIC value for the Oxide samples was 772.55. However, there was no need to use this tool because the correlation output was satisfactory.

The results of Stepwiselm used the data from Appendix F and the final output is shown in Table 5-4.

Table 5-4: Stepwiselm output using the Sulphide ion responses

	Estimate	SE	tStat	pValue
(Intercept)	231	2351.2	9.852	9.2415e-11
x2	-6.03	2.091	-2.87	0.0074
x4	6.10	2.03	3.007	0.0054
x5	-6.31	1.62	-3.899	0.00053
x7	-6.81	2.03	-3.345	0.0022
x22	-6.95	2.21	-3.145	0.0037
x29	-4.55	1.29	-3.501	0.0014
x52	-7.45	2.85	-2.61	0.0141
x64	-3.81	1.67	-2.281	0.0297

Where X# stands for:

X	Elements
2	C III@229.69
4	Ag II@241.32
5	Al II@281.62
7	Ba II@455.4
22	Ga I@294.36
29	Mg III@239.51
52	Ta I@362.66
64	Zr III@262.06

Stepwiselm will use the independent variables for computing either alone or multiplied by another independent variable. This means that for the Sulphide samples, there are no binomials that will show a good fit for the correlation using a p-value threshold of 0.05.

Using this information, it was inferred that the p-value of 0.05 was too low to invalidate the correlation. It was necessary to increase the threshold p-value to 0.08. Testing was conducted several times for 0.06 and 0.07, however same results were obtained.

Table 5-5: Correlation output for variables computed with 0.07 p-value

Binomial	Coefficient	p-value	Std. Error
Al II@281.62*Cd II@274.85	-5.47	0.00041	1.394
Ba II@455.4*Ca II@317.93	-14.5	0.00074	3.907
C III@229.69*Ga I@294.36	-9.61	9.86485E-06	1.844
Cu I@324.75*Cu I@324.75	-8.1	0.01381	3.138

5.4 First procedure run analysis for the regression of Sulphide samples

The problem with increasing the p-value is that the procedure will accept more values with a higher error than for 2 standard deviations. In other words, the correlation will not be as good as expected. The correlation was computed using a 0.08 p-value for the interaction effect variables.

Table 5-6: Results of the first run using Stepwise Fit regression in MATLAB for Sulphide samples

Binomial	Coefficient	p-value	Std. Error
Ag II@232.02*Ag II@241.32	1.290	0	0
Al II@281.62*Ba II@455.4	-11.784	0	0
Al II@281.62*Cd II@274.85	-3.314	0	0
Al II@281.62*Cr I@427.48	-1.084	0	0
Ba II@455.4*Be II@272.89	-7.853	0	0
Ba II@455.4*Ca II@317.93	-3.278	0	0
Ba II@455.4*Si II@413.09	9.481	0	0
C III@229.69*Ga I@294.36	-6.833	0	0
Ca I@422.67*Zr III@262.06	-1.206	0	0
Ca II@317.93*W II@248.92	0.655	0	0
Cd II@274.85*Mn I@279.83	12.620	0	0
Cd II@274.85*Si I@288.16	-0.001	0	0
Cu I@324.75*Cu I@324.75	-16.317	0	0
Cu I@327.4*Si I@288.16	50.920	0	0
Fe I@374.95*O III@393.48	0.560	0	0
Fe II@234.35*O III@393.48	3.223	0	0
Fe II@238.2*Pb I@283.31	-7.528	0	0
In II@294.1*Zr III@262.06	6.014	0	0
Ir I@269.42*P I@253.56	-11.868	0	0
Mg I@285.21*Mn I@279.83	-6.416	0	0
Mg III@239.51*O III@393.48	-1.503	0	0
Mn I@279.83*N IV@347.87	-2.375	0	0
Na II@298.42*Zr III@262.06	-12.288	0	0
O III@393.48*Tl I@351.92	-0.486	0	0
P I@253.56*Pb I@283.31	8.475	0	0
P I@253.56*V II@292.4	0.006	0	0
P I@253.56*Zr III@262.06	-0.873	0	0
P IV@334.77*Sn II@335.2	5.993	0	0
Pb I@283.31*Zr III@262.06	1.547	0	0
Sn II@335.2*Tl I@276.79	-1.402	0	0

As mentioned before, a p-value of 0 and standard error of 0 reflects a computer error because of the large amount of data processed into matrices.

5.5 Second procedure run analysis for the regression of Sulphide samples

The second run for the regression analysis was conducted using a p-value of 0.08. By using a different p-value, the coefficients, standard errors and p-values will change as a result of the mathematical procedure. P-values of less than 0.05 have been added in red.

Table 5-7: Results of the second run using Stepwise Fit regression in MATLAB for Sulphide samples

Binomial	Coefficient	p-value	Std. Error
Ag II@232.02*Ag II@241.32	0.417	0.936	5.201
Al II@281.62*Cd II@274.85	-5.201	0.000	1.157
Al II@281.62*Cr I@427.48	-0.536	0.796	2.058
Ba II@455.4*Be II@272.89	-3.630	0.233	2.983
Ba II@455.4*Ca II@317.93	-8.198	0.031	3.623
Ba II@455.4*Si II@413.09	1.841	0.509	2.756
C III@229.69*Ga I@294.36	-10.010	4.62E-07	1.550
Ca I@422.67*Zr III@262.06	-0.638	0.79	2.438
Ca II@317.93*W II@248.92	1.863	0.495	2.7006
Cd II@274.85*Mn I@279.83	-2.162	0.252	1.852
Cd II@274.85*Si I@288.16	0.486	0.75	1.544
Cu I@324.75*Cu I@324.75	-21.010	0.000	4.690
Cu I@327.4*Si I@288.16	34.875	0.002	10.71
Fe I@374.95*O III@393.48	-0.661	0.660	1.49
Fe II@234.35*O III@393.48	-0.789	0.593	1.462
Fe II@238.2*Pb I@283.31	-3.009	0.03	1.350
In II@294.1*Zr III@262.06	2.705	0.23	2.232
Ir I@269.42*P I@253.56	-5.502	0.014	2.119
Mg I@285.21*Mn I@279.83	-2.025	0.362	2.189
Mg III@239.51*O III@393.48	-0.157	0.913	1.440
Mn I@279.83*N IV@347.87	-1.316	0.651	2.88
Na II@298.42*Zr III@262.06	3.232	0.321	3.202
O III@393.48*Tl I@351.92	0.314	0.835	1.499
P I@253.56*Pb I@283.31	3.447	0.13	2.230
P I@253.56*V II@292.4	0.118	0.962	2.495
P I@253.56*Zr III@262.06	-2.158	0.4391	2.749
P IV@334.77*Sn II@335.2	3.392	0.218	2.696
Pb I@283.31*Zr III@262.06	0.150	0.964	3.380
Sn II@335.2*Tl I@276.79	-0.176	0.956	3.186

MATLAB calculates the matrices for correlation based on a p-value of 0.08. However, binomials with a value of less than 0.05 are selected. This is done to isolate the binomials with higher significance.

5.6 Proposed correlation of Sulphide samples

Selected binomials from Table 5-7 were joined with the ions selected from Table 5-2. Due to the reduced amount of independent variables favourable for correlation, geological background information was not included for this correlation. However, elements such as Cu, Si and Ca are related to the Copper Sulfide ores. MATLAB computed the variables for the third time, as seen in Table 5-8.

Table 5-8: Binomial correlation for Sulphide samples with maximum 0.08 p-value

1st I. E.	2nd I. E.	Variables	Coefficient	p-value	Std. Error
Good	Poor	Al II@281.62*Cd II@274.85	-5.170	0.000	1.219
Good	Poor	Ba II@455.4*Ca II@317.93	-9.736	0.014	3.736
Unknown	Unknown	C III@229.69*Ga I@294.36	-9.529	0.000	1.616
Very Good	Very Good	Cu I@324.75*Cu I@324.75	-21.521	0.000	4.935
Very Good	Very Good	Cu I@327.4*Si I@288.16	32.521	0.007	11.226
Very Good	Good	Fe II@238.2*Pb I@283.31	-2.801	0.058	1.419
Unknown	Good	Ir I@269.42*P I@253.56	-4.530	0.046	2.178
Unknown		C III@229.69	2.680	0.578	4.763
Good		Ag II@241.32	0.281	0.886	1.945
Good		Al II@281.62	-2.302	0.307	2.214
Good		Ba II@455.4	-0.398	0.854	2.144
Unknown		Ga I@294.36	-1.647	0.398	1.921
Good		Mg III@239.51	0.518	0.719	1.425
Unknown		Ta I@362.66	-2.665	0.347	2.789
Good		Zr III@262.06	-2.867	0.100	1.687
		Intercept	16154.47		

This time, variables with p-values of less than 0.08 were coloured in red, and this set of variables represents the variables proposed for a final correlation of the Sulphide ores at Escondida Mine. Negative coefficients express the mathematical shaping of the predictive equation.

$$Predicted\ Cu(ppm) = 16154.4 + Al\ II@281.62 * Cd\ II@274.85 * -5.170 + Ba\ II@455.4 * Ca\ II@317.93 * -9.736 + C\ III@229.69 * Ga\ I@294.36 * -9.529 + Cu\ I@324.75 * Cu\ I@324.75 * -21.521 + Cu\ I@327.4 * Si\ I@288.16 * 32.521 + Fe\ II@238.2 * Pb\ I@283.31 * -2.801 + Ir\ I@269.42 * P\ I@253.56 * -4.530$$

Equation 5 - Predicted Copper for Sulphide samples

Table 5-9: ICP Cu vs Predicted Cu values for Sulphide samples in ppm

Accuracy	ICP Cu	Predicted Cu
52%	6,560	3,157
11%	8,470	7,569
10%	11,400	10,249
55%	7,420	11,526
8%	12,200	13,232
33%	5,150	3,448
3%	15,000	14,483
120%	1,330	(266)
2%	9,620	9,398
86%	1,500	2,792
4%	2,510	2,408
8%	15,000	16,207
65%	6,160	10,139
368%	1,370	6,418
34%	25,700	17,017
302%	1,180	(2,381)
2%	5,490	5,576
91%	4,430	8,472
28%	13,700	17,519
11%	5,540	6,137
8%	1,060	973
38%	19,100	11,822
30%	6,950	9,046
89%	4,190	7,900
25%	3,340	2,519
51%	4,610	6,941
144%	5,420	13,243
39%	2,300	3,187
10%	9,210	8,287
30%	6,130	7,950
418%	393	2,037
48%	20,100	10,438
8%	849	784
0%	14,100	14,121
2%	10,400	10,192
8%	18,300	16,817
13%	19,200	16,793
16%	4,690	3,924
60%		

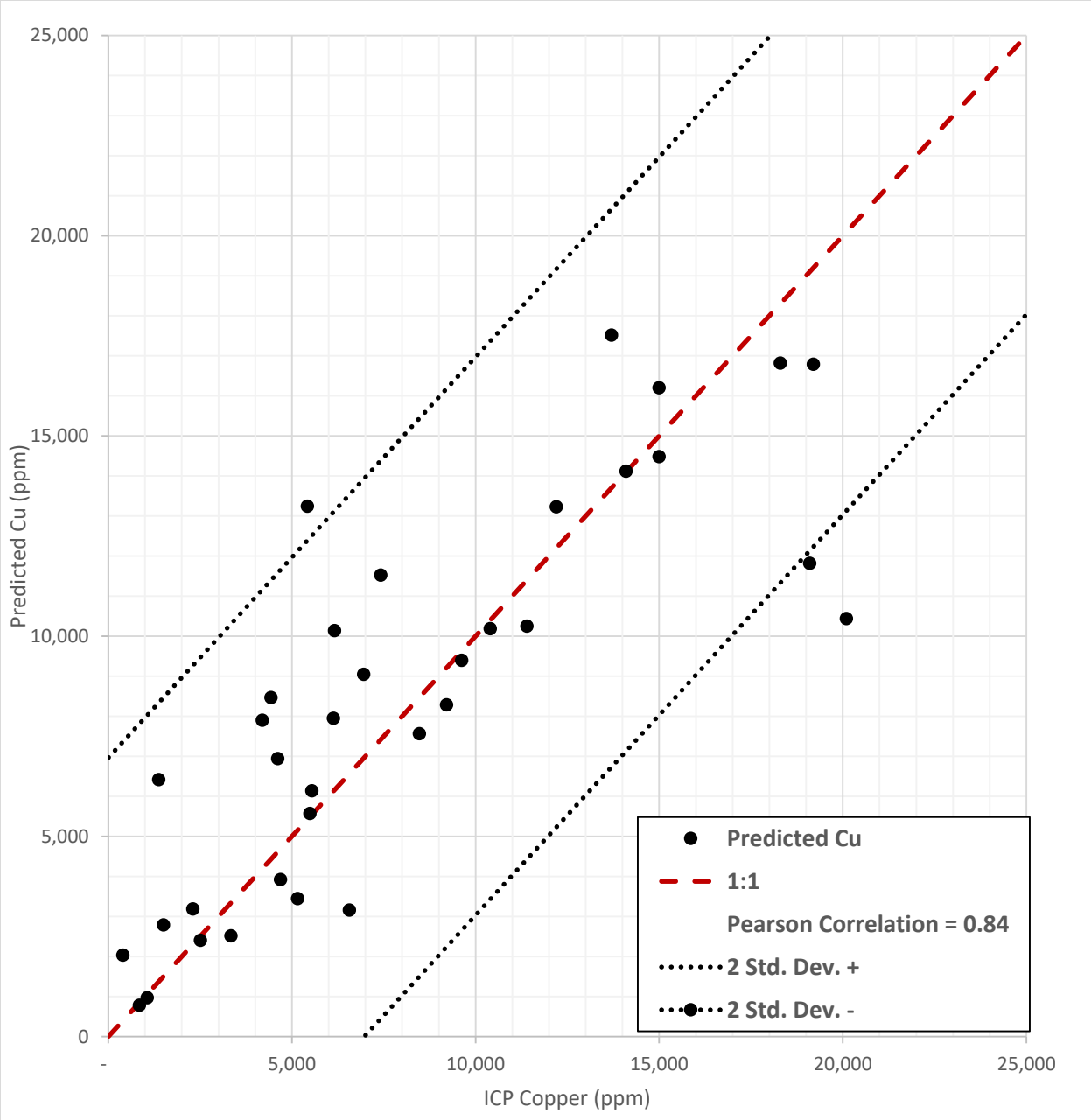

Figure 5-4: Final correlation for Sulphide samples

Figure 5-4 shows the final correlation for the Sulphide ores. The Pearson Correlation Coefficient is 0.84, which is close to the 0.82 coefficient value for the correlation of elements only. It is interesting to note the similarities between the correlations in Table 5-2 and Table 5-4,

which look very similar in terms of the variables used. The Linear Stepwise or “Stepwiselm” did not suggest any binomial, as it had for the Oxide samples. This means that the best fits obtained in Figure 5-4 are not necessarily the best possible fits. We can confirm this information by analyzing the Pearson Correlation Coefficients that are lower than 0.9.

The lines corresponding to the 2 standard deviations calculated from the correlation have been added to the chart. As mentioned previously, a p-value of 0.05 suggests that only 1 out of 20 samples will be out of the two standard deviations. In this case, a p-value of 0.08 was used to calculate this correlation. This means that 2 out of 25 values will be out of the range. As such, a projection of the number of samples that will be out of the range for 38 samples is 3.04, and in the graph, we see that 3 samples are outside of the lines for the two standard deviation.
If material is sorted on a daily basis, 8% of the material will result in blind sorting. Blind sorting could be defined as the material that sensors cannot read properly.

A good way to control for and measure blind sorting is through the use of histograms of standard deviations, as shown in Figure 5-5. This histogram shows the trend of the prediction as being mostly slightly above the real value. The optimum situation would see the histogram inclined to the negative standard deviation so that the sensor could take the response as a low value instead of as processing waste.

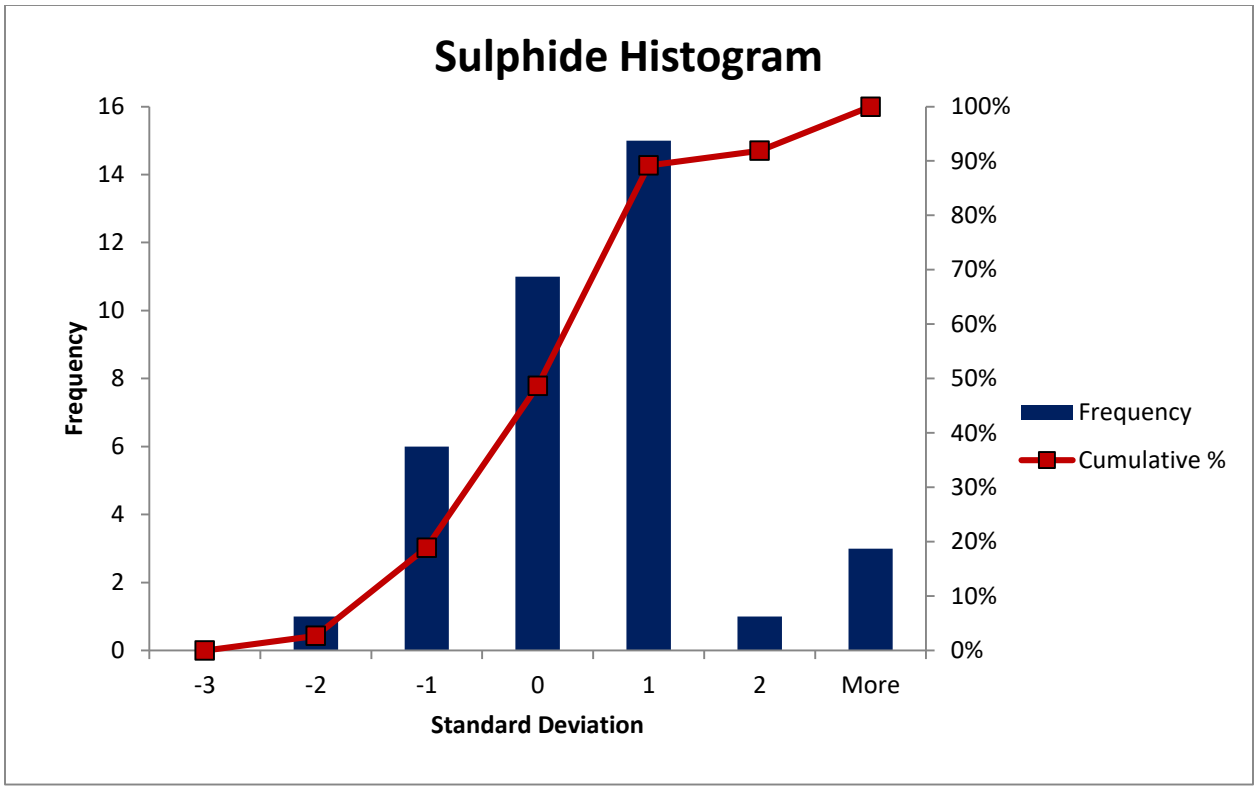

Figure 5-5: Histogram for the final correlation for Sulphide samples

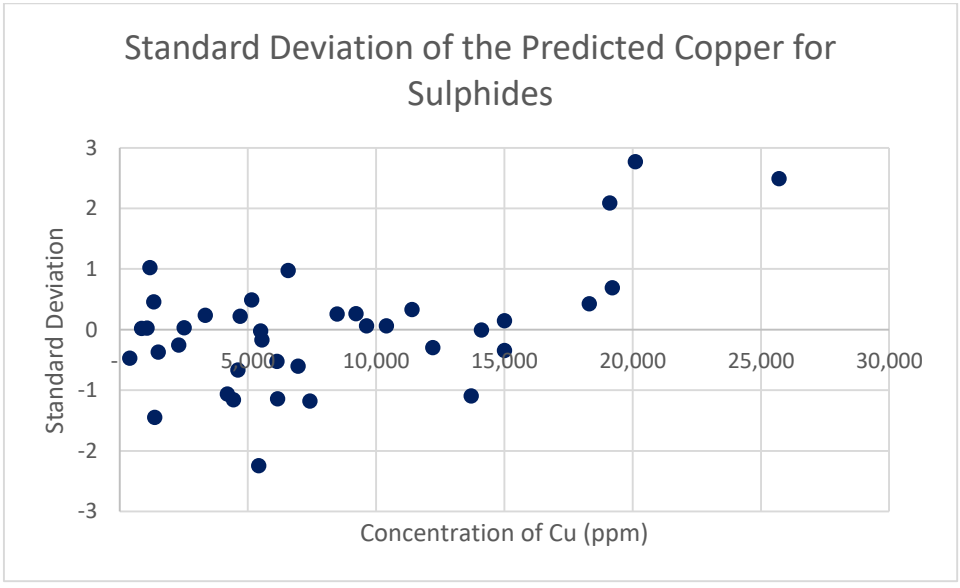

Figure 5-6: Standard Deviation for the final correlation for Sulphide samples

Chapter 6: Sulphide versus Oxide discrimination

The determination of an ore as an Oxide or a Sulphide is crucial for mine-mill reconciliation. The main purpose of the determination of Oxide or Sulphide ores during the mining process is to select the recovery method to be used for that ore. Sulphides are usually processed in the concentrator, while Oxides are usually leached. Although a discussion of the efficiency of each method is not the subject of this research, the economic impact of dilution in mining is an issue that has an effect on the efficiency of the recovery method, and can be solved through LIBS sorting.

6.1 Spectroscopy ambiguity regarding S III and O III for our LIBS machine

The wavelengths taken for the ions were obtained from the NIST database. The use of S III and O III are based solely on the probabilities of transition shown in the NIST database, and represent the only options available for the bandwidth used by FiberLIBS. A detailed discussion of the selection of the wavelengths can be found in Chapter 3:. However, there is ambiguity in defining the most appropriate wavelengths for Oxygen and Sulphur. Wavelengths were identified according to following pattern:

1. Transition strength (Aki)
2. Accuracy (Acc.)
3. Relative Intensity

The rocks analyzed for this research belong either to Oxide or Sulphide ores. There is a characteristic triplet of spin around the wavelengths at 393.42, 394.45 and 396.15 nm. According to the theory of Nuclear Magnetic Resonance Spectroscopy, spins happen because ions have slightly different chemical shifts, represent slightly different spin flip energies, or have nucleii with slightly different magnetic environments.

The wavelength characteristics for these 3 wavelengths were verified using the NIST database as:

- 393.42 nm for O III
- 394.45 for O III
- 396.15 for S III and O III in overlap situation, favourable for S III

6.2 Spectroscopy and observation of multiple strong lines

The main reason that it is necessary to analyze this ambiguity is because the LIBS machine used for this research has limitations with respect to bandwidth. The bandwidth of the machine can detect a range from 229 nm to 500 nm, creating smaller wavelength pixels possible to analyze in comparison to broader LIBS bandwidths. Stronger lines for Oxygen and Sulphur can be found beyond 500 nm with a higher definition, however this limitation does not limit LIBS' capacity to recognize an Oxide or Sulphide sample.

In order to define the parameters to allow LIBS to recognize an Oxide or Sulphide, it is necessary to understand the wavelength characteristics for Oxygen and Sulphur. Table 6-1 shows the spectroscopies taken from the NIST database (National Institute of Standards and Technology NIST), providing a mining search criteria of C+ for accuracy.

Table 6-1: Spectroscopies for ambiguity between O III and S III

Spectrum	Observed Wavelength Air (nm)	Ritz Wavelength Air (nm)	Rel. Int. (?)	Aki s^-1	Acc.	Ei (cm-1)	Ek (cm-1)	Ei eV	Ek eV
Nd II	393.482	393.4815+	610	1.37E+07	B+	2585.46	27992.425	0.32	3.46
O III		393.4823		9.93E+07	C+	366802.62	392209.53	45.284274	48.42093
C IV		393.489		3.30E+07	A	445368.5	470775	54.98	58.12
W II	393.54325	393.54325	39	3.09E+06	B	13173.337	38576.313	1.63	4.76
Fe I	393.58122	393.58124	9300	1.14E+07	C+	22838.323	48238.847	2.82	5.96
Fe I	394.33404	394.33404	3630	6.46E+05	C+	17726.988	43079.023	2.19	5.32
Al I	394.40058	394.4006	24g	4.99E+07	B+	0	25347.756	0.00	3.13
Ar II	394.42712	394.42712	49	4.10E+06	B	132327.36	157673.41	16.34	19.47
O III		394.4854		1.17E+08	C+	366488.45	391830.76	45.25	48.37
Fe I	394.4889	394.4889	2820	1.40E+06	B	24118.819	49460.902	2.98	6.11
Fe I	396.02789	396.02786	1000	4.10E+06	C+	29356.744	54600.35	3.62	6.74
F V		396.08		1.52E+06	B	784099	809339.5	96.80	99.92
W II	396.08582	396.08601	5	4.24E+05	B	19637.309	44877.209	2.42	5.54
S III	396.1516	396.1526	12	9.45E+06	B	147551.6	172787.26	18.22	21.33
Al I	396.152	396.15201	26g	9.85E+07	B+	112.061	25347.756	0.01	3.13
O III	396.159	396.1573	200	1.25E+08	B	306586.08	331821.44	37.85	40.97
Nd II	396.221	396.2205+	510	7.10E+06	B+	2585.46	27816.795	0.32	3.43
Ti I	396.28508	396.28507	2500	4.71E+06	A	0	25227.222	0.00	3.11
Nd II	396.3114	396.3105+	1400	3.98E+07	B+	3801.93	29027.535	0.47	3.58
Nd II	396.39	396.3905+	270	1.14E+07	B+	5085.64	30306.15	0.63	3.74

An extraction from this chart, along with the surrounding ions that could be used to define and understand this ambiguity, can be found in Table 6-1. For 393.48 nm, the biggest transition strength is given to O III, with a total Aki of 9.93E+07. Similar conditions are set for the O III at 394.48, with an Aki of 1.17E+08. The biggest problem regarding the triplet definition is with respect to wavelength 396.15. The only surrounding ion with a higher Aki value is Al I, but it has a “g” comment which stands for “Transition involving a level of the ground term.” The best fits for its Aki and Accuracy are S III or O III. We conclude that this is a case of overlap, as discussed

in Chapter 5 of the "Handbook of Laser Induced Breakdown Spectroscopy" (Cremers and Radziemski). In order to define this ambiguity, it is possible to analyze the ionization energies with respect to the expected energy provided by the laser. As shown in Table 6-2, higher ionization levels require the provision of higher energy. For LIBS, the energy is limited, and it is likely to have greater certainty over smaller ionization energies than higher ones. The O III has a 54.93 eV in contrast to the S III 34.79 eV. This means that S III has a higher probability of being seen. However, the Relative Intensity of O III is 200 in comparison to S III with only 12 (Relative Intensity does not have units).

Table 6-2: Extraction of Ionization Energies (eV)

Element		I	II	III	IV	V
Hydrogen H	1	13.5984				
Helium He	2	24.5874	54.41776			
Lithium Li	3	5.3917	75.64	122.45429		
Beryllium Be	4	9.3227	18.21114	153.89661	217.71865	
Boron B	5	8.298	25.1548	37.93064	259.37521	340.2258
Carbon C	6	11.2603	24.3833	47.8878	64.4939	392.087
Nitrogen N	7	14.5341	29.6013	47.44924	77.4735	97.8902
Oxygen O	8	13.6181	35.1211	54.9355	77.41353	113.899
Fluorine F	9	17.4228	34.9708	62.7084	87.1398	114.2428
Neon Ne	10	21.5646	40.96296	63.45	97.12	126.21
Sodium Na	11	5.1391	47.2864	71.62	98.91	138.4
Magnesium Mg	12	7.6462	15.03527	80.1437	109.2655	141.27
Aluminum Al	13	5.9858	18.82855	28.44765	119.992	153.825
Silicon Si	14	8.1517	16.34584	33.49302	45.14181	166.767
Phosphorus P	15	10.4867	19.7695	30.2027	51.4439	65.0251
Sulfur S	16	10.36	23.33788	34.79	47.222	72.5945

In conclusion, we can say that both ions might be seen at 396.16 for this set of rock samples.

6.3 Definition of the spectrum for Oxides and Sulphides

In contrast to the belief that Oxygen will be found present in any reading because it exists in the air or because is abundant in rock samples, LIBS has shown the ability to recognize an Oxide or a Sulphide. This recognition is based on the plasma formation created by LIBS during the reading. Once excited, the ion of Oxygen or Sulphur will create a wavelength that cannot be contaminated by the air, at least for the particular wavelength we are examining in this section.

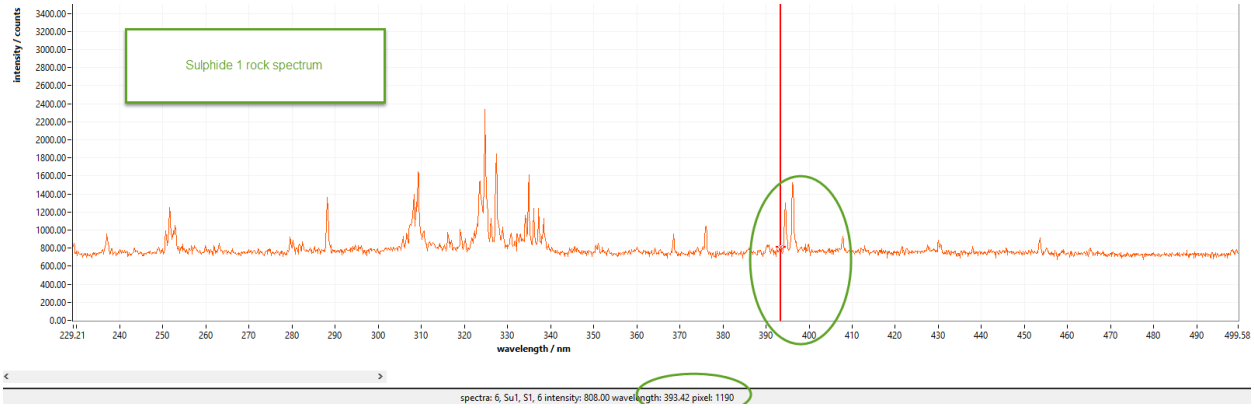

Figure 6-1: Spectrum for Sulphide 1

This set of figures showing the spectrums of the Sulphide and Oxide samples, provides a typical characterization of the spectrum. Three wavelengths together define that we can be seeing either an Oxide or a Sulphide sample.

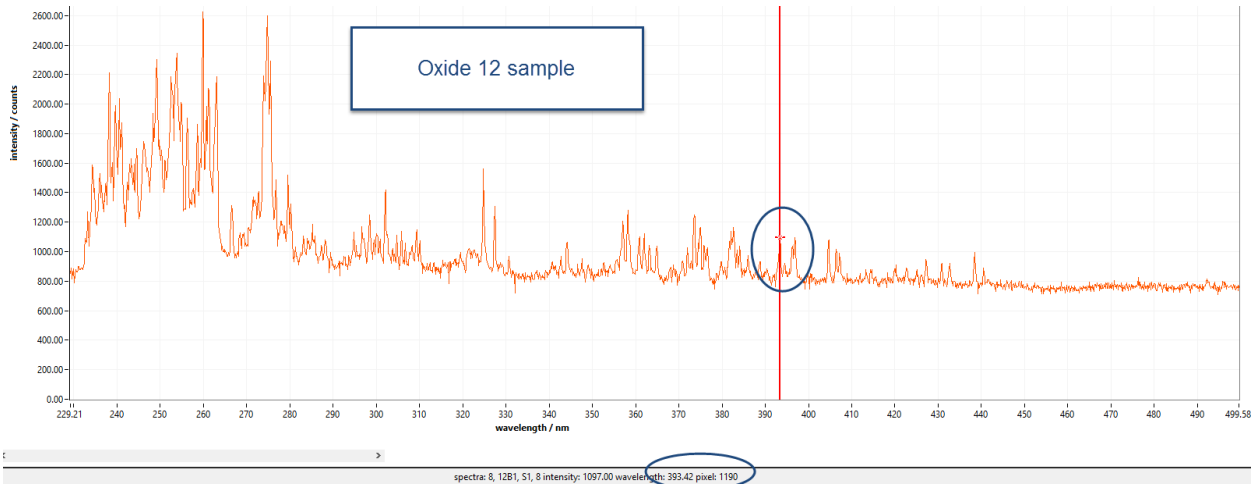

Figure 6-2: Spectrum for Oxide 12

Although Oxide samples will show as 3 wavelengths with peaks, the critical key for their identification will be a wavelength at 393.48 nm. For example, if we analyze another sample that is known to contain ions of Oxygen, then we should be able to see at least 2 of these mentioned wavelengths.

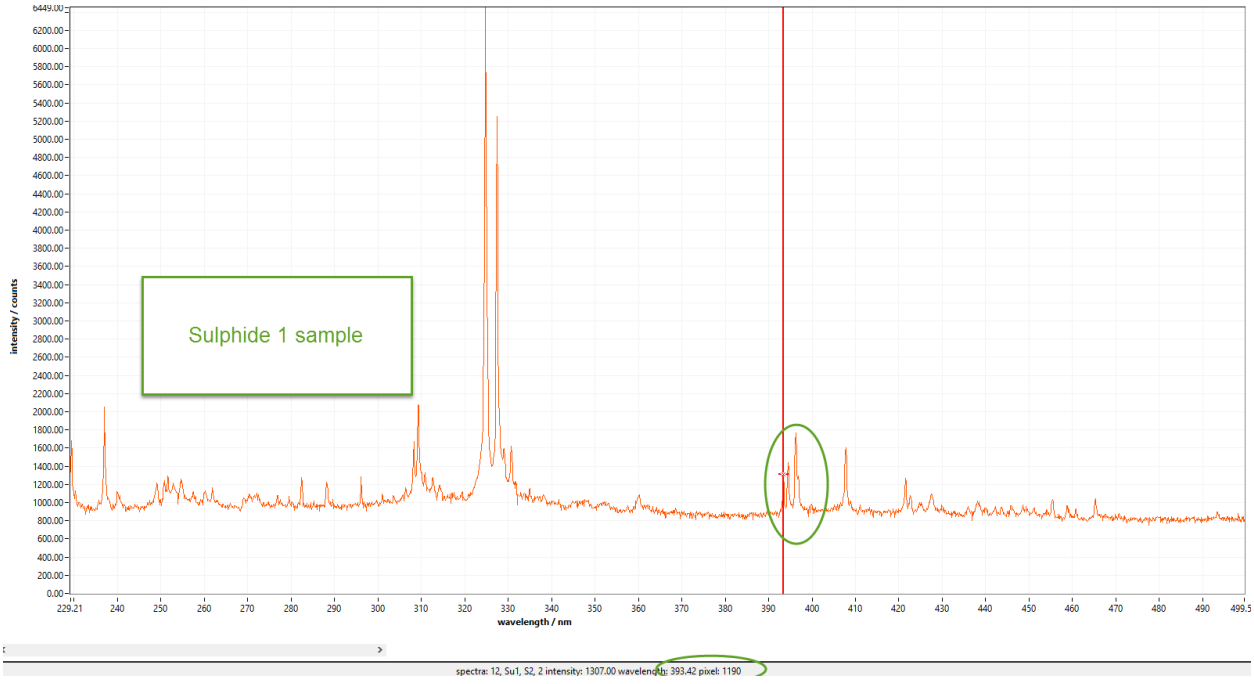

Figure 6-3: Spectrum for Sulphide 1

This turns out to be false as Figure 6-5 shows the spectrum for steel, which contains oxygen ions and it does not have the same 3 peak configuration as do the ore samples. Figure 6-6 shows another sample of a steel plate, and in this case, the spectrum reads the presence of an oxygen ion, possibly because of oxidation. The next peak for this spectrum is 396.8 nm, which does not correspond to the wavelengths mentioned. This particular ionization configuration and arrange of peaks can be seen in Oxide and Sulphide ores with this particular ore deposit.

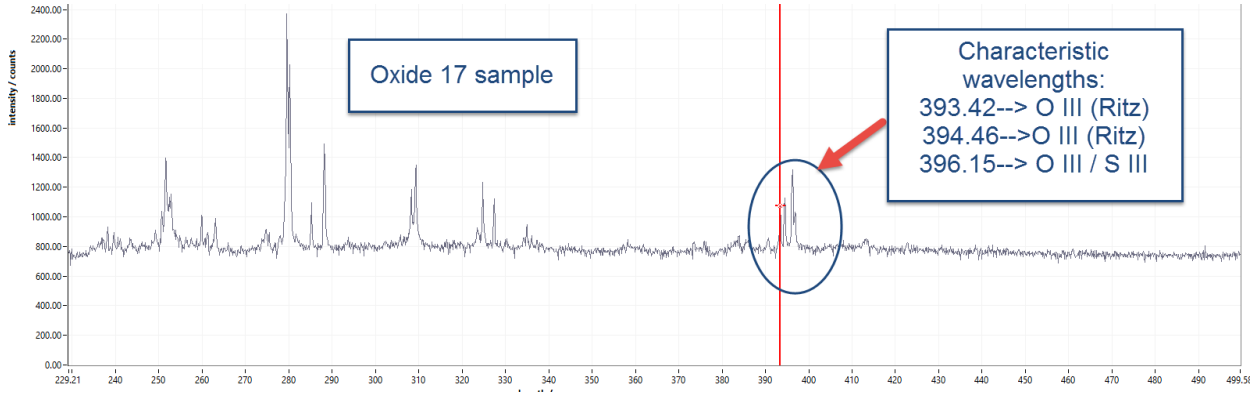

Figure 6-4: Spectrum for Oxide 17 with characteristic wavelengths for Oxide/Sulphide definition

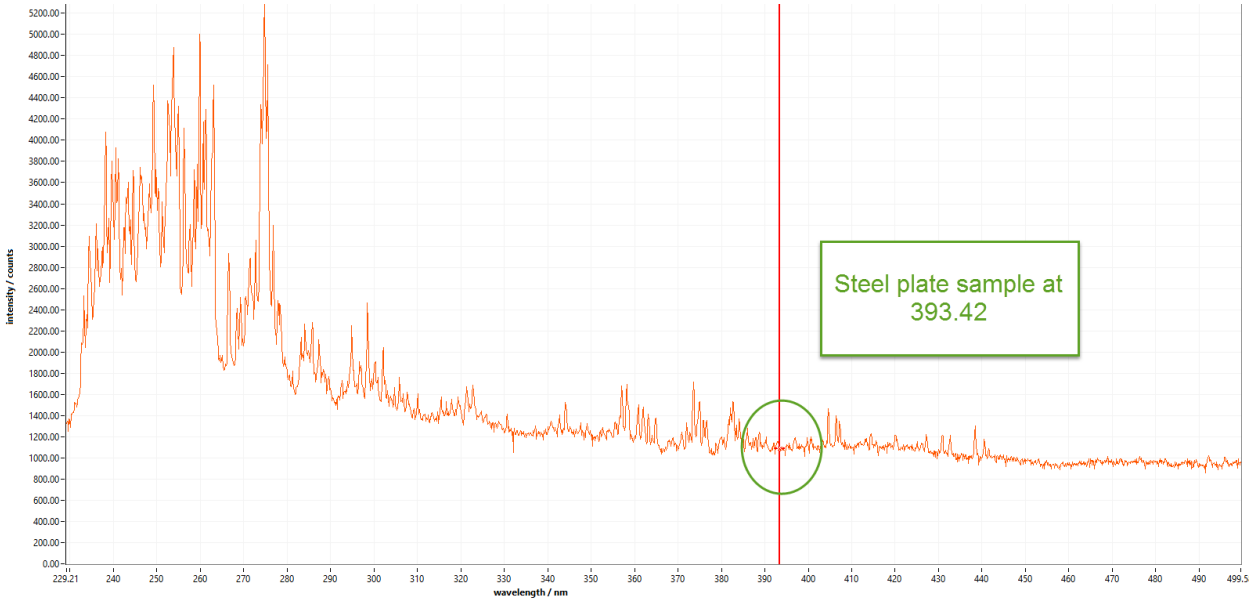

Figure 6-5: Steel pointed at 393.42 nm

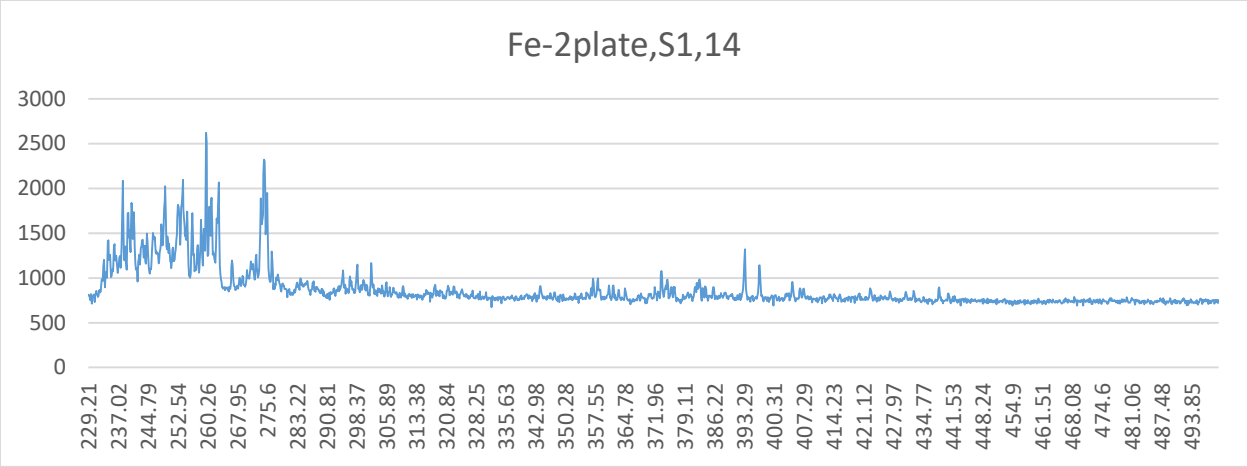

Figure 6-6: Steel spectrum with 393.42 nm wavelength peak

6.4 Proposed solution for Oxide/Sulphide recognition using LIBS

It is recommended that an automated script be developed with the following parameters.

1. Recognize the wavelength 396.15 as a peak
2. Recognize the wavelength 394.48 as a peak
3. Recognize the wavelength 393.42 as a peak
4. Normalize the spectrum from 0 to 1
    a. Calculate the mode based on the noise, as shown in Table J-5
    b. Subtract the mode from the whole spectrum and divide the rest by the maximum value of the current spectrum
5. Set a threshold of 0.15 and above for Oxides and 0.15 and below for Sulphides

Table 6-3: Final results table for Oxide versus Sulphide recognition

	Oxides			Sulphides			
	O III@393.48	O III@394.46	S III@396.15	O III@393.48	O III@394.46	S III@396.15	
OXIDE	0.261	0.255	0.369	0.084	0.224	0.330	SULPHIDE
OXIDE	0.203	0.215	0.310	0.115	0.278	0.411	SULPHIDE
OXIDE	0.204	0.219	0.317	0.054	0.129	0.198	SULPHIDE

	Oxides			Sulphides			
	O III@393.48	**O III@394.46**	**S III@396.15**	**O III@393.48**	**O III@394.46**	**S III@396.15**	
OXIDE	0.184	0.174	0.252	0.092	0.226	0.337	SULPHIDE
OXIDE	0.691	0.203	0.301	0.096	0.238	0.353	SULPHIDE
SULPHIDE	0.117	0.279	0.398		0.238	0.351	SULPHIDE
OXIDE	0.317	0.217	0.303	0.082	0.172	0.257	SULPHIDE
OXIDE	0.211	0.240	0.347	0.164	0.154	0.223	OXIDE
OXIDE	0.486	0.253	0.309	0.215	0.214	0.324	OXIDE
SULPHIDE	0.128	0.222	0.323		0.318	0.461	SULPHIDE
OXIDE	0.434	0.199	0.245	0.095	0.169	0.254	SULPHIDE
OXIDE	0.187	0.135	0.248	0.073	0.280	0.411	SULPHIDE
OXIDE	0.221	0.194	0.280	0.119	0.249	0.337	SULPHIDE
SULPHIDE	0.101	0.183	0.271	0.068	0.243	0.361	SULPHIDE
OXIDE	0.184	0.176	0.262	0.054	0.257	0.382	SULPHIDE
OXIDE	0.292	0.218	0.321	0.070	0.229	0.333	SULPHIDE
SULPHIDE	0.131	0.160	0.241	0.152	0.243	0.358	OXIDE
OXIDE	0.495	0.360	0.544	0.067	0.279	0.407	SULPHIDE
OXIDE	0.237	0.203	0.301	0.103	0.287	0.424	SULPHIDE
OXIDE	0.574	0.258	0.225	0.087	0.251	0.373	SULPHIDE
OXIDE	0.297	0.194	0.280	0.115	0.196	0.291	SULPHIDE
SULPHIDE	0.111	0.207	0.306	0.107	0.195	0.288	SULPHIDE
SULPHIDE	0.096	0.237	0.353	0.125	0.209	0.314	SULPHIDE
OXIDE	0.156	0.302	0.438	0.088	0.290	0.420	SULPHIDE
OXIDE	0.254	0.255	0.370		0.247	0.373	SULPHIDE
OXIDE	0.188	0.257	0.373	0.093	0.225	0.340	SULPHIDE
OXIDE	0.283	0.174	0.205	0.068	0.187	0.284	SULPHIDE
OXIDE	0.278	0.200	0.288	0.104	0.275	0.418	SULPHIDE
OXIDE	0.203	0.184	0.267	0.067	0.314	0.457	SULPHIDE
OXIDE	0.407	0.196	0.266	0.113	0.247	0.361	SULPHIDE
OXIDE	0.157	0.246	0.349	0.053	0.335	0.498	SULPHIDE
OXIDE	0.179	0.175	0.261	0.109	0.211	0.324	SULPHIDE
OXIDE	0.301	0.324	0.474		0.292	0.430	SULPHIDE
OXIDE	0.420	0.247	0.361	0.137	0.246	0.363	SULPHIDE
OXIDE	0.282	0.145	0.198	0.097	0.215	0.330	SULPHIDE
OXIDE	0.285	0.181	0.258	0.065	0.266	0.389	SULPHIDE
SULPHIDE	0.103	0.183	0.267	0.051	0.274	0.394	SULPHIDE
OXIDE	0.167	0.191	0.279	0.105	0.154	0.235	SULPHIDE
SULPHIDE	0.117	0.228	0.335				
OXIDE	0.529	0.243	0.311				
OXIDE	0.196	0.174	0.255				

Table 6-3 shows the 41 Oxide rock samples and the 38 Sulphide samples in order of magnitude. Based on the criteria provided, the algorithm recognizes whether the rock is an Oxide or a Sulphide rock. It is interesting to mention that the algorithm can be used to classify the degree of oxide or sulphide. Some of the rocks can be seen to display either less or more Oxide, thus providing even more value to sorting.

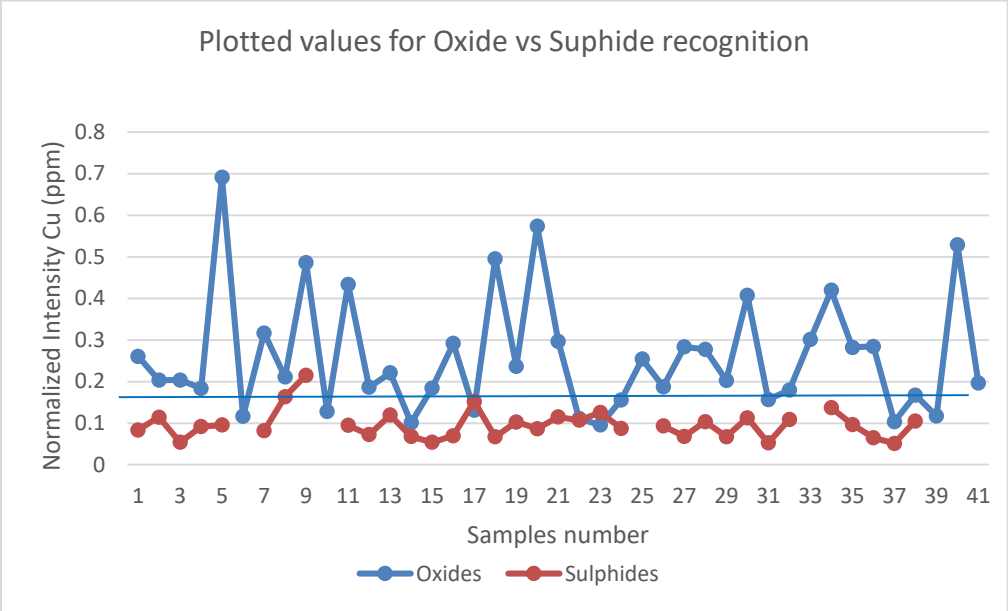

Figure 6-7: Final results table for Oxide versus Sulphide recognition

Chapter 7: Discussion and recommendations

The main purpose of this research has been to develop a greater understanding of the capabilities of LIBS for ore sorting, and to provide the sensor system with a response. The responses of the sensors should be based on good quality readings, statistics, and machine learning processes through which it is possible to train the machine to achieve better predictions. Currently, ore sensors base their responses on the statistical correlations and geological information available for tuning the correlation parameters. LIBS cannot rely solely on the correlations made from field readings, and while a prototype for its sensor is developed, it must have a constant machine learning process available to it through which to gather data and tune itself. One of the purposes of this research was to train the machine to achieve good values for decision making. The main reason that this is not possible is because of the limited amount of data available to build an artificial neural network (ANN).

Also, the architecture of the LIBS sensor would need to be examined for every single mine, depending on the characteristics of the mine, and the needs of the spectrometer. Finally, it would be necessary to define the needs of the LIBS features and capabilities (such as bandwidth, intensity of the laser, resolution, and frequency) to achieve total control over the LIBS sorting sensor. In this chapter, suggestions are offered with respect to useful information that was gathered throughout the progress of the research, and recommendations are made with regarding its potential impact on the performance of the LIBS sensor.

7.1 Data quality and confidence

The data presented in this research is unreliable due to the limited number of rock samples analyzed through ICP. The results are considered unreliable to less 2 standard deviations of

confidence, or at a greater than 5% of error rate. Indeed, this was expected as of the beginning of the project, and does not signify a problem for the next stage of research and development. Empirical data simulated through Montecarlo Simulation suggests that for an expected R^2 =0.05, the estimated error is 9% (approximately) for the 41 Oxide samples, or 10% used for the 38 samples (Austin and Steyerberg).

The minimum recommended number of Subjects Per Variable (SPV) is 100. In order to improve the quality of the data using this methodology, it is necessary to use between 100 to 400 samples, as is statistically recommended when using the Montecarlo Simulation. This concept, as well as the technology, is statistically scalable to the universe of samples subject to prediction while using a sorter in a mine.

The final Pearson Correlation factor for Oxide is 0.94, and for Sulphide it is 0.84. As such, it is possible that the data obtained could be improved upon if expecting correlations close to 3 standard deviations. Also, it is important to note that, within this research, calculations and predictions are not as important as the methodology described because the intention of this research is to provide solid foundations for prediction and correlation, and not final values.

7.1.1 Identification of elements and concentration recommendations

It is recommended that the characteristic wavelength or ID Wavelength, as defined in this research, be acquired from the manufacturer in order to confront the ionization transition probabilities assumed. The reason is that the manufacturer has invested in a great deal of research to find the most probable transitions using its LIBS machine, and as such, spending time and effort towards developing potential ionization transition wavelengths for different LIBS machines is not recommended.

Also, it is necessary to recognize that in contrast to XRF, LIBS is capable of reading the concentration of a sample in nanoseconds. For this reason, at the Research and Development level, it would save time to acquire the software of the manufacturer for element recognition and concentration in order to make it possible to correlate percentages rather than peaks with varying magnitudes.

7.2 LIBS data acquisition and architecture

The data acquisition of LIBS is based on the Nd:YAG, 3 mJ laser pulse at 100 Hz. For LIBS sensors, the data acquisition method is linked to the architecture of the LIBS machine. The main problem with respect to this topic is the reading of white surfaces, mostly for Sulphide rock material. The primary challenge held by the LIBS sorting sensors involves how to acquire reliable data for all types of rock material. As shown in Figure 3-5 and Figure 3-6, several LIBS readings show evidence of high amounts of invalid data obtained during this research. The main reasons of acquiring large numbers of invalid readings are:

a. the low amount of energy absorbed by the surface
b. the capacity of the surface to reflect the energy

Details regarding the white colouring problem were provided in section 2.6. However, the problem was avoided rather than solved. The use of such a strategy will not address the problem once the sensor is placed in operation in a mine.

Robert Noll, in his book “Laser-Induced Breakdown Spectroscopy, Fundamentals and Applications” (Noll), proposes the following chart shown in Figure 7-1.

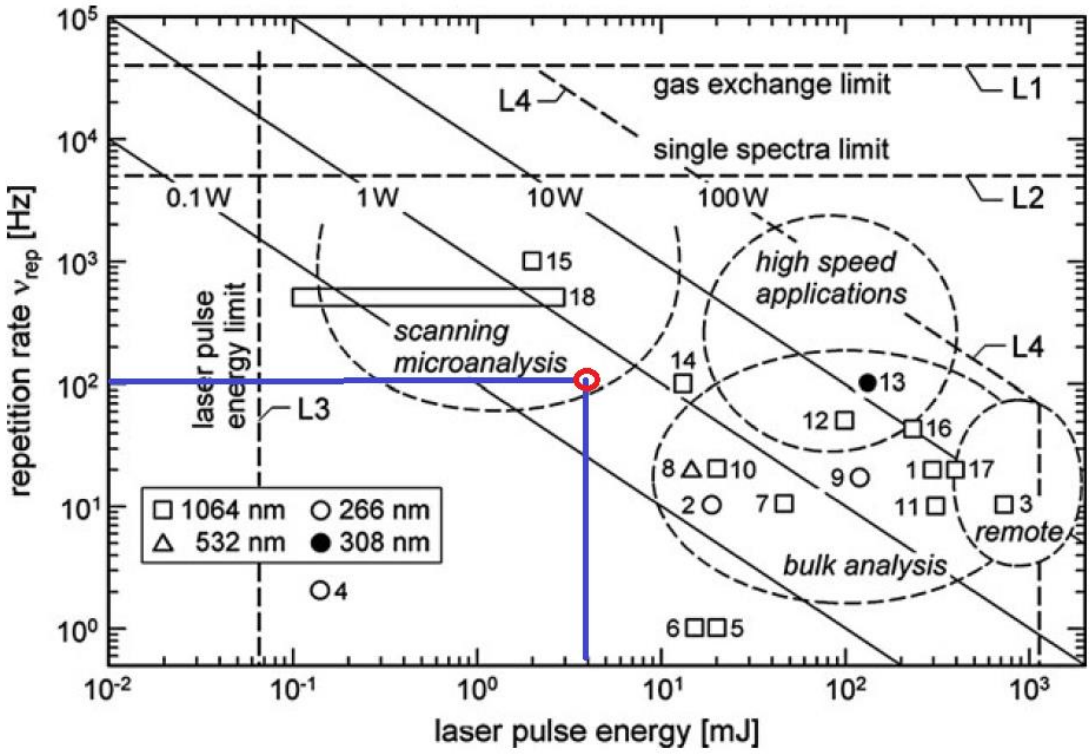

Figure 7-1: Technical specifications for LIBS machine performance (Noll)

This chart provides a location of LIBS applications given the frequency, or repetition rate (Hz) versus the laser pulse energy (mJ). The red circle indicates the current location of the LIBS machine used for this research. This red location suggests that this machine works well for scanning microanalysis. However, LIBS sensors need high speed application capabilities with high pulse energy, and this is currently still limited with respect to commercial availability. (Noll).

An increase in the laser pulse energy will increase the probability of achieving reliable instant readings over mining material. The capacity of energy absorption by the surface of the rock is increased if the laser energy is increased, and the temperature of the crater created by the laser is made larger within a short period of time.

As made evident in Figure 7-1, the use of a LIBS machine with a laser pulse energy in the range of 100 to 500 mJ is recommended.

7.3 LIBS statistics and repeatability analysis

In terms of the repetition rate, the LIBS machine uses electro-optical Q-switching with rates of between 10 to 100 Hz or 0.1 to 0.01 seconds per reading. The ideal velocity of bulk material processed on a belt conveyor is 3 m/s. If a rock with an average size of 3 cm crosses the laser sensor, then the time frame for the LIBS sensors is 0.01 s.

Table 7-1 shows the values for the minimum number of readings needed to gather information from the two ions that conform the interaction effects. These ions were taken in the order in which LIBS acquired the data. The information provided is based purely on the geo-spatial characterizations that the LIBS sensor is sorting.

Table 7-1: Minimum number of readings using LIBS to calculate each of the interaction effects used for the prediction of Oxides

Binomials	#readings needed
Be II@272.89*Ti I@399.86	2
Ti I@399.86*Zr III@266.43	2
Be II@272.89*Cu I@324.75	3
P I@253.56*F II@350.56	2
Al II@281.62*Ba II@455.4	15
Be II@272.89*Cu I@327.4	3
Mg III@239.51*Si I@288.16	1
Ca II@317.93*Cr I@427.48	9
Ca II@317.93*Cl II@481.01	2
Ba II@455.4*Fe I@374.95	60
O III@393.48*P I@253.56	71
N II@399.5*P I@253.56	38
Fe I@374.95*Fe I@374.95	1
Ti II@376.13*Tl I@276.79	2
Be II@272.89*Na II@298.42	1
Fe II@234.35*P I@253.56	7
Be III@448.73*Cr I@427.48	3
Pb I@280.2*Tl I@276.79	13
Ga I@294.36*Ni I@349.3	10
Ba II@455.4*Ca II@317.93	9
Average	12.7

For example, a rock might have a reading of Barium in one small spot of the analyzed rock sample, and LIBS will not provide a value to the interaction effects of Ba II@455.4*Fe I@374.95

until the laser takes a good reading over this small spot. This data was calculated in similar way as was done in Table 4-13. For example, in order to calculate the binomial Be II@272.89*Cu I@327.4, we need at least 3 good readings. The values highlighted belong to the group of binomials that are part of the final prediction equation for Copper Oxides. The binomial O III@393.48*P I@253.56 is a special case because it has a fairly large number of occurrences (refer to Table 4-15). However, LIBS needed to take up to 71 good readings in order to obtain 1 value for this binomial. In addition, this calculation was based on the assumption that 100% of the readings are valid. This is not the case, as shown in Figure 3-5 and Figure 3-6.

If it is necessary to take 71 readings to complete the prediction equation, then addressing the introductory problem in this section about the frequency of the LIBS machine under a belt moving at 3 m/s, we can conclude that the needed frequency is 10^4 hertz.

$$X\left(\frac{seconds}{reading}\right) * 71\ (readings) = 0.01\ (seconds)$$

$$x = 1.4E-4\left(\frac{seconds}{reading}\right) \approx 10^4 Hz$$

There are no current commercial LIBS machines available at this frequency. The use of the highest frequency possible with a tentative range of 10^3 hertz is recommended.

7.4 LIBS future developments

This section discusses an optional method that have been attempted by the author, but not developed further due to lack of time and resources regarding the amount of ICP assays. One of the most important methods applicable to the LIBS ore sorting method is Artificial Neural Networks (ANN). Previous research on ANN (Alexander Koujelev) suggests that the Mean

Deviation is in the range of 5% to 20% for direct measurement concentration instead of through the use of correlation. An argument regarding the preference of ANN over that of LIBS is that most previous experiments have been based on homogenously prepared material. This research attempts to break the heterogeneity problem with respect to LIBS sorting and the reading of moving material.

The ANN algorithm attempts to acquire the target output by summing all of the input and adding the bias to obtain a transfer function, and finally, the output.

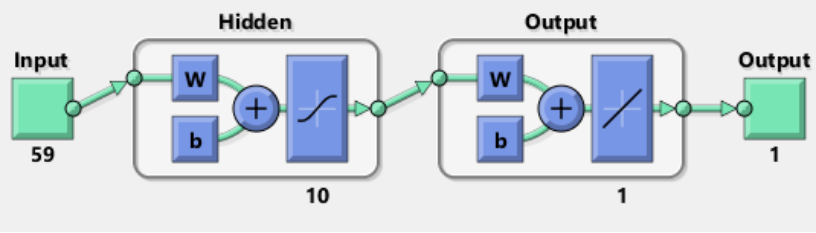

Figure 7-2: Neural Network Scheme for the Oxide samples using 10 neurons

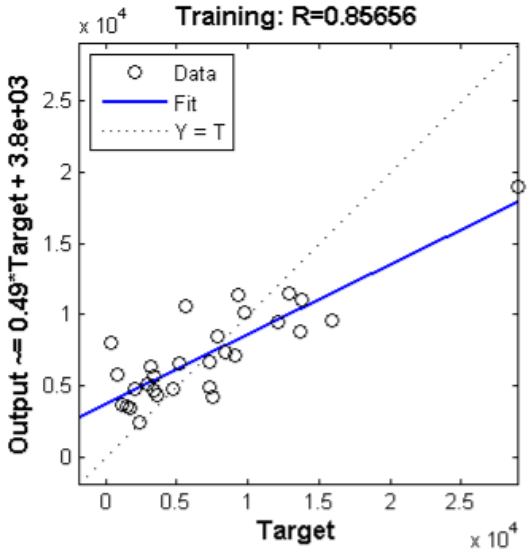

Figure 7-3: Neural Network Fitting for Oxide rocks

It is not the intention of this thesis to present an analysis regarding Artificial Neural Network, but rather to comment on the potential applicability of ANN to the Oxide and Sulphide

ore analysis conducted in this research. One particular aspect of ANN application is the final correlation coefficient obtained out of the 59 ions gotten from LIBS for the Oxide samples. It is possible to differentiate the only high grade sample at the x-axis value of 29000 ppm of Copper. For this set of samples, a better correlation coefficient was obtained in section 4.9.2. However, for the Sulphide rocks, ANN provides an unexpected correlation coefficient of 0.95. This correlation works better than the prediction equation proposed in section 5.6

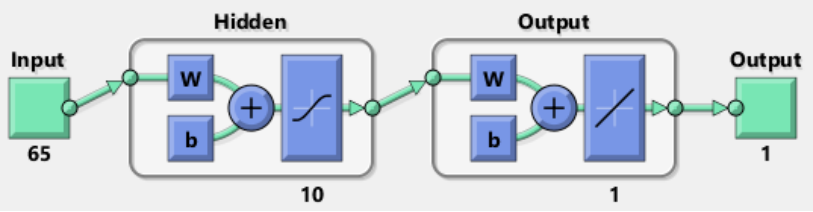

Figure 7-4: Neural Network Diagram for Sulphide samples

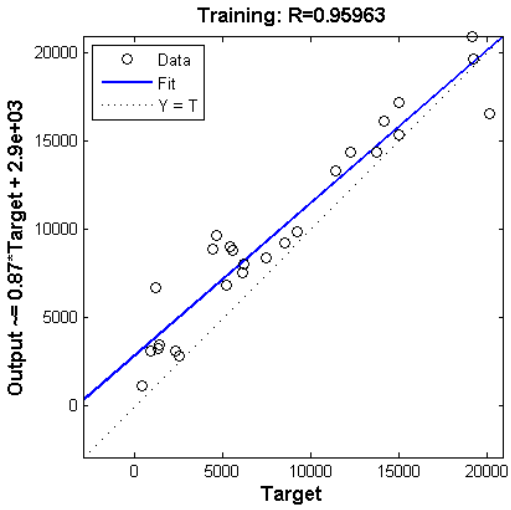

Figure 7-5: Neural Network Fitting for Sulphide rocks

It is important to note that there were problems in reading the Sulphide samples with the LIBS machine, and that most of the readings did not show any type of direct correlation between ICP Cu% and LIBS Cu concentration. In conclusion, it is suggested that further investigation be

conducted into the use of ANN for LIBS sorting systems when looking for a positive outcome for difficult readings such as those with white surfaces.

Chapter 8: Conclusion

Although some conclusions can be drawn based on the findings of this study, there remain questions that would require more research on the LIBS sorting system in order to develop a better understanding regarding its potential uses and applicability.

1. The first conceptual question regards LIBS' capabilities for ore sorting. LIBS can sort rock samples very efficiently if proper statistical and mineralogical information is provided to the computer in charge of processing the spectrums.
2. LIBS can perform to a proven Pearson Correlation Coefficient of 0.94 for Oxides and 0.84 for Sulphides.
3. LIBS achieves a lower performance when sorting Sulphide ore.
4. LIBS has demonstrated proven capacities to act as an ore sorting sensor, and it is recommended that LIBS be brought to a level of Research and Development.
5. Approaches were used to identify elements associated with wavelengths, but in some cases, ICP results showed that the identified element was not probable. Despite this and for simplicity, the element symbol was used to represent the wavelength response.
6. It is necessary to work with specific LIBS machines for different mine projects, depending on the needs of the bandwidth spectrum with respect to acquiring data that is easy to correlate.
7. The Experimental Approach Design used here was correct, but inefficient in terms of theoretical workload. It is necessary to divide the development of LIBS into specialized groups to develop the Computational, Chemometrics and Mining parts separately.

8. The current LIBS laser should be upgraded to a higher pulse laser in order to acquire better readings and obtain better repeatability and data reliability.
9. Developments with respect to the Python Script's ability to recognize peaks and wavelengths should be reviewed and tuned to the maximize LIBS capacity for data acquisition, and its ability to work with moving samples.
10. The purpose of this research was to develop correlation without measuring grades. However, it is a good proactive process for the Python Script to determine the limits of detection and the grades of the rock samples by using a calibrated homogenous scale for all of the available ions.
11. LIBS provides good and reliable readings for Oxide ores, but not for Sulphide ores.
12. Some of the wavelengths overlap for different elements. It is necessary to increase the bandwidth capabilities of the LIBS machine in order to more clearly distinguish between elements with overlapping wavelengths.
13. The Sulphide ores showed better correlation performance using Artificial Neural Networks than through using Stepwise correlations.

Bibliography

Alberty, Robert A. and Robert J. Silbey. *Physical Chemistry*. New York: John Wiley & Sons, Inc, 1996.

Alexander Koujelev, Vincent Motto-Ros, Daniel Gratton, and Alexander Dudelzak. "Laser-induced breakdown spectroscopy as a geological tool for field planetary analogue research." *Can. Aeronaut. Space* (2009): 97-106. Document.

Anderson, Steven T. "2005 Minerals Yearbook." 2007. Document.

Austin, Peter C and Ewout W Steyerberg. "The number of subjects per variable required in linear regression analyses." *ELSEVIER* (2015): 627-636.

Cremers, Davi and Leon J. Radziemski. *Handbook of Laser-Induced Breakdown Spectroscopy*. Alburquerque, NM: Wiley, 2013.

Cyberphysics group. *Cyberphysics*. Date retrieved: 2 Dec 2016. November 2016. <http://www.cyberphysics.co.uk/topics/light/emspect.htm>.

DAGDIGIAN, P. J. *Laser spectroscopy for sensing. Fundamentals, techniques and applications*. Baltimore: The John Hopkins University, 2014. Publication.

Darling, Peter. *Mining Engineering Handbook*. Society for Mining, Metallurgy, and Exploration, 2011. Document.

Fleischer, Sharly. *Physical Chemistry Laboratory*. Date retrieved: 2 December 2016. October 2016. <http://www.tau.ac.il/~phchlab/experiments_new/SemB01_Hydrogen/02TheoreticalBackground.html>.

Geological Association of Canada. *Journal of the Geological Association of Canada*. 2008. January 2016. <https://journals.lib.unb.ca/index.php/gc/article/view/11269/12010>.

Idaho Nationl Engineering & Environmental Lab, Bechtel BWXT. *Development of a Mine Compatible LIBS Instrument for Ore Grading*. Confidential. Washington, DC, 2001.

INEEL. *Mine Compatible LIBS Instrument for Ore Grading*. Idaho, March 2000. Document.

John Tyson, George Asimellis, Stu Rosenwasser. *Development of a Mine Compatible LIBS Instrument for Ore Grading Phase II –Final Report*. Washington DC: Idaho National Engineering & Environmental Lab; Bechtel BWXT Idaho LLC (BBWI), 2001.

Laboratory, Physical Measurement. *NIST database*. Date retrieved: 2011. June 2016. <http://physics.nist.gov/PhysRefData/ASD/lines_form.html>.

Marsden, John and Iain House. "The Chemestry of Gold Extraction." *The Chemestry of Gold Extraction*. Colorado: SME, 2006.

MathWorks. "Matlab Documentation." 2016. *https://www.mathworks.com/help/matlab/ref/nan.html.* Document. Date retrieved: 31 October 2016.

National Institute of Standards and Technology NIST. *NIST lines help*. July 2012. Date retrieved: February 2016. <http://physics.nist.gov/PhysRefData/ASD/Html/lineshelp.html#OUTACC>.

Noll, Reinhard. *Laser Induced Breakdown Spectroscopy*. Berlin: Springer, 2012.

Reader, Joseph; Corliss, Charles. "Wavelengths and Transition Probabilities for Atoms and Atomic Ions." 1980 Date retrieved: September 2016.. *National Institute of Standards and Technology.* <https://www.google.ca/url?sa=t&rct=j&q=&esrc=s&source=web&cd=1&cad=rja&uact=8&ved=0ahUKEwi23OP467nLAhUN1WMKHXjgDKMQFggbMAA&url=http%3A%2F%2Fwww.nist.gov%2Fdata%2Fnsrds%2FNSRDS-NBS-68.pdf&usg=AFQjCNEGlOc9cloW1NIVpdUH6Ar7c02QOA&sig2=OOTgWDeR0hX7JBuTUdcIkQ&b>.

Rehse, Steven J. "Wayne State University." Date retrieved: 1 June 2010. <www1.uwindsor.ca/people/.../final%20draft%20Rehse%20May%2031%202010.pdf>.

Ruben Padilla Garza, Specer Titley, Francisco Pimentel. "Geology of the Escondida Porphyry Copper Deposit, Anofagasta Region, Chile." *Economic Geology* (2001): 307-324. Document.

Ryer, Alex. *Manipulating Light*. 26 September Date retrieved: 1997. March 2016. <http://homepages.inf.ed.ac.uk/rbf/CVonline/LOCAL_COPIES/RYER/ch04.html>.

Samuel M. Clegg, a,* Roger Wiens,a Anupam K. Misra,b Shiv K. Sharma,b James Lambert,Steven Bender,a Raymond Newell,a Kristy Nowak-Lovato,a Sue Smrekar,c M. Darby Dyar,dSylvestre Mauricee. "Spectroscopy, Planetary Geochemical Investigations Using Raman and Laser-Induced Breakdown." *Applied Spectroscopy* (2014): 935-936. Document.

SECOPTA. *Secopta Analytics GmbH*. n.d. Product catalog. 27 November 2016.

Senesi, Giorgio S. "Laser-Induced Breakdown Spectroscopy (LIBS) applied to terrestrial and extraterrestrial analogue geomaterials with emphasis to minerals and rocks." *ELSEVIER* (2014): 231-267. Document.

Senesi, Giorgio S. "Laser-Induced Breakdown Spectroscopy (LIBS)applied to terrestrial and extraterrestrial analogue geomaterials with emphasis to minerals and rocks." *ELSEVIER* (2016): 231-267. Document.

Skoog, Douglas and James Leary. *Análisis Instrumental*. Madrid: McGraw'Hill, 1994.

Yaroshevsky, A. A. "Abundances of Chemical Elements in the Earth's Crust." *Geochemistry International* (2006): 48-55.

Appendices

Appendix A Compiled LIBS responses for Oxide rock samples from Escondida Mine

Sample	Ag II 232.02	Ag II 241.32	Al II 281.62	Ba II 455.40	Be II 272.89	Be III 448.73	Bi I 306.77	Ca I 422.67	Ca II 317.93	Cd II 274.85	Cl II 481.01	Co I 347.40	Cr I 427.48
1			912		937			904		1007			
2					952			880		1038			
3								877	891	947			
4								888		1017			
5			940					995	943	981	779		
6			870					872		952			
7			971					923		929			
8			1092		1312		1167	887		1248			
9		908	850		1411			984	1029	1165	848		
10					1028		1044	866		1176			
11			942	797	1383			999	1348	1134			830
12		874			1298		1108	886	941	1861			931
13				932	1109			893		1021			
14		863	1006					842		1006			
15		865						800		904			
16			928	820				903		958	824		
17				842	1130	870		857	977	1045			952
18			932		1064		1002	979	1031	1639			
19					1088		943	886	954	1168			
20			919		994		970	982	1015	1009			
21				827	964			885	871	1085	816		822
22			945		1282		1220	871		1463			
23		858	880		1379		1039	893		1116			
24			945		1145		977	910	1068	1283		891	
25					962			897	936	1018			
26					1245		1059	894	856	1203			
27								897	967	991			
28				829	1136			930	981	1265			916
29								886		955			
30				773	962			906	1003	1214			
31					1063			882		1146			
32	1374	1803						854		1091			
33		985	975	1015				978		997			1135
34			881	803				945	916	1025	892		
35					1098			918	953	1157			
36								879	920	974			
37					1096			869	871	1070			
38					1249		1124	874	880	1533			
39					1020			878		1316			
40								989	1009	938			
41					1270			927		1119	854		

Sample	Cu I 324.75	Cu I 327.40	Cu II 271.35	F II 350.56	Fe I 374.95	Fe II 234.35	Fe II 238.20	Ga I 294.36	Hf I 368.22	In II 294.10	Ir I 269.42	Mg I 285.21
1	998	944		970	860	865	955					1165
2	1205	1051			945	905	974					1150
3	1118	1004		1013		869	916			1035		1192
4	1207	1058			986	903	965					1177
5	1269	1124			934	979	934				948	1057
6	985	910			913	879	928					1122
7	1083	980		1018		829	892			929		1132
8	1160	1061	1268	926	1098	1142	1133			959	1077	1166
9	1428	1230	1129	985	1043	1219	1086					1129
10	1070	966	1024	953	971	961	1095					1207
11	1446	1272		1090	1120	1046	1054					1119
12	1244	1090	1157		1052	1329	1596		897		1061	1145
13	1165	1051		1018	1115	897	969					1166
14	1059	953		1103	957	883	945	1002		978		1128
15	907	866		1122		799	876	965				1083
16	1271	1121				861	926					1137
17	1775	1532			914	966	988			988		1119
18	1166	1014	1041	1011	1019	1127	1441			981	931	1094
19	1052	971	1165	1078	978	1035	1082	1129			1000	1167
20	1186	1038			921	922	952					1067
21	1387	1224			889	923	1030					1098
22	1065	978	1026		1127	1156	1276					1185
23	1121	1018		1055	1185	1155	1000	1005			1089	1135
24	1257	1114	1127	979	1003	1011	1186					1159
25	1048	961	954		953	930	976					1130
26	1084	1002	925		981	1043	1121				1081	1173
27	1023	951			862	873	947					1209
28	1571	1404	1033	1125	1047	1148	1130	1031			1057	1105
29	1016	942		986	847	839	917					1195
30	1250	1084	1016	947	935	966	1124					1128
31	1022	958		1104	949	956	1069	1017				1124
32	1153	1029			890	900	1030					1161
33	1186	1106		1450			960	1347		1047		1104
34	1604	1372			906	900	985					1101
35	1013	928		902	948	969	1067					1201
36	1061	970		860		900	934					1142
37	982	945		1119	1022	1004	1002	1034				1159
38	1187	1059	1030		977	1123	1354				1097	1243
39	1106	1018	999		953	997	1205					1136
40	974	933			942		893					1099
41	1071	991	1245		1065	1139	1039					1175

Sample	Mg II 279.55	Mg III 239.51	Mn I 279.83	Mn II 261.02	N II 399.50	N IV 347.87	Na II 298.42	Na II 307.83	Ni I 349.30	O III 393.48	O V 278.10	P I 253.56
1	2195	901		928			871	1437	838	1135	969	1028
2	2182	921		956			866	1165		1048	972	1026
3	2311	883		915			836	1388		1091	962	
4	2353	928		937			886			1071	958	
5	1846	927		925			985			1832	975	
6	2226	900		909			881		833	1000	924	
7	2177	859		879			846	1285	822	1248	957	
8	2177	1092		901		841	1156			1087	953	
9	2154	1022		959			1090		927	1520	976	1084
10	2412	1018		1036		847	947	1376		1005	985	1135
11	1990	1035		984			1006	1481	1014	1396	989	1126
12	1842	1430		1343			1155	1158		1072	1023	
13	2209	923		922			966	1001		1114	960	968
14	2229	896		930			905	1547	908	930	919	1061
15	2031	838		859		846	914	1503	930	981	900	
16	2283	886		917			888			1209	949	
17	1748	948	2207	975			1009	1031		978	985	1212
18	1987	1260		1130			1028	1496	863	1520	964	1166
19	2179	1015		988			996	1337		1127	961	1032
20	1956	926		932			906			1564	940	
21	2128	979		979			886			1227	916	1084
22	2146	1184		1097			1103	1374		954	983	1295
23	2133	1040		900		892	1141	1488	827	940	946	
24	2190	1081		1041			999	1457	933	1042	957	1244
25	2308	921		907			943			1164	929	
26	2322	1028		982			1014			1091	963	
27	2443	894		926			881			1202	1027	1031
28	1944	1078		967			1046	1571	925	1207	1001	1237
29	2353	874		897			901	1368	846	1061	984	
30	2115	1042		1024		788	902	1300	836	1345	952	1123
31	2215	990		973			948	1536	891	1033	961	
32	2233	966		986			877			1057	977	1080
33	2000	918		943		946	1082	1827	1084	1289	922	1443
34	2161	940		953			901			1409	929	
35	2427	1019		1031			937	1081		1250	1024	1182
36	2262	894		914			858	1122		1194	960	1118
37	2206	949		960		904	978	1376		945	961	
38	2381	1244		1095	882		1011	1206	943	1048	1028	1399
39	2178	1100		1113			954			970	973	1344
40	1982	889		883						1615	912	
41	2285	990		908	938		1057			1087	989	990

Sample	P IV 334.77	Pb I 280.20	Pb I 283.31	S VI 419.89	S VI 420.08	Sc III 269.91	Si I 288.16	Si II 413.09	Sn II 335.20	Ti I 399.86	Ti II 376.13
1							1360			892	1082
2	861						1207			852	927
3		1739					1291			852	953
4					818		1276			871	915
5	935	1234					1156			947	890
6	929						1281			887	903
7	925	1315					1196			855	1072
8	916	1568	1195		926		1250			917	909
9	916	1377	1084		1003		1391			938	881
10			967				1285			872	1141
11	892	1332	1215	875	884		1339			969	1003
12		1369	1062	903	879		1196	912			984
13		1727					1269			1020	898
14	925						1232			895	1357
15	915	1167					1101			863	1080
16	904	1147					1319				891
17		1340					1175				897
18		1611	958	869	861		1524	866		892	
19		1639	1039	825	874		1315	959		900	1163
20	889	1168					1333		846		893
21		1311					1335	837			896
22		1731	1182	943	975		1264	906		923	957
23	996	1298	1110	918	915		1161	906		915	1105
24		1658	1189		1000		1399	918	964	928	1250
25		1685					1475			869	
26	900	1825					1429	934		845	885
27	859						1227			827	870
28		1396	1083	959	914		1293	893		958	1406
29		1717	940				1201	916		926	1251
30	983	1303					1238			881	1074
31	921	1497			905		1471	954	886	897	1357
32	890	1060					1198			859	858
33	1006	1388				977	1454			1105	1807
34		1390					1359				842
35	896	1642					1133				968
36	869						1238				931
37	895	1563		907	871		1210	910		912	1154
38	917	1603	1112	874	890		1400	890		894	
39				913	889		1368	945			
40		1219					1228				
41	899	1651	1052		929		1247				866

Sample	Ti III 251.61	Tl I 276.79	Tl I 351.92	V II 292.40	W I 400.88	W II 248.92	Y II 371.03	Zn I 334.50	Zn II 491.16	Zr III 266.43
1	1314	864				922		960		888
2	1177	927				849	848			901
3	1258	912								
4	1254	928				1009	837	931		892
5	1148	1017					845	978		953
6	1237	883								
7	1154						814			
8	1321	1334		1096			920			1216
9	1398	1171		942			960	1000		1237
10	1292	977				860	858			1002
11	1301	1037				885	892			1053
12	1314	1308				900	903			1192
13	1228	1037				901				1060
14	1213	898	915			894				
15	1067		890			880				
16	1297	941				843		949		
17	1186	986				917				992
18	1557	1067					882			1002
19	1294	1071				940	878			1006
20	1273	916				890		982		922
21	1315	896					829	980		886
22	1288	1271		1089		908	1009			1210
23	1193	1246					966	892		1252
24	1428	1032				958	932			1036
25	1428	991					881			941
26	1422	1079				926	940	944		1068
27	1199	947				876				
28	1291	1100	911				916			1064
29	1177	817				914				
30	1291	933				1067	866			918
31	1425	981				943	928			1027
32	1212	903		850						856
33	1451		1146		1132	960	922		966	
34	1372	894				920		1198		887
35	1166	998		946			898			962
36	1201	863				930				838
37	1216	1044		873						1048
38	1441	1115					922			1079
39	1422	989					900	932		938
40	1171									
41	1248	1145		985		880	898	916		1095

Appendix B ICP certified assay results for the 41 Oxide Escondida samples

ANALYTE	WtKg	Ag	Al	As	Ba	Be	Bi	Ca	Cd
METHOD	G_WGH79	GE_ICP14B	GE_ICP14B	GE_ICP14B	GE_ICP14B	GE_ICP14B	GE_ICP14B	GE_ICP14B	GE_ICP14B
DETECTION	0.01	2	0.01	3	5	0.5	5	0.01	1
UNITS	kg	ppm	%	ppm	ppm	ppm	ppm	%	ppm
EscOx1B2	0.05	<2	1.91	<3	75	<0.5	<5	0.05	<1
EscOx2B2	0.114	<2	2.66	4	40	<0.5	<5	0.04	<1
EscOx3B2	0.068	<2	1.33	4	80	0.9	<5	0.22	<1
EscOx4B2	0.048	<2	4.94	4	49	0.6	<5	0.12	<1
EscOx5B2	0.035	<2	1.3	4	86	0.7	<5	0.26	<1
EscOx6B2	0.04	<2	1.73	9	47	<0.5	<5	0.22	<1
EscOx7B2	0.035	<2	1.66	4	116	0.9	<5	0.16	<1
EscOx8B2	0.219	<2	3.73	8	96	<0.5	<5	0.04	<1
EscOx9B2	0.125	<2	1.03	<3	68	<0.5	<5	0.37	<1
EscOx10B2	0.119	31	3.81	3	51	<0.5	<5	0.05	<1
EscOx11B2	0.044	<2	1.11	<3	61	<0.5	<5	0.3	<1
EscOx12B2	0.033	<2	2.63	19	91	0.5	<5	0.06	<1
EscOx13B2	0.227	<2	1.23	<3	41	<0.5	<5	0.13	<1
EscOx14B2	0.081	3	1.1	15	81	0.5	<5	0.05	<1
EscOx15B2	0.051	6	3.91	6	59	0.6	<5	0.04	<1
EscOx16B2	0.097	<2	1.28	4	128	<0.5	<5	0.14	<1
EscOx17B2	0.3	2	0.8	10	105	<0.5	<5	0.08	<1
EscOx18B2	0.035	<2	1.25	<3	26	<0.5	<5	0.75	<1
EscOx19B2	0.03	<2	1.51	3	50	<0.5	<5	0.04	<1
EscOx20B2	0.074	<2	2.08	4	64	<0.5	<5	0.14	<1
EscOx21B2	0.037	<2	1.08	3	66	0.8	<5	0.28	<1
EscOx22B2	0.056	12	3.07	7	62	<0.5	<5	0.05	<1
EscOx23B2	0.032	<2	2.43	14	73	0.5	<5	0.04	<1
EscOx24B2	0.044	<2	1.9	11	52	3.3	<5	0.05	<1
EscOx25B2	0.06	<2	1.16	3	44	0.8	<5	0.03	<1
EscOx26B2	0.083	<2	0.79	3	71	<0.5	<5	0.04	<1
EscOx27B2	0.091	<2	2	4	58	<0.5	<5	0.07	2
EscOx28B2	0.049	<2	0.93	<3	62	<0.5	<5	0.18	<1
EscOx29B2	0.052	<2	2.29	4	95	<0.5	<5	0.03	<1
EscOx30B2	0.05	<2	1.05	<3	45	0.8	<5	0.35	<1
EscOx31B2	0.269	<2	0.77	<3	90	0.6	<5	0.16	<1
EscOx32B2	0.167	<2	3.61	6	45	<0.5	<5	0.28	<1
EscOx33B2	0.205	<2	1.39	3	86	<0.5	<5	0.05	<1
EscOx34B2	0.177	2	1.09	3	86	<0.5	<5	0.53	<1
EscOx35B2	0.082	<2	2.91	4	64	<0.5	<5	0.53	1
EscOx36B2	0.159	<2	1.06	4	63	<0.5	<5	0.22	<1
EscOx37B2	0.084	<2	1.14	7	83	<0.5	<5	0.04	<1
EscOx38B2	0.087	<2	0.98	5	64	<0.5	<5	0.04	<1
EscOx39B2	0.119	<2	0.84	12	55	0.5	<5	0.14	<1
EscOx40B2	0.104	<2	0.94	3	59	<0.5	<5	0.11	<1
EscOx41B2	0.117	<2	1.06	4	72	0.6	<5	0.18	<1

Co	Cr	Cu	Fe	Hg	K	La	Li	Mg	Mn
GE_ICP14B	GE_ICP14B	GE_ICP14B	GE_ICP14B	GE_ICP14B	GE_ICP14B	GE_ICP14B	GE_ICP14B	GE_ICP14B	GE_ICP14B
1	1	0.5	0.01	1	0.01	0.5	1	0.01	2
ppm	ppm	ppm	%	ppm	%	ppm	ppm	%	ppm
10	8	1540	2.57	<1	0.45	11.7	6	0.68	293
16	12	>10000	4.11	<1	0.35	14.4	14	1.43	237
3	6	7240	1.16	<1	0.39	24.7	5	0.35	160
24	17	>10000	5.19	<1	0.31	19	28	2.48	180
4	4	>10000	1.21	<1	0.42	14.6	4	0.28	114
5	3	3080	1.69	<1	0.58	20.9	7	0.58	355
4	5	4750	1.36	<1	0.49	24.3	7	0.48	188
12	25	3130	3.42	<1	0.39	16	18	1.87	572
4	8	9320	1.7	<1	0.22	17.9	4	0.37	138
19	25	2890	5.27	<1	0.38	14	15	1.24	344
4	8	5600	1.68	<1	0.22	14.1	5	0.41	127
9	15	7170	6.03	<1	0.46	13.3	21	1.33	1010
6	5	3600	2.05	<1	0.14	16.7	6	0.5	152
3	3	2350	1.38	<1	0.46	20.5	4	0.41	221
27	27	8440	5.14	<1	0.37	10.3	25	2.52	527
7	7	9720	1.28	<1	0.3	16.7	6	0.5	141
2	6	>10000	1.37	<1	0.38	18.5	2	0.21	95
1	4	774	1.79	<1	0.77	2.3	<1	0.07	74
4	5	1680	2.16	<1	0.2	11	6	0.51	234
14	20	>10000	4.39	<1	0.36	10.8	15	1.12	341
5	7	>10000	1.9	<1	0.19	19.8	6	0.49	125
16	20	2990	4.41	<1	0.38	18.9	14	1.23	1000
5	11	3410	3.09	<1	0.52	15.6	10	0.93	183
2	4	5680	2.02	<1	0.48	25.5	4	0.19	87
4	7	2100	1.6	<1	0.26	13	4	0.44	145
2	5	1110	0.99	<1	0.31	16.2	2	0.21	101
11	6	9150	2.67	<1	0.23	15.1	15	1.19	286
4	6	5230	1.58	<1	0.19	12.2	4	0.39	145
9	5	7480	2.27	<1	0.25	26.5	11	1.07	245
4	6	7310	1.78	<1	0.14	16.4	7	0.47	133
3	4	1930	1.42	<1	0.34	12.5	2	0.16	107
15	22	>10000	4.95	<1	0.27	11.3	16	1.42	398
<1	3	370	0.68	<1	0.42	22.5	2	0.15	35
3	3	1940	1.23	<1	0.36	14.2	4	0.35	122
18	21	8790	5.65	<1	0.39	8	17	1.51	478
6	5	4710	1.75	<1	0.21	17.7	8	0.48	129
5	5	1530	1.49	<1	0.31	30.9	5	0.42	139
4	5	1410	1.52	<1	0.26	23.7	4	0.41	132
7	2	7360	1.58	<1	0.25	9.1	3	0.27	242
4	7	3450	1.6	<1	0.09	16.2	7	0.47	116
5	6	7820	1.91	<1	0.2	14.4	7	0.52	144

Mo	Na	Ni	P	Pb	S	Sb	Sc	Sn	Sr
GE_ICP14B	GE_ICP14B	GE_ICP14B	GE_ICP14B	GE_ICP14B	GE_ICP14B	GE_ICP14B	GE_ICP14B	GE_ICP14B	GE_ICP14B
1	0.01	1	0.01	2	0.01	5	0.5	10	5
ppm	%	ppm	%	ppm	%	ppm	ppm	ppm	ppm
15	0.16	10	0.03	22	<0.01	<5	5.2	<10	41
14	0.11	14	0.12	11	0.01	<5	10.7	<10	41
22	0.13	5	0.23	30	0.27	<5	1.4	<10	76
7	0.12	20	0.06	15	0.02	<5	13.7	<10	50
30	0.14	5	0.16	11	0.36	<5	1.7	<10	73
7	0.09	6	0.03	6	0.24	<5	1.2	<10	17
16	0.11	6	0.11	17	0.17	<5	1.8	<10	73
109	0.1	22	0.04	31	0.02	<5	14.8	<10	147
13	0.13	12	0.09	14	0.41	<5	2	<10	62
11	0.11	23	0.02	31	0.02	<5	12.7	<10	71
11	0.14	6	0.04	8	0.31	<5	2	<10	46
412	0.09	12	0.13	552	0.04	<5	8.4	<10	20
10	0.11	5	0.08	6	0.12	<5	1.7	<10	83
135	0.04	4	0.13	136	0.04	<5	2.1	<10	20
43	0.11	25	0.03	9	0.01	<5	10.3	<10	29
67	0.12	9	0.08	18	0.25	<5	1.6	<10	54
17	0.09	4	0.06	7	0.9	6	1.5	<10	33
16	0.05	3	<0.01	22	0.66	<5	<0.5	<10	13
6	0.16	5	0.07	13	0.02	<5	1.4	<10	42
34	0.11	16	0.14	5	0.02	<5	15	<10	38
10	0.14	7	0.05	8	0.48	<5	2.2	<10	80
22	0.11	20	0.05	98	0.02	<5	9.5	<10	120
96	0.05	9	0.2	83	0.05	<5	10.9	<10	65
37	0.08	4	0.87	159	0.04	<5	1.2	<10	18
33	0.11	5	0.2	19	0.02	<5	1.3	<10	32
46	0.07	4	0.03	25	0.02	<5	0.6	<10	14
77	0.1	12	0.08	7	<0.01	<5	8.2	<10	28
44	0.12	7	0.06	6	0.22	<5	1.3	<10	29
38	0.1	7	0.07	5	0.02	<5	4.3	<10	135
87	0.12	6	0.11	9	0.38	<5	3.1	<10	76
152	0.08	4	0.04	29	0.22	<5	<0.5	<10	36
21	0.1	18	0.13	4	0.02	<5	13.8	<10	38
11	0.14	2	0.02	48	0.23	<5	0.7	<10	74
32	0.1	5	0.08	17	0.48	<5	0.8	<10	32
15	0.17	18	0.1	3	<0.01	<5	15.8	<10	36
19	0.13	6	0.05	6	0.23	<5	3	<10	72
22	0.09	7	0.05	17	0.03	<5	0.7	<10	114
19	0.09	5	0.04	10	0.02	<5	0.8	<10	97
12	0.08	8	0.09	82	0.24	<5	0.8	<10	16
5	0.1	6	0.06	7	0.11	<5	3.2	<10	97
23	0.09	7	0.08	9	0.31	<5	2.1	<10	45

Ti	V	W	Y	Zn	Zr	Au	Al2O3	Ba	CaO
GE_ICP14B	GE_ICP14B	GE_ICP14B	GE_ICP14B	GE_ICP14B	GE_ICP14B	GE_FAA313	GO_ICP95A	GO_ICP95A	GO_ICP95A
0.01	1	10	0.5	1	0.5	5	0.01	0.001	0.01
%	ppm	ppm	ppm	Ppm	ppm	ppb	%	%	%
0.02	85	<10	4.2	465	0.7	54	18.1	0.079	0.66
0.09	149	<10	9.8	102	1.1	21	18.9	0.025	0.85
<0.01	22	<10	49.6	132	<0.5	18	17.2	0.056	0.67
0.11	164	<10	10.5	347	1.1	7	18.8	0.032	0.93
<0.01	20	<10	5.2	165	<0.5	28	17.2	0.068	0.85
<0.01	22	<10	4.4	281	<0.5	5	19.2	0.036	0.34
<0.01	22	<10	12.1	256	<0.5	21	17.6	0.05	0.76
0.05	167	<10	3.1	375	0.9	7	21.4	0.024	0.39
0.02	32	<10	8.2	169	0.5	53	16.2	0.078	1.32
0.04	203	<10	124	734	1.2	<5	19.7	0.018	0.47
0.03	31	<10	5	138	0.7	28	16.2	0.075	1.34
<0.01	114	<10	2.1	1030	1.2	8	18.4	0.041	0.1
0.03	34	<10	2.8	114	0.6	22	17.8	0.056	1.67
<0.01	23	<10	4.1	121	<0.5	30	19.1	0.065	0.09
<0.01	129	<10	9.4	282	1.3	9	19.2	0.026	0.54
<0.01	19	<10	1.1	164	<0.5	82	16.2	0.077	0.7
<0.01	20	<10	0.7	63	<0.5	135	13.7	0.057	0.21
<0.01	7	<10	0.6	23	0.5	17	18.6	0.007	1.09
0.01	34	<10	0.8	103	0.7	9	18.4	0.027	1.14
0.17	203	<10	14	909	1.3	107	17.8	0.028	2.71
0.04	34	<10	16.8	143	0.7	65	16.4	0.085	1.57
0.03	156	<10	27.7	714	1.2	<5	19.5	0.028	0.37
<0.01	101	<10	3.6	250	1	9	18.3	0.036	0.06
<0.01	13	<10	1.9	182	0.5	7	17.7	0.037	0.08
<0.01	23	<10	0.8	159	<0.5	5	16.6	0.081	0.35
<0.01	12	<10	3.3	223	<0.5	29	14.9	0.057	0.11
0.07	91	<10	9.2	814	1.1	128	18.9	0.041	1.38
<0.01	24	<10	1.3	160	0.6	25	15.5	0.063	0.99
0.01	64	<10	10.8	160	0.8	7	19.4	0.042	0.75
0.04	34	<10	5.7	166	0.7	40	16	0.065	1.63
<0.01	13	<10	2.8	116	<0.5	43	15.6	0.056	0.31
0.16	170	<10	13.9	307	1.7	<5	18.1	0.025	1.53
<0.01	16	<10	0.7	16	<0.5	93	18.8	0.047	0.14
<0.01	14	<10	0.7	125	<0.5	194	17.3	0.052	0.9
0.24	206	<10	12.3	558	1.8	17	17.8	0.021	3.56
0.08	37	<10	21.5	243	0.7	71	17.2	0.048	2.05
<0.01	16	<10	1.7	189	<0.5	5	15.7	0.077	0.26
<0.01	16	<10	1.1	121	<0.5	13	16.1	0.073	0.36
<0.01	16	<10	2.5	188	0.5	54	16.9	0.048	0.3
0.04	34	<10	118	118	0.6	53	16.8	0.073	1.85
0.02	27	<10	3	239	0.6	42	16	0.078	0.95

Cr2O3	Fe2O3	K2O	MgO	MnO	Na2O	Nb	P2O5	SiO2	Sr
GO_ICP95A	GO_ICP95A	GO_ICP95A	GO_ICP95A	GO_ICP95A	GO_ICP95A	GO_ICP95A	GO_ICP95A	GO_ICP95A	GO_ICP95A
0.01	0.01	0.01	0.01	0.01	0.01	0.001	0.01	0.01	0.001
%	%	%	%	%	%	%	%	%	%
<0.01	4.39	3.05	1.42	0.04	4.28	0.002	0.08	65.1	0.039
<0.01	6.82	1.91	2.7	0.03	4.01	0.002	0.28	55.3	0.039
<0.01	2.05	2.52	0.86	0.02	5.1	0.001	0.45	66.6	0.045
<0.01	7.85	1.4	4.16	0.02	2.29	0.002	0.14	53.3	0.026
<0.01	2.18	3.24	0.75	0.02	4.38	0.001	0.36	68.3	0.054
<0.01	3.07	4.59	1.61	0.05	0.18	0.001	0.07	63.6	0.004
<0.01	2.45	3.08	1.16	0.03	3.11	0.001	0.21	65.1	0.038
<0.01	5.61	1.89	3.44	0.08	2.16	0.003	0.06	54.7	0.031
<0.01	2.69	2.64	0.72	0.02	5.06	0.001	0.22	65.3	0.055
<0.01	8.14	1.78	2.28	0.05	1.38	0.003	0.04	54.3	0.022
<0.01	2.63	2.71	0.79	0.02	5.01	0.001	0.11	66	0.063
<0.01	9.09	4.07	2.63	0.13	0.23	0.003	0.25	55.4	<0.001
<0.01	3.22	1.79	0.94	0.02	5.53	0.001	0.17	64.9	0.078
<0.01	2.77	5.63	1.66	0.05	0.12	0.002	0.24	61.2	0.004
<0.01	7.71	2.09	4.36	0.07	2.69	0.002	0.09	54.1	0.026
<0.01	2.17	2.76	1.03	0.02	4.61	0.001	0.26	67.4	0.047
<0.01	2.18	2.85	0.68	0.01	3.4	<0.001	0.18	65.1	0.02
<0.01	2.6	4.84	0.49	0.02	0.12	0.002	<0.01	65.3	0.004
<0.01	3.43	1.26	0.97	0.03	5.67	0.001	0.12	67.7	0.071
<0.01	6.56	1.23	1.89	0.05	4.34	0.003	0.3	54.4	0.059
<0.01	2.92	2.77	0.9	0.02	5.15	0.001	0.15	64.4	0.066
<0.01	7.21	2.74	2.43	0.14	1.5	0.003	0.11	55.2	0.027
<0.01	5.03	3.94	2.16	0.04	0.13	0.003	0.41	59.8	0.005
<0.01	3.41	4.05	1.02	0.03	0.14	0.001	1.81	62.1	0.003
<0.01	2.63	3.42	0.96	0.02	4.57	0.001	0.49	67.2	0.037
<0.01	2	3.47	0.85	0.02	1.51	0.001	0.08	68.8	0.005
<0.01	4.27	1.94	2.2	0.04	5.21	0.002	0.2	59.7	0.044
<0.01	2.61	1.92	0.77	0.02	5.25	0.001	0.13	68.1	0.054
<0.01	3.85	1.81	2.05	0.03	4.52	0.002	0.13	61.4	0.051
<0.01	2.79	2.23	0.9	0.02	5.45	0.001	0.29	63.8	0.067
<0.01	2.56	2.92	0.64	0.02	3.28	0.001	0.1	67.6	0.019
<0.01	7.64	1.66	2.53	0.06	2.99	0.002	0.27	55.3	0.035
<0.01	1.74	2.83	0.78	<0.01	2.53	0.002	0.06	65.2	0.022
<0.01	2.29	2.87	1.01	0.02	4.08	0.002	0.17	66.4	0.026
<0.01	8.04	1.29	2.51	0.07	3.41	0.002	0.22	54.2	0.049
<0.01	2.68	1.66	0.84	0.02	5.89	0.002	0.18	64.4	0.076
<0.01	2.52	3.31	0.99	0.02	3.57	0.001	0.14	66.3	0.039
<0.01	2.7	2.96	0.92	0.02	4.63	0.001	0.12	68.8	0.049
<0.01	2.7	2.43	0.8	0.04	4.62	0.001	0.18	65.9	0.021
<0.01	2.54	2.05	0.84	0.02	5.33	0.001	0.12	66.6	0.075
<0.01	3.07	2.98	1.03	0.02	4.42	0.001	0.2	65.7	0.052

TiO2	Y	Zn	Zr	LOI	Cu
GO_ICP95A	GO_ICP95A	GO_ICP95A	GO_ICP95A	G_PHY01K	GO_ICP13B
0.01	0.001	5	0.001	0.01	0.01
%	%	ppm	%	%	%
0.77	0.001	487	0.015	3.22	N.A.
0.96	0.001	121	0.012	4.77	1.59
0.43	0.005	170	0.015	3.35	N.A.
0.91	0.001	375	0.012	7.1	1.21
0.45	<0.001	233	0.015	3.65	1.37
0.53	<0.001	449	0.017	6.07	N.A.
0.43	0.001	381	0.015	4.06	N.A.
1.26	0.001	378	0.013	7.28	N.A.
0.39	<0.001	211	0.014	3.36	N.A.
1.07	0.014	708	0.011	7.7	N.A.
0.38	<0.001	157	0.014	2.76	N.A.
1.05	0.001	1010	0.011	6.31	N.A.
0.46	<0.001	128	0.015	2.54	N.A.
0.68	0.001	151	0.016	4.08	N.A.
1.08	0.002	285	0.011	6.17	N.A.
0.38	<0.001	200	0.014	3.02	N.A.
0.33	<0.001	89	0.012	4.95	2.9
0.51	<0.001	26	0.017	5.94	N.A.
0.49	<0.001	119	0.016	3.09	N.A.
1	0.002	908	0.01	3.44	1.38
0.42	0.002	177	0.014	2.71	1.29
1.06	0.003	737	0.012	6.94	N.A.
0.89	0.001	250	0.01	5.66	N.A.
0.41	<0.001	341	0.015	6.5	N.A.
0.42	<0.001	190	0.015	2.58	N.A.
0.37	<0.001	365	0.012	3.27	N.A.
0.78	0.001	770	0.015	3.84	N.A.
0.36	<0.001	221	0.013	2.54	N.A.
0.64	0.002	176	0.016	4.36	N.A.
0.41	<0.001	207	0.015	3.53	N.A.
0.34	<0.001	216	0.014	3.07	N.A.
1.01	0.002	336	0.011	5.9	1.53
0.44	<0.001	22	0.015	6.76	N.A.
0.46	<0.001	194	0.014	4.39	N.A.
1	0.002	574	0.011	3.77	N.A.
0.49	0.002	297	0.015	2.53	N.A.
0.37	<0.001	222	0.014	3	N.A.
0.38	<0.001	154	0.015	2.27	N.A.
0.46	<0.001	263	0.014	3.61	N.A.
0.38	0.013	155	0.015	2.08	N.A.
0.4	<0.001	347	0.014	3.21	N.A.

Appendix C Python Script for the processing of LIBS responses

```
from __future__ import division
from __future__ import division

import matplotlib.pylab as plt
import pandas as pd
import numpy as np
from scipy.optimize import leastsq
import os
import matplotlib.ticker as plticker

import mtl.processing.convolution2 as conv
from mtl.misc import gaussianDerivKernel, gaussianKernel
from mtl.sensors.xray import lorentz
from scipy.ndimage.filters import convolve
from scipy.optimize import leastsq # Levenberg-Marquadt Algorithm

saveplot=False
readingsFilename = 'Oxido_Escondida_unified.csv'
SIGMA = 2.
outDir = readingsFilename+'_plots'
if saveplot:
        os.makedirs(outDir)   #******************
'''
columns = df.columns[1:]
table = []
for name in columns:
        table.append(name.split(','))
'''

### Load database of wavelengths and elements, and clean it up
badChar = u'\xa0'

def fixValue(x):
        if (isinstance(x, unicode)):
                return x.strip().replace(badChar,'')
        else:
                return x

def clean(col):
        return col.apply(fixValue)



### Load ID wavelengths
```

```
idWavelengths = pd.read_csv('ID wavelength.csv')


### Load spectra
TOL = 0.132

spectra = pd.read_csv(readingsFilename)
wavelengths = spectra['wavelength']
for col in spectra.columns:
        print col
readingtoplot = raw_input('Enter the reading to plot from the list:')

matches = []
for whichReading in spectra.columns:
        if whichReading != 'wavelength':
                spectrum = spectra[whichReading]

                ########################################
                PEAK_THRESHOLD = 890


                ########################################
                ### NUMERICAL DERIVATIVE WRT X
                kernel = gaussianDerivKernel.get(sigma=SIGMA, threshold=0.005)
                deriv = -1 * convolve(spectrum, kernel)

                ### FIND PEAKS
                ### by looking for when derivative crosses 0 from positive to negative
                min2ndDeriv = 1.0
                peakIndices = []
                prevSlope = False
                for idx, slope in enumerate(deriv):
                        if (prevSlope > 0 and slope <= 0 and abs(slope-prevSlope) > min2ndDeriv):
                                #print abs(slope-prevSlope)
                                peakIndices.append(idx)

                        prevSlope = slope

                peakIndices = np.array(peakIndices)

                ############ 2nd deriv example
                kernel2 = np.array([-1,0,1])
                deriv2 = -1 * convolve(deriv, kernel2)
                if saveplot or whichReading == readingtoplot:
                        # if whichReading==readingtoplot:
                        # plot example
```

```
                    fig, ax = plt.subplots(1,1, figsize=(30,20))
                    loc = plticker.MultipleLocator(base=10) # this locator puts ticks at regular
intervals
                    yaxis_loc = plticker.MultipleLocator(base=0.1)
                    ax.xaxis.set_major_locator(loc)
                    ax.yaxis.set_major_locator(yaxis_loc)
                    ax.plot(wavelengths, spectrum, c='b')
                    ax.plot(wavelengths, deriv, c='r')
                    ax.plot(wavelengths, deriv2, c='g')
                    ax.set_xlim((wavelengths.min(), wavelengths.max()))

            # for peakIdx in peakIndices:
            #       ax.axvline(wavelengths[peakIdx], ls='--', c='#555555')

            peakTable = []

            BELOW = False
            x0 = None
            x1 = None
            maxval = 10
            for idx, value in enumerate(deriv2):
                    if (BELOW):
                            maxval = max(abs(value), maxval)

                    if (value < 0 and not BELOW):
                            BELOW = True
                            x0 = idx

                    if (value >= 0 and BELOW):
                            BELOW = F23alse
                            x1 = idx

                            if (maxval >= 10):
                                    # accept as peak
                                    peakIdx = spectrum[x0:x1+1].argmax()
                                    peakTable.append([peakIdx,              wavelengths[peakIdx],
spectrum[peakIdx]])

                                    if saveplot or whichReading == readingtoplot:
                                            ax.fill_between([wavelengths[x0],wavelengths[x1]],      -
0.2, 1, alpha=0.3, colour='y')

                                    maxval = 0
            maxval = 0

            if len(peakTable)==0:
```

```
                print ("No peaks found")
        if saveplot:
                plt.savefig(os.path.join(outDir, 'Plot'+whichReading+'.jpg'))  #********
        if whichReading==readingtoplot:
                plt.show()
        if saveplot or whichReading == readingtoplot:
                plt.close()

        peakTable_df = pd.DataFrame(peakTable, columns=['pixel', 'wavelength',
'peakIntensity'])

        ########################################
        ### FIND MATCHING ELEMENTS


        TOL = 0.132

        for pIdx, row in idWavelengths.iterrows():
                w = row['Observed Wavelength Air (nm)']

                # print '>>> w = ', w
                idx = (peakTable_df['wavelength'] - float(w)).abs().argmin()
                matchedRow = peakTable_df.iloc[idx]

                if (abs(matchedRow['wavelength'] - w) < TOL):
                        # Found a match
                        concentration = (matchedRow['peakIntensity'] )
                        matches.append([whichReading, matchedRow['wavelength'], row['Ion'],
concentration, row['Acc.'],w])



matches_df = pd.DataFrame(matches, columns=['Sample Rock','Peak Wavelength', 'Element',
'Intensity','Acc.','Observed Wavelength Air'])
matches_df.to_excel('Matches_'+readingsFilename+'.xlsx')
########################################
### FIT LORENTZIAN
if (False):
        OFFSET = 800.0
        lorKernel = lorentz.makeLorentzKernel_FWHM(4)

        def residual(peakAmounts, peakLocations, observedSpectrum):
                peakArray = np.zeros(len(observedSpectrum))
                peakArray[peakLocations] = peakAmounts

                # to generate spectrum: convole peak array with lorentzian kernel
```

```
        reconstructedSpectrum = convolve(peakArray, lorKernel) + OFFSET

        return np.abs(observedSpectrum - reconstructedSpectrum)

initAmounts = np.array([1000.0]*len(peakIndices))
results = leastsq(residual, initAmounts, args=(peakIndices, spectrum), full_output=1)

# get results
solnAmounts, cov_x, infodict, mesg, ier = results

peakArray = np.zeros(len(spectrum))
peakArray[peakIndices] = solnAmounts
reconstructedSpectrum = convolve(peakArray, lorKernel) + OFFSET

# plot example
fig, ax = plt.subplots(1,1)
ax.plot(wavelengths, spectrum, c='b', label='LIBS spectrum')
ax.plot(wavelengths, deriv, c='r', label='Derivative of spectrum')
ax.plot(wavelengths, reconstructedSpectrum, c='g', lw=2, alpha=0.7, label='Reconstruction')
ax.set_xlim((wavelengths.min(), wavelengths.max()))
ax.legend()

for peakIdx in peakIndices:
        ax.axvline(wavelengths[peakIdx], ls='--', c='#555555')

plt.show()
```

Appendix D Python Script for the multiplication of the LIBS responses

```
from __future__ import division
from __future__ import division

import matplotlib.pylab as plt
import pandas as pd
from pandas import DataFrame
import numpy as np
from scipy.optimize import leastsq
import os
import matplotlib.ticker as plticker
import xlrd


def fixValue(x):
        if (isinstance(x, unicode)):
                return x.strip().replace(badChar,'')
        else:
                return x

def clean(col):
        return col.apply(fixValue)



readingFilename='pythonbinomial2.csv'
spectra=pd.read_csv(readingFilename)
##rocks=spectra['Rocks']

result_data = {}

for col1 in spectra:
   for col2 in spectra:
      result_data[col1+'*'+col2] = spectra[col1]*spectra[col2]
pd.DataFrame(result_data).to_csv('result2.csv')
```

Appendix E Number of responses per sample for each ion for the Oxide samples

Row	Ag II 232.02	Ag II 241.32	Al II 281.62	Ba II 455.40	Be II 272.89	Be III 448.73	Bi I 306.77	Ca I 422.67	Ca II 317.93	Cd II 274.85	Cl II 481.01	Co I 347.40	Cr I 427.48
1			1		1			26		39			
2					2			21		35			
3								28	1	38			
4								27		37			
5			2					38	2	25	1		
6			1					15		33			
7			2					23		35			
8			8		7		4	29		39			
9		1	1		3			36	5	37	2		
10					3		1	19		40			
11			1	3	2			24	3	37			1
12		1			20		3	22	5	39			1
13				1	1			28		40			
14		7	1					18		33			
15		2						25		35			
16			1	1				29		38	1		
17				1	1	1		14	1	31			1
18			6		21		7	35	5	39			
19					3		3	26	2	38			
20			4		1		1	33	5	31			
21				1	1			38	3	40	1		2
22			1		9		4	14		38			
23		1	1		2		2	8		33			
24			1		6		1	27	1	39		1	
25					1			34	1	39			
26					4		3	30	1	40			
27								24	2	38			
28				3	8			28	2	35			3
29								18		40			
30				1	5			37	4	37			
31					1			24		37			
32	1	1						29		36			
33		7	2	2				28		30			1
34			1	1				37	2	36	2		
35					3			25	5	40			
36								33	1	40			
37					3			18	1	39			
38					10		1	25	1	40			
39					8			15		40			
40								36	1	20			
41					3			14		39	1		

Row	Cu I 324.75	Cu I 327.40	Cu II 271.35	F II 350.56	Fe I 374.95	Fe II 234.35	Fe II 238.20	Ga I 294.36	Hf I 368.22	In II 294.10	Ir I 269.42	Mg I 285.21
1	26	24		5	4	10	40					40
2	38	37			1	8	39					40
3	39	36		1		3	39			1		40
4	39	39			1	8	38					40
5	40	40			1	2	27				1	33
6	33	25			1	6	36					40
7	31	29		1		1	35			1		39
8	30	24	3	1	8	15	39			1	1	40
9	40	40	1	1	8	7	38					39
10	37	26	2	5	5	22	40					40
11	36	33		2	4	13	38					39
12	39	38	4		27	30	40		1		3	39
13	39	34		1	1	9	40					40
14	34	35		6	1	7	38	2		2		40
15	30	22		3		1	37	3				39
16	40	39				4	40					40
17	38	37			2	8	35			1		24
18	40	39	3	4	27	33	39			1	3	40
19	30	25	1	2	7	14	38	1			1	40
20	40	40			2	7	33					40
21	40	39			13	18	40					40
22	28	17	2		17	25	40					40
23	26	22		6	4	8	37	2			1	40
24	40	39	2	2	17	26	39					40
25	40	39	2		5	8	40					40
26	40	37	1		11	17	40				1	40
27	40	35			1	11	39					40
28	32	29	1	7	11	13	38	1			1	40
29	28	26		2	1	2	39					40
30	39	39	1	3	9	23	36					38
31	38	37		2	7	16	39	2				40
32	40	37			2	20	36					38
33	24	23		11			30	6		3		38
34	40	40			2	10	39					40
35	40	35		1	8	21	40					40
36	39	32		1		2	40					40
37	36	26		2	3	8	40	1				40
38	39	39	1		29	31	40				3	40
39	39	35	2		19	33	40					40
40	15	11			1		26					27
41	39	35	2		4	7	40					40

Row	Mg II 279.55	Mg III 239.51	Mn I 279.83	Mn II 261.02	N II 399.50	N IV 347.87	Na II 298.42	Na II 307.83	Ni I 349.30	O III 393.48	O V 278.10	P I 253.56
1	40	34		32			9	3	3	38	24	1
2	40	34		21			11	7		37	26	2
3	40	24		17			1	1		30	25	
4	40	29		20			3			37	27	
5	39	15		10			1			37	11	
6	40	18		16			4		1	19	25	
7	40	26		24			2	3	2	31	20	
8	40	31		17		1	9			39	21	
9	40	33		14			8		1	40	14	1
10	40	37		24		1	16	2		31	28	2
11	40	27		21			11	4	2	32	14	1
12	40	40		11			28	1		31	10	
13	40	31		27			3	3		34	21	1
14	40	33		22			12	4	3	37	22	1
15	40	23		19		1	3	3	1	33	25	
16	40	28		16			2			39	17	
17	35	28	1	19			2	1		26	10	1
18	40	39		9			33	6	3	38	5	1
19	40	35		23			13	3		33	28	1
20	40	24		21			8			38	14	
21	40	32		23			14			38	15	2
22	40	38		21			21	1		31	16	5
23	40	21		14		2	7	8	1	18	17	
24	40	39		22			19	2	1	37	19	3
25	40	33		25			6			40	19	
26	40	40		25			11			36	15	
27	40	31		22			3			37	27	1
28	40	32		20			16	6	5	36	12	1
29	40	28		24			1	2	1	26	32	
30	39	33		18		1	25	3	2	39	20	1
31	40	38		23			9	2	1	35	14	
32	40	34		16			12			38	25	6
33	40	21		15		4	9	8	7	32	13	1
34	40	29		24			7			40	10	
35	40	33		25			17	2		37	28	3
36	40	31		17			2	3		37	23	1
37	40	33		22		1	5	2		33	26	
38	40	38		18	1		30	2	1	39	25	1
39	40	40		18			23			29	18	1
40	31	10		12						38	19	
41	40	33		16	1		6			35	26	1

Row	P IV 334.77	Pb I 280.20	Pb I 283.31	S VI 419.89	S VI 420.08	Sc III 269.91	Si I 288.16	Si II 413.09	Sn II 335.20	Ta I 362.66	Ti I 399.86	Ti II 376.13
1							35			8	7	40
2	1						26			3	4	40
3		3					36			3	7	40
4					1		24			1	4	39
5	2	13					34			1	1	36
6	3						34			3	7	40
7	1	4					33			2	4	40
8	1	3	2		4		26			3	8	39
9	1	10	3		2		32			3	3	39
10			1				26			5	6	40
11	1	13	2	1	2		28			3	3	39
12		21	9	2	9		26	3			3	19
13		2					24			1	9	40
14	1						28			10	10	40
15	3	3					30			2	8	40
16	3	1					30				1	40
17		2					29				2	33
18		30	3	5	9		39	5		10		40
19		5	2	1	2		30	1		5	7	37
20	2	13					36		1		6	40
21		9					38	1			3	40
22		2	5	3	8		27	2		10	2	32
23	1	3	2	1	3		26	1		9	18	39
24		5	1		2		28	3	2	6	3	39
25		2					35			2		40
26	2	4					31	1		1	1	40
27	1						32			1	9	40
28		18	3	1	3		36	2		8	4	39
29		1	1				33	1		3	3	40
30	1	5					33			3	8	36
31	2	5			1		32	1	1	3	2	40
32	2	2					28			2	5	40
33	1	7				1	24			12	16	40
34		5					35				1	40
35	1	1					31				4	39
36	1						26				9	40
37	1	3		1	2		29	1		4	7	39
38	2	4	3	3	7		28	1		4		37
39				1	2		25	1				39
40		3					37					40
41	1	3	1		1		27				2	40

Row	Ti III 251.61	Tl I 276.79	Tl I 351.92	V II 292.40	W I 400.88	W II 248.92	Y II 371.03	Zn I 334.50	Zn II 491.16	Zr III 266.43
1	4				2		1		1	1
2	7				1	1			3	3
3	2									
4	3				2	1	2		2	2
5	1					1	8		1	1
6	1									
7						1				
8	8		2			4			8	8
9	7		1			4	5		4	4
10	13				1	3			4	4
11	11				1	7			5	5
12	26				1	19			25	25
13	2				2				1	1
14	3	2			1					
15		1			1					
16	1				1		7			
17	5				2				2	2
18	30					18			29	29
19	8				3	5			8	8
20	6				2		3		2	2
21	13					3	1		3	3
22	16		7		1	9			13	13
23	6					4	1		4	4
24	18				1	6			10	10
25	3					1			3	3
26	11				3	2	2		8	8
27	4				2					
28	14	1				7			10	10
29	1				1					
30	19				1	2			11	11
31	7				1	2			3	3
32	11		1						2	2
33		6		2	2	2		1		1
34	6				1		17		1	1
35	14		1			2			8	8
36	3				3				1	1
37	5		1						3	3
38	26					7			18	18
39	27					2	1		22	22
40										
41	6		1		1	3	1		5	5

Appendix F Compiled LIBS responses for Sulphide rock samples from Escondida Mine

	C I	C III	Ag II	Ag II	Al II	Au I	Ba II	Be II	Bi I	Ca I	Ca II	Cd II	Cl II	Cr I
Row	**247.86**	**229.69**	**232.02**	**241.32**	**281.62**	**242.80**	**455.40**	**272.89**	**306.77**	**422.67**	**317.93**	**274.85**	**481.01**	**427.48**
1		727		798			881			922		1007		908
2		743	730	835	861					876				
4							830							878
8					878		904			905				881
9								1295	1102	864		1455		927
10		715		900	916					875		957		858
11						984				855		1102		875
12					972			1132	974	875	913	1505	801	865
13	1065			928	935					992		1196		875
14		777						1174				1815		
15					1048		806		983	856		1315		1006
16										873				836
18					928					849		898		843
20				811	935		846			876		1255		1039
22				893								941		919
25		742		831	913					831		916		873
27		800					821	1319	1090	920	978	2149		
30				847	885							893		869
31				851	935					835				1065
32				808	882					943		1076		827
33							843	1107		849	938	1213		849
35							826			840		961		834
37		884						1522	1245	951	1059	2596		828
39		718		846	883									
42		774		846	924				1340					941
44		771		828			835	1103		854		1181		906
45				890						846		1167		920
46		778		885	1030			1257	1020	848	928	1146		894
48		783		869	1390							921		
49					849			1178	1079	944		2030		858
50		751		861	906		888	1012		847		1321		793
51				846	914					891		1165		971
54		752			906			1118	1122			1450		
55								1179	1098			1580		862
57				827	957							969		952
58					890									874
59		824		819				1568	1224	927	1052	1787		847
62		885		825				1640	1220	984	1086	2907	988	

	Cu I	Cu I	Cu II	F II	Fe I	Fe II	Fe II	Ga I	Hf I	Hg II	In II	Ir I	Mg I
Row	**324.75**	**327.40**	**271.35**	**350.56**	**374.95**	**234.35**	**238.20**	**294.36**	**368.22**	**284.77**	**294.10**	**269.42**	**285.21**
1	2619	2175		1049	969	908	1043	928			986		856
2	2146	1596		1106				964			957		881
4	2520	2151		1017							920		884
8	2713	2261											862
9	2368	1979	1269	1026	1048	1121	1300	928			925	1054	930
10	2350	1996		1165			897	1024			1028		
11	2290	1986			891	955	1060						876
12	2360	1960	1059		1065	1043	1302	948				944	1044
13	2357	1853	1022	1203	956	1041	1021	1131			1110		1064
14	2136	1841	1135	1029	1079	1227	1435	942			988	994	934
15	3036	2562			1021	1049	1192			995			964
16	2290	1909		1027				958			927		899
18	2439	1993		1004			884	896					900
20	2530	1903		1024	958	1012	1064	916			931		881
22	2408	2015		1060			896	905			1005		897
25	2631	2037		1047			865	963			990		906
27	1760	1510	1114		1199	1324	1789		894			1018	1062
30	2176	1677		1036			844	972			948		955
31	2161	1746		1071				939			1029		862
32	2359	1952		1052	932	891	999	920			957		898
33	2369	1983	1047	998	948	993	1106	892					818
35	2258	1913			931	904	924						904
37	2160	1795	1170		1307	1556	2110					1042	1054
39	2068	1687		1051			822	965			978		872
42	2385	1637		1113				1009			1017		871
44	2373	1954		1033	940	974	1122	960			905		901
45	2532	2118		1129	929	973	1088	949			1018		936
46	2019	1635		1150	1355	1185	1000	1059	895		1015		941
48	1863	1440	1022	1137			866	946		1779	1067		968
49	2325	1939		976	1204	1244	1252	905			909		843
50	2141	1819	990	1041	1073	995	1164	990			935		913
51	2319	1882		1063	1072	961	1104	966			940		926
54	1741	1106	1125	1046	1123	1104	1258	922			990		949
55	2184	1822	1093	1134	1084	1212	1355						836
57	2249	1696		1111			918	959			1018		953
58	2245	1980		1008				904			911		813
59	2028	1713	1363	1143	1219	1306	1578		984		983		956
62	2391	1935	1208	938	1404	1659	2336	1024	1050			1077	1175

	Mg II	Mg III	Mn I	Mn II	Mo VI	Mo VI	N IV	Na II	Na II	Ni I	Ni I	O III	O V	P I
Row	**279.55**	**239.51**	**279.83**	**261.02**	**329.33**	**338.70**	**347.87**	**298.42**	**307.83**	**341.48**	**349.30**	**393.48**	**278.10**	**253.56**
1	962	1012	879				867	908	1468		878	971		
2	974			818			877	938	1585		869	964		
4	953		794				844		1448			859		
8	955					976						1005		
9	1044	1208		1273			863	1021	1470		889	924		
10	913	843		930			878	974	1582		914			
11	1005	1041	912	1112				921				894		1163
12	1339	1183		1229				1022	1105		828	1008	962	1449
13	1040	1010		956			855	1026	1804		958	1156		1207
14	1038	1434		1388			871	1076	1507		892			1869
15	1142	1177		1259				1001		984		919		
16	964							840	1462		830	882		
18	1048						812	884	1421		846	1078		
20	988	1092		1082			860	938	1501		819	936		
22	976						913	988	1606		948			
25	1006	880		857			831	897	1521		841	888		
27	1197	1587		1509				1219	958			1035		1461
30	962						879	924	1539		863	881		
31	1026			825			966	1091	1565		884	936		
32	947	949		1033			815	888	1476		849	922		
33	896	1064		1020			809	901	1398		825	956		995
35	950	926		944				863				908		
37	1307	1867		2091				1354	1119		903	1018		
39	922			830			880	934	1520		877			
42	967			879			891	949	1621		901			
44	1017	1062		1145			867	938	1526		853	948		
45	981	1024	982	1134			856	963	1491		916	910		1035
46	1059	1151		968			909	1000	1696		881	942		
48	1073			904	1436		876	983	1644		892	919		
49	996	1488	852					1153	1566		816	921		
50	1008	1084		1123			877	999	1538		872	929		1084
51	1104	1034		1084			892	950	1551		883	999		1283
54	1071	1176		1115			859	1026	1550		893			1048
55	952	1331		1360			860	1102	1671		869	964		
57	1014	884		946			893	918	1580		876			
58	915			807			829	852	1447		830	820		
59	1087	1536		1206				1181	1684		931			1079
62	1295	2027		2030				1416	1570			1025		

	P IV	Pb I	Pb I	Pd I	S VI	S VI	Sb I	Si I	Si II	Sn II	Ta I	Ti I	Ti II
Row	**334.77**	**280.20**	**283.31**	**340.46**	**419.89**	**420.08**	**231.15**	**288.16**	**413.09**	**335.20**	**362.66**	**399.86**	**376.13**
1		1004			841	841		1138				912	1319
2		970	990					1234		913		907	1452
4	1014	923						1026		882		888	1089
8	947	988						1209					869
9	906	1037	1118		852	885		1263	985			915	1167
10	999							1225				937	1534
11	847	1035			815	815		1079				907	
12		1169	1036		871	869		1167	837			879	1000
13		1141						1247				955	1529
14		1042	958		915	906		1296	912			916	1347
15	1064	1138			903	897		1227	893			890	
16	844	966						1206				883	1348
18		1043						1243				908	1329
20		968						1258				886	1284
22	879	1018						1303		911		941	1415
25		1034						1201		825		896	1387
27	922	1085	1041		948	972	905	1289	931			882	
30		995	921					1204		868	795	917	1337
31		1002						1240				933	1334
32	845	993	889		863	863		1136				910	1409
33		899				834		942	821			875	1071
35	856	1052				826		968	827				
37	1104	1239	1181		998	1003		1419	962			948	867
39		1046	962					1221			883	916	1406
42		984	974					1228		837	864	925	1498
44	973	1029				922		1212				894	1387
45	949	1088						1187				913	1353
46		1033	971		1026	1017	805	1305				958	1559
48		1015		1049				1407				939	1472
49	851	1003						1153				885	1094
50		1017	935		870	892	750	1236	885			931	1494
51		1076	906			930		1376				903	1461
54		1047	1021		870	887		1308	891			913	1468
55	857	930	922		876	902		1201	914	883		902	1284
57	995	1051						1253				925	1370
58		934						1146				868	1285
59	993	1080	1157		1016	1041		1275	987			929	1252
62		1234	1246		1006	1043		1376	945		829	962	1753

	Ti III	Tl I	Tl I	V I	V II	W I	W II	Y II	Zn I	Zr III	Zr III
Row	**251.61**	**276.79**	**351.92**	**411.18**	**292.40**	**400.88**	**248.92**	**371.03**	**334.50**	**262.06**	**266.43**
1	1094	968	920	973			840	849		986	843
2	1176		936								
4	1072	913					826			848	
8	1156	924		961			903			1008	
9	1332	1044					1139	916			1057
10	1186		993				866			859	
11	1144	908					815	797			877
12	1278	1012					1195	885	944		981
13	1245	897	1017			869	862	874		858	1001
14	1336	1164			939			916			1088
15	1291	1022			1002		930	908		1076	993
16	1171						849			856	
18	1178	846					872			845	
20	1229	1064					1031				1016
22	1244						906				
25	1145		861				875			839	
27	1603	1268			925		1888	973			1183
30	1187		923				858			845	
31	1197		962				908			843	
32	1115	856	858				804			821	830
33	947	858					829	855		856	1012
35	992	845					909	819			873
37	1580	1459			1240		905	1051		910	1335
39	1164		1014								
42	1189		918				839	880			
44	1232	961	868				946	934			969
45	1200	968	963				890	811		896	874
46	1258	1223	951		948			1009			1133
48	1319		984		1799						
49	1085	1193	851				816	953			1076
50	1249	962	928				984	887			957
51	1342	955	886				991	857			926
54	1299	1090	948		937			916			1047
55	1191	1060	910				960	905			1093
57	1213	875	921								
58	1083	802	807				825			821	
59	1263	1235	906		1127		885	1007			1288
62	1772	1556		969	1182			1080			1407

Appendix G Number of responses per sample for each ion for the Sulphide samples

	C I	C III	Ag II	Ag II	Al II	Au I	Ba II	Be II	Bi I	Ca I	Ca II	Cd II	Cl II	Cr I
Row	247.86	229.69	232.02	241.32	281.62	242.80	455.40	272.89	306.77	422.67	317.93	274.85	481.01	427.48
1		2		1			9			6		5		4
2		1	1	4	1					3				
4							1							5
8					1		6			11				9
9								4	5	10		34		4
10		1		6	1					2		2		2
11						1				10		28		7
12					1			9	11	32	3	39	2	1
13	1			4	1					2		6		2
14		4						13				18		
15					3		2		1	16		25		10
16										5				4
18					2					1		2		10
20				1	2		1			6		5		3
22				2								1		2
25		2		5	4					2		8		5
27		1					2	22	24	18	8	40		
30				4	3							1		1
31				2	5					2				1
32				3	2					3		4		6
33							4	1		7	1	5		7
35							3			9		20		4
37		5						27	18	19	6	37		1
39		1		3	5									
42		1		8	4				1					1
44		1		3			2	3		7		30		4
45				1						1		13		4
46		1		8	3			3	3	11	1	21		3
48		1		8	4							6		
49					1			1	1	1		1		6
50		2		3	4		1	8		4		37		1
51				4	2					11		19		3
54		1			4			10	3			29		
55								9	2			22		3
57				7	3							9		1
58					1									2
59		2		1				8	7	3	3	26		1
62		3		1				27	28	22	13	39	1	

	Cu I	Cu I	Cu II	F II	Fe I	Fe II	Fe II	Ga I	Hf I	Hg II	In II	Ir I	Mg I
Row	324.75	327.40	271.35	350.56	374.95	234.35	238.20	294.36	368.22	284.77	294.10	269.42	285.21
1	28	28		9	2	2	3	6			3		6
2	5	7		17				11			12		4
4	38	38		2							1		2
8	40	40											6
9	36	36	2	2	22	21	33	1			1	1	13
10	20	21		19			3	7			10		
11	38	39			14	11	27						8
12	40	40	3		33	35	40	1				1	32
13	25	30	1	16	1	2	8	6			1		7
14	4	4	9	8	13	16	21	2			3	5	7
15	40	40			20	16	27			1			12
16	33	32		11				2			8		7
18	34	36		5			3	2					15
20	25	31		10	3	4	8	2			7		9
22	34	34		6			2	2			6		7
25	15	18		15			9	12			5		12
27	40	39	2		38	40	40		3			4	10
30	17	18		22			1	9			9		3
31	32	33		13				4			5		13
32	29	31		6	2	2	5	5			3		4
33	38	39	1	1	6	3	5	1					1
35	40	40			9	3	19						2
37	40	40	2		36	36	37					1	18
39	7	7		25			1	12			7		1
42	11	19		23				16			8		4
44	38	36		10	11	19	29	3			4		10
45	36	36		6	5	5	15	3			4		4
46	13	13		22	3	4	26	7	1		9		18
48	11	13	1	17			5	3		1	7		7
49	36	36		5	1	1	2	3			1		16
50	1	1	2	24	14	29	37	2			3		3
51	33	31		18	3	12	16	7			3		19
54	4	8	5	25	12	20	29	5			3		10
55	40	40	8	2	13	14	23						5
57	20	25		18			9	6			10		6
58	23	20		15				3			5		5
59	38	38	1	2	18	19	23		4		2		11
62	39	39	5	1	38	39	39	1	3			2	8

	Mg II	Mg III	Mn I	Mn II	Mo VI	Mo VI	N IV	Na II	Na II	Ni I	Ni I	O III	O V	P I
Row	279.55	239.51	279.83	261.02	329.33	338.70	347.87	298.42	307.83	341.48	349.30	393.48	278.10	253.56
1	31	2	1				7	6	11		2	14		
2	33			1			8	8	31		16	4		
4	20		1				1		2			3		
8	32					1						9		
9	39	28		11			1	25	4		1	18		
10	8	2		3			5	11	13		6			
11	25	19	1	16				14				18		3
12	39	39		13				38	2		2	26	6	3
13	36	5		8			5	9	13		8	2		1
14	26	16		9			4	19	14		4			2
15	20	19		13				18		1		15		
16	35							3	3		7	9		
18	30						1	1	3		2	2		
20	40	5		5			5	5	14		4	7		
22	35						2	1	10		3			
25	30	2		10			11	12	21		11	3		
27	26	40		10				37	1			11		2
30	21						7	5	27		10	1		
31	37			1			3	1	12		5	7		
32	36	4		2			2	5	6		5	4		
33	13	4		1			1	5	1		1	10		1
35	17	10		9				7				20		
37	38	37		10				36	3		2	15		
39	19			2			12	5	30		7			
42	31			1			10	11	25		12			
44	35	24		14			7	17	8		1	14		
45	24	6	1	4			2	6	8		3	1		1
46	36	8		16			11	20	26		11	11		
48	26			6	1		5	10	19		10	1		
49	30	1	1					1	2		1	3		
50	36	33		21			4	34	26		10	2		3
51	40	14		15			3	17	19		6	14		3
54	35	25		20			6	25	28		9			1
55	25	17		7			2	14	2		1	1		
57	34	3		3			2	11	16		8			
58	26			1			6	1	16		5	3		
59	32	19		9				20	2		3			1
62	25	39		5				40	3			11		

	P IV	Pb I	Pb I	Pd I	S VI	S VI	Sb I	Si I	Si II	Sn II	Ta I	Ti I	Ti II
Row	334.77	280.20	283.31	340.46	419.89	420.08	231.15	288.16	413.09	335.20	362.66	399.86	376.13
1		10			1	1		30				17	17
2		11	1					22		1		36	33
4	1	2						30		1		3	5
8	2	7						36					8
9	2	12	3		6	12		35	3			12	3
10	1							28				22	22
11	1	8			1	1		34				1	
12		20	2		5	20		40	5			6	1
13		12						31				20	22
14		3	6		1	9		20	2			19	13
15	1	9			2	5		38	1			5	
16	2	10						36				16	16
18		15						37				7	7
20		12						25				15	15
22	2	3						30		1		11	12
25		14						29		1		24	21
27	1	10	14		10	23	1	37	7			13	
30		3	1					23		1	1	31	31
31		14						30				19	22
32	1	8	1		1	1		35				11	14
33		2				3		34	1			3	6
35	3	3				2		32	3				
37	1	25	17		13	30		37	9			25	1
39		2	1					29			1	33	32
42		8	1					22		1	1	32	31
44	1	10				1		30				13	12
45	2	3						35				11	10
46		20	4		2	3	1	18				31	24
48		13		2				16				26	21
49	2	12						38				7	14
50		16	5		4	8	1	31	2			37	25
51		23	1			1		38				26	20
54		22	6		1	7		31	4			40	21
55	4	4	1		5	10		37	1	2		9	4
57	1	10						32				24	27
58		4						35				17	25
59	2	10	8		2	11		37	5			13	6
62		14	23		13	34		33	10		1	24	2

	Ti III	Tl I	Tl I	V I	V II	W I	W II	Y II	Zn I	Zr III	Zr III
Row	251.61	276.79	351.92	411.18	292.40	400.88	248.92	371.03	334.50	262.06	266.43
1	40	3	1	1			2	2		3	2
2	40		3								
4	33	1					1			6	
8	40	3		1			5			5	
9	37	25					2	11			12
10	40		5				2			1	
11	24	18					1	2			8
12	23	36					3	28	11		29
13	38	3	6			1	1	1		1	1
14	24	16			2			12			16
15	27	19			1		2	7		1	9
16	40						2			1	
18	40	2					5			2	
20	40	3					2				2
22	40						3				
25	37		3				4			1	
27	20	39			2		1	30			36
30	40		2				2			1	
31	40		2				3			2	
32	39	3	2				1			2	1
33	24	6					6	3		8	1
35	22	11					4	3			1
37	22	37			3		1	30		1	34
39	40		1								
42	40		6				1	1			
44	38	17	1				2	1			7
45	39	9	2				4	1		1	1
46	37	3	3		1			3			3
48	30		3		1						
49	40	1	1				5	1			1
50	37	26	3				1	16			17
51	40	8	4				1	3			4
54	37	16	1		1			11			13
55	34	19	1				3	12			12
57	40	1	4								
58	40	2	1				4			1	
59	32	20	1		1		2	13			13
62	9	39		1	2			33			37

Appendix H ICP certified assay results for the 41 Sulphide Escondida samples

ANALYTE	WtKg	Ag	Al	As	Ba	Be	Bi	Ca	Cd
METHOD	G_WGH79	GE_ICP14B	GE_ICP14B	GE_ICP14B	GE_ICP14B	GE_ICP14B	GE_ICP14B	GE_ICP14B	GE_ICP14B
DETECTION	0.01	2	0.01	3	5	0.5	5	0.01	1
UNITS	kg	ppm	%	ppm	ppm	ppm	ppm	%	ppm
Sulfuro-1	0.428	<2	0.85	4	61	<0.5	<5	0.01	<1
Sulfuro-2	0.157	<2	1.69	7	13	<0.5	<5	<0.01	<1
Sulfuro-3	0.181	<2	0.59	11	26	<0.5	<5	0.03	<1
Sulfuro-4	0.07	<2	0.92	11	43	<0.5	<5	0.02	<1
Sulfuro-8	0.101	<2	0.72	3	47	<0.5	<5	0.01	<1
Sulfuro-9	0.346	<2	0.42	5	11	<0.5	<5	0.03	<1
Sulfuro-10	0.402	<2	1.21	4	13	<0.5	<5	<0.01	<1
Sulfuro-11	0.267	<2	0.41	3	16	<0.5	<5	0.01	<1
Sulfuro-12	0.198	<2	0.61	3	31	<0.5	<5	0.13	<1
Sulfuro-13	0.141	<2	0.6	9	17	<0.5	<5	0.02	<1
Sulfuro-14	0.159	<2	0.9	7	7	<0.5	<5	<0.01	<1
Sulfuro-15	0.17	<2	0.43	<3	39	<0.5	<5	0.02	<1
Sulfuro-16	0.065	<2	0.88	6	10	<0.5	<5	0.04	<1
Sulfuro-18	0.06	<2	1.4	7	21	<0.5	<5	<0.01	<1
Sulfuro-20	0.045	<2	1.09	<3	<5	<0.5	<5	0.02	<1
Sulfuro-22	0.028	<2	1.16	4	30	<0.5	<5	0.02	<1
Sulfuro-25	0.026	<2	0.75	6	42	<0.5	<5	0.05	<1
Sulfuro-27	0.038	<2	0.55	5	31	<0.5	<5	0.02	<1
Sulfuro-30	0.014	<2	1.94	10	26	<0.5	<5	0.01	<1
Sulfuro-31	0.026	<2	1.51	5	48	<0.5	<5	0.02	<1
Sulfuro-32	0.018	<2	1.34	3	50	<0.5	<5	0.03	<1
Sulfuro-33	0.025	<2	0.86	<3	62	<0.5	<5	0.02	<1
Sulfuro-35	0.022	<2	0.68	5	50	<0.5	<5	0.03	<1
Sulfuro-37	0.028	<2	0.59	4	23	<0.5	<5	0.03	<1
Sulfuro-39	0.035	<2	1.33	8	12	<0.5	<5	<0.01	<1
Sulfuro-42	0.046	<2	1.01	4	12	<0.5	<5	0.01	<1
Sulfuro-44	0.018	<2	0.74	3	64	<0.5	<5	0.01	<1
Sulfuro-45	0.018	<2	0.82	3	24	<0.5	<5	0.02	<1
Sulfuro-46	0.018	<2	0.87	18	11	<0.5	<5	0.04	<1
Sulfuro-48	0.018	<2	1.1	6	18	<0.5	<5	0.02	<1
Sulfuro-49	0.019	<2	1.66	5	48	<0.5	<5	0.02	<1
Sulfuro-50	0.017	<2	1.32	5	22	<0.5	<5	0.01	<1
Sulfuro-51	0.022	<2	0.69	<3	15	<0.5	<5	0.03	<1
Sulfuro-54	0.03	<2	1.72	10	26	<0.5	<5	0.01	<1
Sulfuro-55	0.029	<2	1.31	7	14	<0.5	<5	0.02	<1
Sulfuro-57	0.019	<2	0.82	9	30	<0.5	<5	0.03	<1
Sulfuro-58	0.018	<2	1.23	5	16	<0.5	<5	0.02	<1
Sulfuro-59	0.015	<2	0.95	<3	40	<0.5	<5	0.02	<1
Sulfuro-62	0.016	<2	0.52	4	39	<0.5	<5	0.03	1

Co	Cr	Cu	Fe	Hg	K	La	Li	Mg	Mn
GE_ICP14B	GE_ICP14B	GE_ICP14B	GE_ICP14B	GE_ICP14B	GE_ICP14B	GE_ICP14B	GE_ICP14B	GE_ICP14B	GE_ICP14B
1	1	0.5	0.01	1	0.01	0.5	1	0.01	2
ppm	ppm	ppm	%	ppm	%	ppm	ppm	%	ppm
<1	<1	6560	0.12	<1	0.2	7.2	<1	0.03	11
<1	<1	8470	0.07	<1	0.07	4.4	3	0.01	12
5	1	6390	0.28	1	0.11	3.1	<1	0.02	17
<1	1	>10000	0.22	<1	0.2	7.6	1	0.03	30
<1	<1	7420	0.12	<1	0.19	6.6	<1	0.03	9
11	<1	>10000	3.26	<1	0.1	<0.5	<1	0.01	8
<1	<1	5150	0.15	<1	0.05	6.9	2	<0.01	7
10	2	>10000	0.71	<1	0.14	0.6	<1	0.01	18
5	3	1330	1.33	<1	0.1	18.7	4	0.51	296
1	1	9620	0.14	<1	0.12	5.1	<1	0.02	15
<1	<1	1500	0.74	<1	0.06	3.5	<1	0.01	19
6	2	2510	0.37	<1	0.16	1.2	<1	0.02	15
<1	<1	>10000	0.13	<1	0.13	0.8	<1	0.02	12
<1	<1	6160	0.28	<1	0.12	7.4	2	0.02	18
<1	<1	1370	0.09	<1	0.12	5.3	2	0.01	9
<1	<1	>10000	0.12	<1	0.11	4.5	<1	0.02	10
<1	1	1180	0.15	<1	0.09	1.2	<1	0.02	11
47	<1	5490	6.91	<1	0.11	<0.5	<1	0.01	14
<1	1	4430	0.18	<1	0.1	7.2	2	0.02	29
<1	<1	>10000	0.11	<1	0.15	6.5	1	0.02	10
1	1	5540	0.21	<1	0.25	4.3	1	0.03	15
4	3	1060	0.48	<1	0.33	1.2	<1	0.03	37
9	2	>10000	3.33	<1	0.32	0.8	<1	0.03	22
43	<1	6950	1.94	<1	0.14	1.4	<1	0.02	11
<1	<1	4190	0.11	<1	0.09	5.8	2	0.01	10
<1	<1	3340	0.09	<1	0.07	6.6	1	0.01	9
15	1	4610	0.65	<1	0.21	4.3	<1	0.03	12
7	1	5420	0.5	<1	0.1	4.7	<1	0.01	15
<1	<1	2300	0.18	<1	0.14	1	<1	0.02	10
4	1	9210	0.38	<1	0.12	6.4	1	0.02	19
<1	1	6130	0.19	<1	0.24	6.5	2	0.03	15
<1	2	393	1.54	<1	0.08	6	2	0.01	45
6	1	>10000	0.56	<1	0.22	<0.5	<1	0.02	19
<1	1	849	0.62	<1	0.13	8	2	0.02	35
1	<1	>10000	0.83	<1	0.07	2.3	2	0.01	6
3	1	>10000	0.25	<1	0.21	1.8	<1	0.03	16
<1	<1	>10000	0.13	<1	0.07	4.1	1	0.01	8
3	1	>10000	0.38	<1	0.29	1.4	<1	0.03	18
32	<1	4690	8.31	<1	0.12	<0.5	<1	<0.01	20

Mo	Na	Ni	P	Pb	S	Sb	Sc	Sn	Sr
GE_ICP14B	GE_ICP14B	GE_ICP14B	GE_ICP14B	GE_ICP14B	GE_ICP14B	GE_ICP14B	GE_ICP14B	GE_ICP14B	GE_ICP14B
1	0.01	1	0.01	2	0.01	5	0.5	10	5
ppm	%	ppm	%	ppm	%	ppm	ppm	ppm	ppm
75	0.03	1	<0.01	3	0.21	<5	<0.5	<10	6
80	0.04	1	<0.01	3	0.3	<5	0.6	<10	10
66	0.03	2	<0.01	<2	0.33	<5	<0.5	<10	8
80	0.05	1	<0.01	5	0.32	<5	0.7	<10	5
77	0.03	<1	<0.01	<2	0.21	<5	<0.5	<10	6
20	0.05	4	<0.01	7	4.31	<5	<0.5	<10	8
15	0.03	<1	<0.01	<2	0.26	<5	<0.5	<10	<5
141	0.03	3	<0.01	7	1.16	<5	0.5	<10	16
7	0.05	5	0.05	154	0.73	<5	0.6	<10	7
106	0.05	1	<0.01	3	0.31	<5	<0.5	<10	7
18	0.03	1	<0.01	<2	0.14	<5	0.6	<10	<5
19	0.03	2	<0.01	<2	0.36	<5	<0.5	<10	14
107	0.1	2	<0.01	6	0.58	<5	1	<10	13
77	0.03	<1	<0.01	2	0.21	<5	0.5	<10	<5
30	0.08	1	<0.01	<2	0.17	<5	0.5	<10	<5
121	0.04	1	<0.01	10	0.69	<5	0.5	<10	15
15	0.07	2	<0.01	<2	0.14	<5	0.6	<10	38
52	0.06	10	<0.01	7	>5	<5	<0.5	<10	16
25	0.04	1	<0.01	<2	0.2	<5	0.8	<10	12
20	0.05	1	<0.01	4	0.43	<5	0.7	<10	21
13	0.08	2	<0.01	<2	0.23	<5	0.9	<10	16
10	0.06	2	<0.01	<2	0.2	<5	0.6	<10	20
1830	0.06	4	<0.01	10	4.48	<5	0.8	<10	18
25	0.05	4	<0.01	4	2.55	<5	<0.5	<10	7
51	0.04	<1	<0.01	<2	0.17	<5	<0.5	<10	<5
31	0.03	1	<0.01	<2	0.16	<5	<0.5	<10	7
13	0.04	3	<0.01	<2	0.8	<5	<0.5	<10	8
19	0.05	3	<0.01	<2	0.61	<5	0.5	<10	6
80	0.11	1	<0.01	<2	0.2	<5	1.1	<10	28
88	0.04	1	<0.01	2	0.55	<5	0.6	<10	6
45	0.04	1	<0.01	<2	0.22	<5	0.9	<10	5
20	0.04	<1	<0.01	<2	0.08	<5	1	<10	8
26	0.05	2	<0.01	6	1.07	<5	0.8	<10	8
31	0.04	<1	<0.01	<2	0.09	<5	0.8	<10	<5
40	0.03	1	<0.01	6	1.38	<5	0.6	<10	11
41	0.06	1	<0.01	<2	0.34	<5	0.6	<10	20
29	0.03	1	<0.01	6	0.55	<5	<0.5	<10	6
280	0.07	2	<0.01	8	0.9	<5	1	<10	27
156	0.06	6	<0.01	6	>5	<5	<0.5	<10	21

Ti	V	W	Y	Zn	Zr	Al2O3	Ba	CaO	Cr2O3
GE_ICP14B	GE_ICP14B	GE_ICP14B	GE_ICP14B	GE_ICP14B	GE_ICP14B	GO_ICP95A	GO_ICP95A	GO_ICP95A	GO_ICP95A
0.01	1	10	0.5	1	0.5	0.01	0.001	0.01	0.01
%	ppm	ppm	ppm	ppm	ppm	%	%	%	%
<0.01	5	<10	0.6	9	<0.5	25.1	0.091	0.04	<0.01
<0.01	5	<10	0.6	5	0.6	28.7	0.029	0.04	<0.01
0.02	4	<10	<0.5	5	<0.5	20.5	0.045	0.08	<0.01
0.02	6	<10	0.6	5	<0.5	20.9	0.045	0.04	<0.01
<0.01	3	<10	<0.5	3	<0.5	21.4	0.079	0.04	<0.01
<0.01	5	<10	<0.5	2	0.6	19.1	0.03	0.24	<0.01
<0.01	3	<10	<0.5	2	<0.5	25.8	0.027	0.03	<0.01
<0.01	4	<10	<0.5	4	0.6	16.3	0.036	0.08	<0.01
<0.01	13	<10	4.3	207	<0.5	15.7	0.037	0.76	<0.01
0.01	3	<10	<0.5	4	<0.5	18.8	0.028	0.07	<0.01
0.03	20	<10	<0.5	4	<0.5	26.1	0.03	0.05	<0.01
<0.01	4	<10	<0.5	4	<0.5	18.4	0.061	0.1	<0.01
<0.01	7	<10	0.6	5	<0.5	19.1	0.016	0.14	<0.01
<0.01	8	<10	0.5	4	<0.5	27.7	0.039	0.03	<0.01
<0.01	5	<10	0.6	5	<0.5	22.9	0.016	0.08	<0.01
<0.01	5	<10	0.6	7	<0.5	24.9	0.04	0.05	<0.01
<0.01	4	<10	0.6	5	<0.5	21.4	0.037	0.15	<0.01
<0.01	5	<10	<0.5	<1	1.2	16.9	0.04	0.2	<0.01
<0.01	6	<10	0.7	8	<0.5	27.4	0.028	0.04	<0.01
<0.01	6	<10	0.6	3	<0.5	26.8	0.059	0.05	<0.01
<0.01	9	<10	0.7	4	<0.5	21.1	0.045	0.07	<0.01
<0.01	9	<10	0.6	6	<0.5	16.6	0.047	0.08	<0.01
<0.01	5	<10	<0.5	1	0.8	16.5	0.055	0.21	<0.01
<0.01	6	<10	<0.5	2	0.7	20.2	0.038	0.15	<0.01
<0.01	4	<10	<0.5	2	<0.5	30.2	0.026	0.04	<0.01
<0.01	3	<10	0.6	5	<0.5	26.4	0.023	0.04	<0.01
<0.01	4	<10	<0.5	3	<0.5	19.7	0.082	0.05	<0.01
<0.01	5	<10	0.6	4	<0.5	22.6	0.032	0.07	<0.01
0.03	6	<10	0.5	4	<0.5	24.5	0.02	0.17	<0.01
<0.01	5	<10	0.6	2	<0.5	25.1	0.03	0.06	<0.01
<0.01	7	<10	0.6	6	<0.5	23.3	0.04	0.04	<0.01
0.07	38	<10	0.6	2	0.5	26.5	0.032	0.05	<0.01
<0.01	9	<10	<0.5	2	<0.5	18.1	0.02	0.13	<0.01
0.03	18	<10	0.7	3	<0.5	28.3	0.028	0.03	<0.01
<0.01	5	<10	0.5	3	<0.5	26.1	0.021	0.06	<0.01
0.01	4	<10	<0.5	2	<0.5	20.3	0.036	0.09	<0.01
<0.01	4	<10	0.6	4	<0.5	26.5	0.026	0.05	<0.01
<0.01	10	<10	0.6	3	<0.5	20.4	0.05	0.09	<0.01
<0.01	5	<10	<0.5	<1	1.5	19.4	0.055	0.24	<0.01

Fe2O3	K2O	MgO	MnO	Na2O	Nb	P2O5	SiO2	Sr
GO_ICP95A	GO_ICP95A	GO_ICP95A	GO_ICP95A	GO_ICP95A	GO_ICP95A	GO_ICP95A	GO_ICP95A	GO_ICP95A
0.01	0.01	0.01	0.01	0.01	0.001	0.01	0.01	0.001
%	%	%	%	%	%	%	%	%
1.41	4.15	0.56	<0.01	0.49	0.002	0.04	56.5	0.014
0.43	1.23	0.14	<0.01	0.59	0.002	0.11	52.1	0.023
1.21	2.61	0.3	<0.01	0.69	0.001	0.08	64.5	0.027
1.14	2.71	0.36	<0.01	0.69	0.002	0.04	64.7	0.012
1.18	3.46	0.43	<0.01	0.48	0.002	0.04	63.9	0.01
5.13	2.38	0.17	<0.01	1.3	0.002	0.36	57.2	0.053
0.53	1.04	0.11	<0.01	0.49	0.002	0.03	57.7	0.011
1.77	3.32	0.29	<0.01	0.56	0.002	0.25	58.8	0.057
2.15	1.4	1.02	0.04	5.44	0.001	0.12	70.1	0.052
0.92	2.44	0.28	<0.01	0.89	0.001	0.08	61.3	0.026
2.27	1.75	0.15	<0.01	0.69	0.002	0.15	52.8	0.03
1.75	3.89	0.44	<0.01	0.61	0.002	0.18	66.7	0.044
0.58	1.75	0.14	<0.01	1.33	0.002	0.2	64.8	0.02
1.03	2.05	0.22	<0.01	0.47	0.002	0.06	55.1	0.012
0.51	1.65	0.16	<0.01	1.19	0.002	0.09	59.2	0.015
0.65	1.83	0.21	<0.01	0.59	0.002	0.06	57.3	0.023
0.62	1.46	0.17	<0.01	1.29	0.002	0.24	64.8	0.068
10.2	1.65	0.1	<0.01	1.11	0.002	0.36	56.9	0.074
0.62	1.33	0.16	<0.01	0.45	0.002	0.06	60.6	0.014
0.71	2.08	0.26	<0.01	0.63	0.002	0.08	56.5	0.026
0.98	2.71	0.3	<0.01	0.83	0.002	0.06	65.8	0.015
1.69	3.61	0.38	<0.01	0.56	0.002	0.15	65.4	0.031
5.1	3.69	0.32	<0.01	0.63	0.003	0.28	58.2	0.038
3.59	2.66	0.27	<0.01	0.99	0.002	0.18	58.5	0.028
0.61	1.63	0.17	<0.01	0.59	0.002	0.04	53.4	0.009
0.5	1.3	0.16	<0.01	0.57	0.002	0.06	58.7	0.015
2.02	3.49	0.36	<0.01	0.7	0.002	0.06	63.8	0.017
1.25	1.93	0.19	<0.01	0.99	0.002	0.04	65.4	0.015
0.81	2.22	0.19	<0.01	1.76	0.002	0.26	60.2	0.03
1.1	2.19	0.22	<0.01	0.69	0.002	0.07	55.4	0.019
0.97	2.51	0.34	<0.01	0.42	0.002	0.03	61	0.006
3.7	1.49	0.14	<0.01	0.63	0.002	0.09	54.3	0.02
1.65	3.17	0.38	<0.01	0.81	0.002	0.17	64	0.024
1.66	1.66	0.22	<0.01	0.51	0.002	0.04	58.1	0.008
1.65	1.06	0.14	<0.01	0.39	0.002	0.1	54.4	0.028
1.2	2.84	0.35	<0.01	0.97	0.001	0.12	62.2	0.026
0.55	1.34	0.13	<0.01	0.47	0.002	0.06	58.2	0.023
1.41	3.67	0.29	<0.01	0.97	0.002	0.22	60.8	0.055
14.1	2.4	0.12	<0.01	1.33	0.003	0.45	45.9	0.074

TiO2	Y	Zn	Zr	LOI	Cu
GO_ICP95A	GO_ICP95A	GO_ICP95A	GO_ICP95A	G_PHY01K	GO_ICP13B
0.01	0.001	5	0.001	-10	0.01
%	%	ppm	%	%	%
0.66	<0.001	9	0.017	6.79	N.A.
0.92	0.001	9	0.021	12.5	N.A.
0.58	<0.001	5	0.015	5.8	N.A.
0.6	0.001	7	0.015	6.08	1.14
0.54	<0.001	16	0.014	5.79	N.A.
0.66	0.001	<5	0.015	8.86	1.22
0.64	<0.001	7	0.017	9.83	N.A.
0.49	<0.001	7	0.011	6.81	1.5
0.3	<0.001	210	0.013	1.88	N.A.
0.6	0.001	9	0.014	5.49	N.A.
0.76	0.001	8	0.017	12.6	N.A.
0.55	<0.001	5	0.013	4.71	N.A.
0.65	<0.001	11	0.014	8.79	1.5
0.83	0.001	8	0.019	10.6	N.A.
0.86	0.002	6	0.02	11.3	N.A.
0.7	0.001	6	0.016	8.92	2.57
0.63	0.001	10	0.016	6.94	N.A.
0.54	<0.001	<5	0.012	10	N.A.
0.85	0.001	9	0.018	10.2	N.A.
0.76	0.001	5	0.017	9.47	1.37
0.62	0.001	5	0.016	6.52	N.A.
0.43	<0.001	7	0.013	4.35	N.A.
0.61	<0.001	5	0.014	6.1	1.91
0.72	0.001	<5	0.016	9.09	N.A.
0.83	0.001	7	0.02	10.8	N.A.
0.79	0.001	6	0.018	9.98	N.A.
0.51	<0.001	11	0.015	5.57	N.A.
0.67	0.001	7	0.016	6.74	N.A.
0.86	<0.001	8	0.019	9.33	N.A.
0.78	0.001	5	0.017	9.1	N.A.
0.73	0.001	7	0.016	8.4	N.A.
0.79	0.001	<5	0.017	10.4	N.A.
0.59	<0.001	6	0.013	6.97	2.01
0.82	0.001	<5	0.018	10.1	N.A.
0.81	0.002	5	0.017	11.4	1.41
0.6	<0.001	7	0.014	5.78	1.04
0.78	0.001	<5	0.016	9.58	1.83
0.55	0.001	8	0.013	9.27	1.92
0.66	0.001	<5	0.014	12.8	N.A.

Appendix I Details regarding the Python Script

GAUSSIAN SMOOTH TECHNIQUE

In order to develop a curve with a valid derivative, it was necessary to use the Gaussian Blur or Gaussian Smoothing Technique.

$$G(x) = \frac{1}{\sigma\sqrt{2\pi}} e^{\frac{-x^2}{2\sigma^2}}$$

Equation 6 Gaussian function used in the construction of the Python Script

$$G'(x) = \frac{1}{\sigma\sqrt{2\pi}} e^{\frac{-x^2}{2\sigma^2}} \left(-\frac{x}{\sigma^2}\right)$$

Equation 7 First derivative of the Gaussian Function

$$G''(x) = -\frac{1}{2\pi\sigma^4} e^{\frac{-x^2}{2\sigma^2}} \left(2 - \frac{x^2}{2\sigma^2}\right)$$

Equation 8 Second derivative of the Gaussian Function

This equation allows for the calculation of the derivative because it smoothens the peaks, converting them into a concave local maximum. The value of sigma is calculated by the Fast Fourier Transform (FFT), which provides the best approach to measuring that which can be considered a noise and that which can be considered a peak. With respect to the examination of the FFT, it was suggested that a sigma value of 2.0 be used. The convolution also plays an important role in converting the peaks into a spectrum that is able to derivate.

The principal algorithm for recognizing a peak is the use of the first derivative of the smoothened spectrum, which has to be previously positive and currently 0 to be considered a local maximum

and, the second derivative has to show a negative value to confirm that this wavelength belongs to a peak.

POSSIBLE NUMBERS TO TUNE FROM THE PYTHON SCRIPT

In this section, some detail that can be modified by the user, is provided for the use of the Python Script. The proposed Python Script provides the option to plot the whole spectrum with the variable "saveplot". "SIGMA=2" can be changed depending on the reliability of the data obtained during the sorting process. It is important to notice that this sigma value smoothens the data and the increase of this value will filter more data that has low peaks, but also will remove potential noise from complicated surfaces such as samples of white rock. "idWavelengths" allows for the choice of which file can be used as the ID Wavelength. "maxval" can be changed to the minimum peak that is required in order be similar to a minimum spectrum threshold.

Appendix J Details of methodology and data treatment or the Oxide samples

Case Arsenic – Oxygen distortion ambiguity

There is an ambiguity with regard to the readings for the quadruple ionization stage of Oxygen (or O V) and the neutral ion of Arsenic (As I). Both readings have a wavelength of around 278.1 nm. Arsenic can be heavily associated with Sulphurs, creating a positive expectancy regarding the presence of Copper, and an optimum material for froth flotation. Paxite can be found in hydrothermal calcite veins, and its composition is $CuAs_2$. The overlapping responses act favourably toward the ion that has the biggest Aki, in this case for O V, which was not expected because ionization stages larger than III are less likely to happen since they are more stable and require higher energy for the transition.

Table J-1: O V vs. As I key indicators for element selection

Ion	Observed Wavelength Air (nm)	Ritz Wavelength Air (nm)	Acc.	Rel. Int. number	Aki
O V	278.101	278.101	B	1000	140,000,000
As I	278.022			170	78,000,000

the distance in terms of Wavelength for As I (272.02 nm) and O V (278.10 nm) creates a confusion that can be easily resolved using LIBS machine. Further information about this feature is explained in Chapter 3:, the distance between each pixel varies between 0.135 nm to 0.15 nm. Distances between wavelengths lesser than 0.15 nm have been avoided for the selection of the ID wavelength.

Table J-2: Arsenic ICP certified results for the 41 rock samples from Escondida Mine

SAMPLE	As (ppm)
1	
2	4
3	4
4	4
5	4
6	9
7	4
8	8
9	
10	3
11	
12	19
13	
14	15

SAMPLE	As (ppm)
15	6
16	4
17	10
18	
19	3
20	4
21	3
22	7
23	14
24	11
25	3
26	3
27	4
28	

SAMPLE	As (ppm)
29	4
30	
31	
32	6
33	3
34	3
35	4
36	4
37	7
38	5
39	12
40	3
41	4

To gain a better understanding of how the LIBS machine works, the LIBS responses and the ICP Certified Analysis have been contrasted.

Rhenium response found in Laser Induced Breakdown Spectroscopy

It is unlikely to find Rhenium. Rhenium is the 70th most abundant element in the earth's crust (Yaroshevsky) with $7x10^{-8}$ % ($7x10^{-4}$ ppm). This is in contrast with Oxygen with 47%, Si with 29.5% or Al with 8.05%. Chile has the largest reserves of Rhenium in the world (Anderson). However, even in Chile, obtaining a trace of Rhenium from a sensor is difficult as the area sensed is relatively small (100 um for LIBS), and the occurrence Rhenium is limited.

Tests conducted on Oxide rocks only showed 1 reading out of 1640 readings that successfully detected Rhenium. LIBS was sensitive enough to provide a reading for such a small amount that was not even traceable using ICP.

Table J-3: Trace of Rhenium in Oxide sample in Escondida Mine

Sample Rock	Peak Wavelength	Element	Intensity	Acc.	Observed Wavelength Air
33B1,S3,1	346.09	Re I	1046		346.046

The reason that this trace can be accepted as a valid reading is because it has a valid Intensity that is statistically outside of the 3 standard deviations of the total noise.

Table J-4: Statistical analysis of the spectrum for sample 33B1, S3, 1

u	884.4361	
Stan Dev	50.39881	
2*S D	985.2337	783.6384
3*S D	1035.632	733.2396

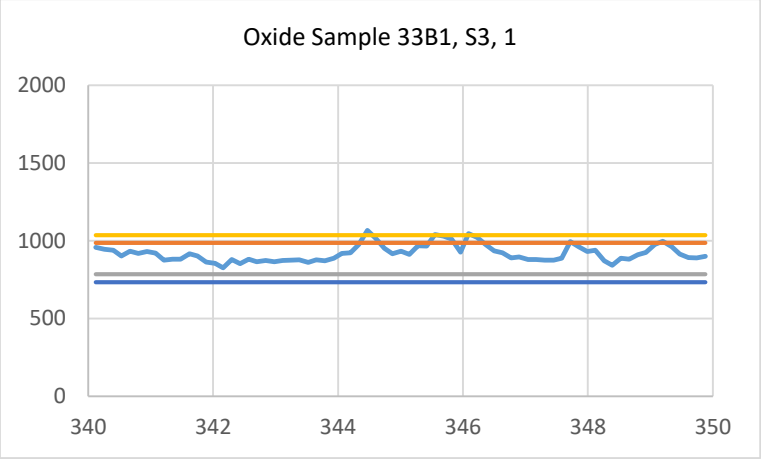

Figure J-1: Zoomed spectrum of sample 33B1,S3,1

In Figure J-1 the spectrum has been zoomed between the wavelengths 340 nm to 350 nm. The full spectrum of the same rock sample is shown in Figure J-2. The chart shows the peak of interest of Re I at 346.09 nm. Table J-4 indicates the calculation of the standard deviation of the noise as

represented with red and green lines in Figure J-2. An algorithm was built to calculate this standard deviation of the noise.

The logic behind this algorithm is to find

$$If\ \|X_i - avg(X_i)\| <\ 2 * STD\ (X_i)\ then\ X_i$$

$$else\ \emptyset$$

Where:

$X_i = Intensity\ pixel\ of\ the\ spectrum$

This pseudocode finds the 2 and 3 standard deviations of the whole noise in the spectrum by removing all the peaks, and leaving only that which the algorithm can recognize as noise. It is necessary to repeat the algorithm until the final output achieves the same value.

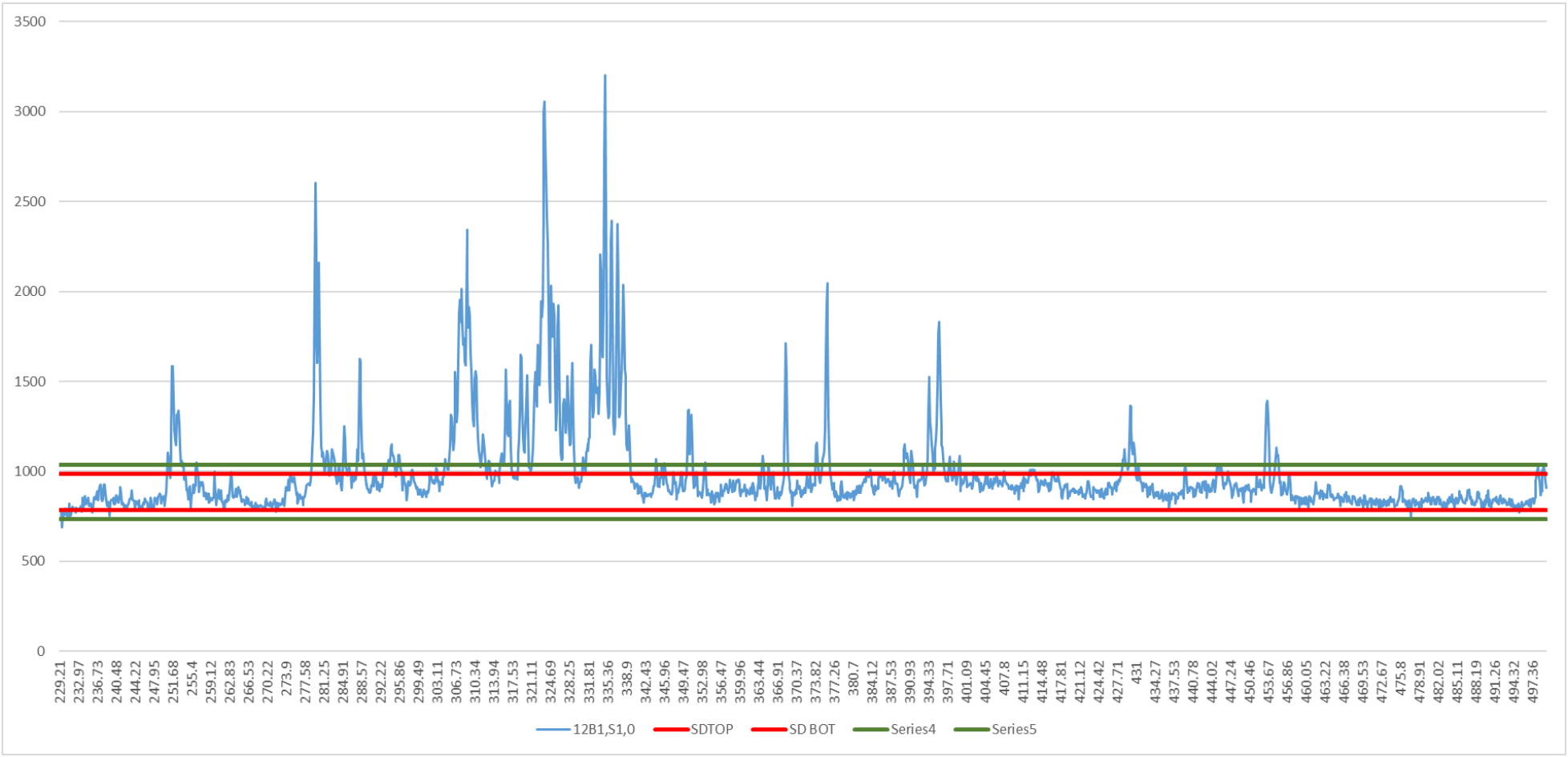

Figure J-2: Spectrum for sample 33B1, S3,1

Table J-5: Statistical analysis of noise to recognize LIBS responses

		Avg	982.14	933.02	909.9	898.66	893.39	890.74	888.5	887.36	886.38	885.4	884.84
Wavelength	**33B1, S3,1**	**Std. Dev**	254.74	124.67	81.5	66.31	59.58	56.35	54.25	53.33	52.35	51.35	50.81
229.21	788		788	788	788	788	788	788	788	788	788	788	788
229.36	788		788	788	788	788	788	788	788	788	788	788	788
229.5	774		774	774	774	774							
229.65	691		691	691									
229.79	752		752	752	752								
229.94	776		776	776	776	776	776						
230.08	754		754	754	754								
230.22	785		785	785	785	785	785	785	785	785	785	785	785
230.37	793		793	793	793	793	793	793	793	793	793	793	793
230.51	758		758	758	758								
230.66	774		774	774	774	774							
230.8	741		741	741									
230.95	762		762	762	762								
231.09	824		824	824	824	824	824	824	824	824	824	824	824
231.24	773		773	773	773	773							
231.38	755		755	755	755								
231.53	756		756	756	756								
231.67	799		799	799	799	799	799	799	799	799	799	799	799
231.82	804		804	804	804	804	804	804	804	804	804	804	804
231.96	792		792	792	792	792	792	792	792	792	792	792	792
232.11	781		781	781	781	781	781	781	781	781			
232.25	782		782	782	782	782	782	782	782	782	782		
232.4	771		771	771	771	771							
232.54	800		800	800	800	800	800	800	800	800	800	800	800
232.68	796		796	796	796	796	796	796	796	796	796	796	796
232.83	788		788	788	788	788	788	788	788	788	788	788	788

This back-calculated formula creates blank cells that represent the peaks of the spectrum, leaving just the values that do not correspond to a LIBS response. In the first row, Table J-5 shows the average value of the previous sample group. E.g. 928.14 is the average of all of the values in the second column, which are the LIBS responses for the sample 33B1,S3,1. Likewise, the standard deviation of 254.74 is calculated using all of the LIBS responses. In the next column, 933.02 is calculated from the values previously processed, removing the responses that do not fit with the logic, and 124.67 is the standard deviation for the value in the 4th column previously processed. Once it has been tested that 2 contiguous columns do not change, the variation in the statistical analysis becomes insignificant, and then, it can be concluded that the standard deviation calculated

is the correct response for all of the noise responses. In this case it is 50.39, which is calculated from all of the values for the last column.

The occurrence of Rhenium in geological deposits can be found as part of the Platinum Group Metals PGM (Pt, Re, Os, Ir) or Tarkianite (Cu0.85 Fe2+0.1Re2.8Mo1.2S8), which can be found in mineral grain sulfide concentrates.

We can conclude that the response for Rhenium is correct, providing evidence for the geological occurrence of the mineral, the statistical analysis of the response, and the 3 filters described in section 3.7 and used by the Python Script to analyze a correct signal.

The value of the Rhenium case analysis does not have to do with the need for getting the Re signal. Indeed, Re is not significant, and is very unlikely to be observed. However, the importance of this exercise is to provide an idea of the real capabilities of LIBS, which can read an element that in the earth's crust is less than $7x10^{-8}$ %. This provides LIBS with a qualitative capability rate and a quantitative capability, leaving behind certified methods such as ICP.

The main reason that this same response has not been repeatable, despite the 40 readings in the rock, is because the laser beam is small (100 um), with a chance of 0.008% of shooting back in the same position. Rhenium, as mentioned, is a very scarce element in the environment. For practical purposes, Rhenium has been taken away from the ID wavelength input for the Python Script and for the analysis of the rock samples.